THE UNIVERSITY OF OKLAHOMA

GRADUATE COLLEGE

INELASTIC FINITE ELEMENT ANALYSIS OF STIFFENED END-PLATE MOMENT CONNECTIONS

A THESIS

SUBMITTED TO THE GRADUATE FACULTY

in partial fulfillment of the requirements for the

degree of

MASTER OF SCIENCE

By

MEHDI GHASSEMIEH

Norman, Oklahoma

1983

INELASTIC FINITE ELEMENT ANALYSIS OF STIFFENED END-PLATE MOMENT CONNECTIONS

A THESIS

APPROVED FOR THE SCHOOL OF CIVIL ENGINEERING

AND ENVIRONMENTAL SCIENCE

By

[redacted]

ACKNOWLEDGMENTS

The writer wishes to express his sincere appreciation to Dr. Anant Kukreti and Dr. Thomas M. Murray for their guidance and assistance in this study. The financial support of the American Institute of Steel Construction is gratefully acknowledged. Appreciation is also extended to the project committee chairman, Mr. John D. Griffiths and to the project committee members, Dr. Duane S. Ellifritt, Mr. Gerald B. Emerson, Mr. Jim Wooten, and Mr. Nestor Iwankiw of the AISC staff for their guidance and constructive suggestions. Further thanks are expressed to Professor Leon R.L. Wang for serving as a thesis committee member. The assistance given by Mr. Ali Mazroi and Mr. E. Bryant Davidson for conducting the experiments is acknowledged. Finally, special thanks are expressed to Ms. Lori E. Creech for typing the thesis.

The prototype test specimens were provided by Capitol Steel Corporation, Oklahoma City. Plates for the tee-hanger specimens were provided by Robberson Steel Company and Star Manufacturing Company, both of Oklahoma City. The generous contributions of these three companies are sincerely appreciated.

TABLE OF CONTENTS

LIST OF FIGURES

Figure Page

Figure		Page

LIST OF TABLES

ABSTRACT

This study involves the development of a methodology for the design of stiffened end-plate moment connections having two rows of high strength bolts on either side of the beam tension flange. This geometric configuration results in a highly indeterminate problem as the bolt forces cannot be determined directly. Thus, an analytical study with modeling of the connection as an assemblage of finite elements was conducted. In the analysis, it was assumed (which was later verified experimentally) that the tension beam flange and the surrounding plate acts as a stiffened tee-hanger. Only one-quarter of a symmetric section of this tension region was analyzed using eight-noded isoparametric brick elements for the end-plate elements. Bilinear stress-strain behavior is considered for both the bolt and end-plate material. To consider the inelastic steel behavior in each cycle, the elastic moduli of the yielded elements is reset to their secant values.

A sensitivity and feasibility study was conducted with information from sufficient cases so as to select parameters, within practical ranges, from the pertinent geometry and force related variables governing the connection behavior. Finite element analyses were carried out for the cases and the results regressed to yield predicting equations for maximum deflection in the end-plate, maximum bending stresses in the end-plate and near (to the beam flange) bolt force. Certain analytical results were compared with test results from tee-hanger and prototype connection tests. Finally, the predicting equations were used to develop a design methodology. This study is restricted to A36 steel and A325 bolts with maximum diameter of 1½ in. Based on comparison of experimental and analytical results, it is concluded that the prediction equations developed adequately explain the connection behavior.

INELASTIC FINITE ELEMENT ANALYSIS OF STIFFENED END-PLATE MOMENT CONNECTIONS

CHAPTER I

INTRODUCTION

1.1 General

Beam-to-column connections play an important role in the performance of structural steel frames used in buildings. The major function of these connections is to safely transfer moments at beam-column interfaces; a secondary, but equally important, function is to transfer shear forces. There are many types of beam-to-column moment connections used in steel structures. Usually they are classified by the load path developed at the time of erection: (a) all bolted, using A325 or A490 F-, N- or X-type bolts; (b) all welded; or (c) welded and bolted using A325 or A490 F-type bolts.

In recent years, end-plate moment connections of the type shown in Figure 1.1, which are shop welded and field bolted type connections, are becoming more widely used. The typical end-plate moment connection (referred to henceforth as "end-plate connection") is composed of a steel plate welded to the end of the beam section with attachment to an adjacent member made using rows of pre-tensioned high-strength bolts. The connection may be made between two beams (splice plate connection) as shown in

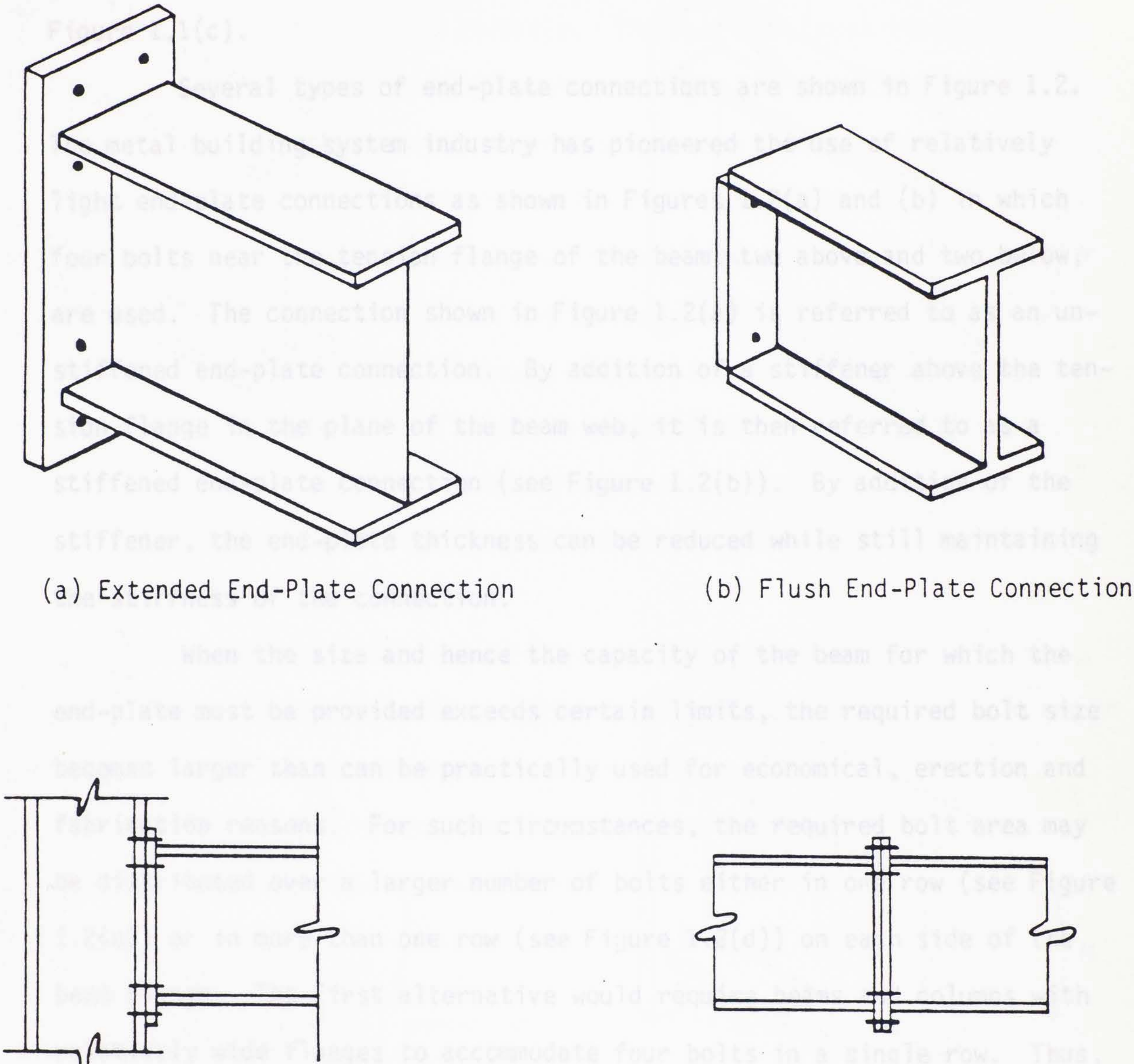

(a) Extended End-Plate Connection

(b) Flush End-Plate Connection

(c) Beam-to-Column Connection

(d) Beam-to-Beam Connection (Splice Connection)

Figure 1.1 Typical End-Plate Connections

Figure 1.1(d) or more typically between a beam and a column as shown in Figure 1.1(c).

Several types of end-plate connections are shown in Figure 1.2. The metal building system industry has pioneered the use of relatively light end-plate connections as shown in Figures 1.2(a) and (b) in which four bolts near the tension flange of the beam, two above and two below, are used. The connection shown in Figure 1.2(a) is referred to as an unstiffened end-plate connection. By addition of a stiffener above the tension flange in the plane of the beam web, it is then referred to as a stiffened end-plate connection (see Figure 1.2(b)). By addition of the stiffener, the end-plate thickness can be reduced while still maintaining the stiffness of the connection.

When the size and hence the capacity of the beam for which the end-plate must be provided exceeds certain limits, the required bolt size becomes larger than can be practically used for economical, erection and fabrication reasons. For such circumstances, the required bolt area may be distributed over a larger number of bolts either in one row (see Figure 1.2(c)) or in more than one row (see Figure 1.2(d)) on each side of the beam flange. The first alternative would require beams and columns with relatively wide flanges to accommodate four bolts in a single row. Thus, the second alternative may be a better choice, that is, two rows of two bolts above and two rows of two bolts below the tension flange, as shown in Figure 1.2(d). However, at the present time, no design criteria is available for this configuration.

The objective of this study is to investigate the behavior of the type of end-plate connection shown in Figure 1.2(d). This type of

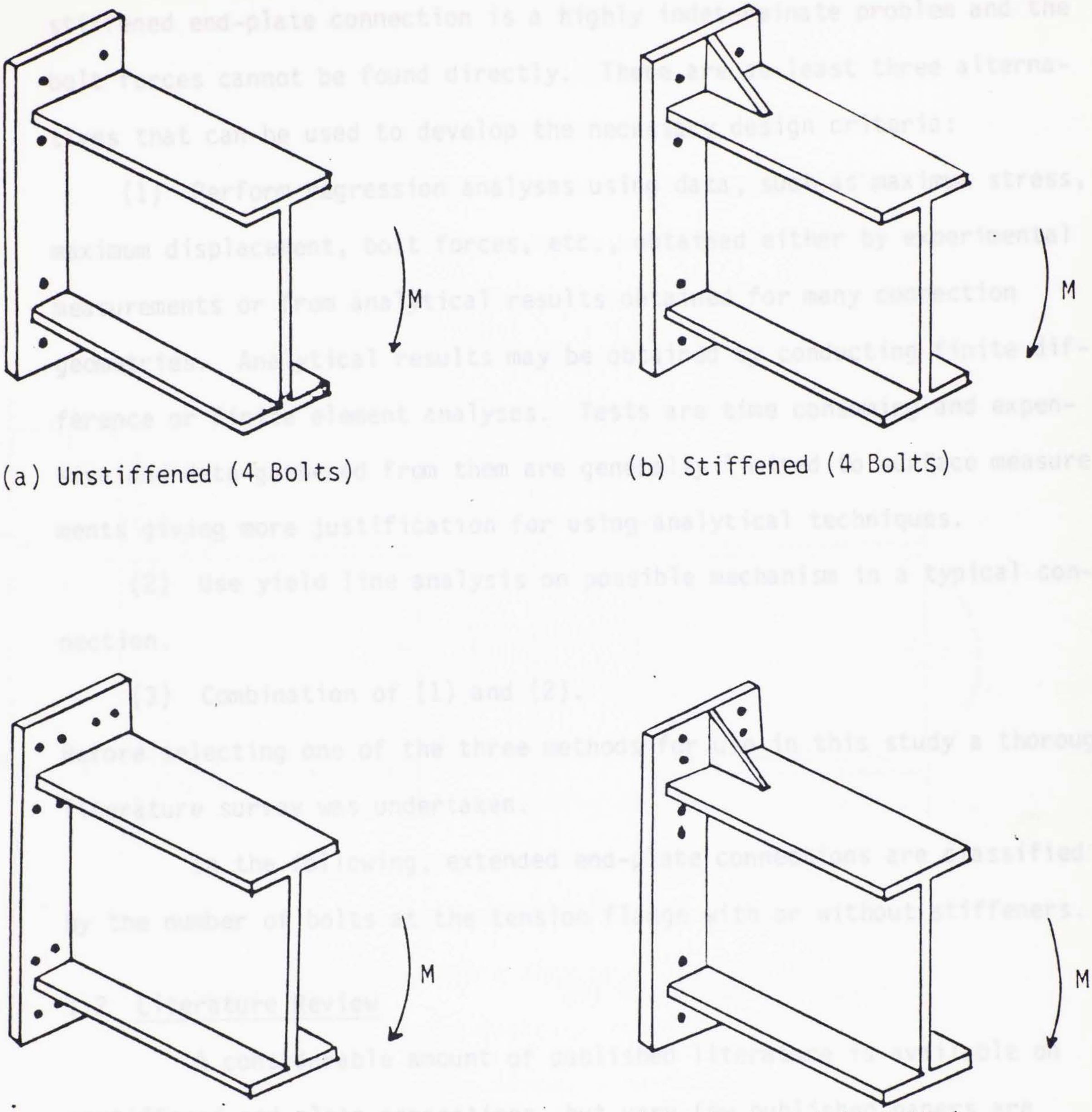

(a) Unstiffened (4 Bolts)

(b) Stiffened (4 Bolts)

(c) 4 Bolts Wide

(d) Stiffened (8 Bolts)

Figure 1.2 Typical Extended End-Plate Connections stiffened end-plate connection is a highly indeterminate problem and the bolt forces cannot be found directly. There are at least three alternatives that can be used to develop the necessary design criteria:

(1) Perform regression analyses using data, such as maximum stress, maximum displacement, bolt forces, etc., obtained either by experimental measurements or from analytical results obtained for many connection geometries. Analytical results may be obtained by conducting finite difference or finite element analyses. Tests are time consuming and expensive and data gathered from them are generally limited to surface measurements giving more justification for using analytical techniques.

(2) Use yield line analysis on possible mechanism in a typical connection.

(3) Combination of (1) and (2).

Before selecting one of the three methods for use in this study a thorough literature survey was undertaken.

In the following, extended end-plate connections are classified by the number of bolts at the tension flange with or without stiffeners.

1.2 Literature Review

A considerable amount of published literature is available on unstiffened end-plate connections, but very few published papers are available regarding design of stiffened end-plate connections. Apparently, the steel building industry has been designing such connections by rule of thumb or on the basis of experience.

Early attempts (prior to 1970) to develop a design methodology for end-plate connections were based on the tee-stub analogy. Figure 1.3(a) shows a typical unstiffened tee-stub connection. On comparison

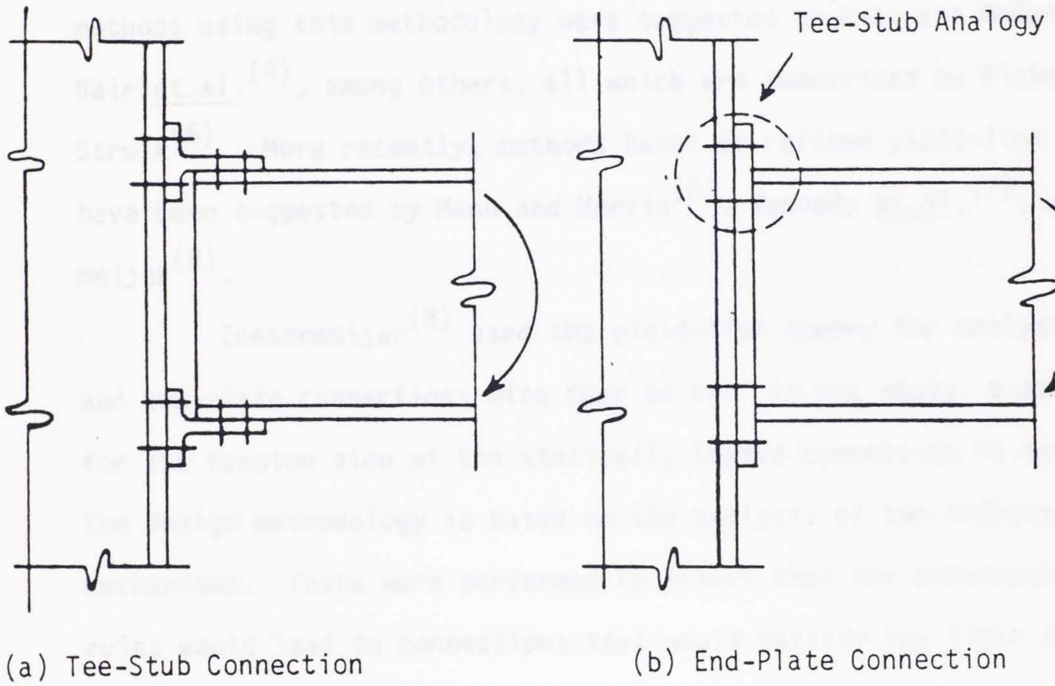

Figure 1.3 Tee-Stub Analogy for End-Plate Connection

with the unstiffened end-plate connection of Figure 1.3(b), it can be seen that the tension region of this connection may possibly be treated as a tee-stub. All the early research on end-plate design resulted in large end-plate thicknesses and large bolt diameters. The reason being that a prying force was conservatively assumed to act at the edge of the end-plate. One of these methods was developed by Douty and McGuire[1] and was later presented in the 7th edition AISC Manual of Steel Construction[2]. Other methods using this methodology were suggested by Kato and McGuire[3] and Nair et al.[4], among others, all which are summarized by Fisher and Struik[5]. More recently, methods based on refined yield-line analyses have been suggested by Mann and Morris[6], Kennedy et al.[7], and Zoetermeijer[8].

Zoetermeijer[8] used the yield-line theory for analysis of T-stub and end-plate connections with four bolts. In his study, a design method for the tension side of the statically loaded connection is developed. The design methodology is based on the analysis of two different collapse mechanisms. Tests were performed to insure that the developed design rules would lead to connections that would satisfy the limit state of deformations as given in the European regulations for Constructional Steel Work. The test results showed a satisfactory agreement with the proposed design rules.

Krishnamurthy[9] has shown that the design rules presented by Zoetermeijer[8] lead to unnecessarily thick plates if only strength is considered.

Krishnamurthy[9] developed the finite element methodology specifically for the analysis of unstiffened, four bolt, extended, end-plate connections (Figure 1.2(a)). Based on an extensive analytical study of the end-plates along with a series of experimental tests, Krishnamurthy developed the design procedure found in the 8th edition of the AISC Manual of Steel Construction[10]. From Krishnamurthy's theoretical studies it was found that even though prying action is present, it is overly conservative to assume it to be acting at the edge of the plate since this results in thicker than necessary plates.

Krishnamurthy[11] also studied the splice end-plate connection (flush end-plate connection) with multiple bolt rows at the tension flange using the finite element method, yield-line theory and some prototype testing. Yield-line mechanisms were suggested to determine the plate thickness. A parametric study was conducted using two dimensional finite element analyses and the results were regressed to develop prediction equations for connection rotation, critical plate stress, and bolt forces. Also five specimens, with plate thicknesses selected according to the proposed procedure, were tested. The test results were used to validate the design procedure. It was observed that plate thickness or bolt diameter could be reduced with an increase in the number of bolt rows. It was also observed that the increase in the number of bolt rows generally reduced the flexibility of the connection at the maximum test load.

Krishnamurthy[12] also investigated the behavior of stiffened end-plate connections using four bolts in the tension region. For this study, the tension region was modeled as a tee-stub. A hybrid 2D-3D finite element model of the tee-stub was developed in which the beam flange and stiffener elements were modeled using a family of two dimensional elements and the end-plate elements were modeled using Levy's eight noded brick element[13]. Thus, the transverse behavior of the tee-stub flanges (i.e., end-plate) was introduced. Also, a parametric study on the influence of the stiffener on the tee-stub behavior was studied. From results of analyses of 72 different combinations of geometric dimensions, prediction equations were developed for maximum deflection, maximum stress in the end-plate and near bolt force. The results are reported to be within a 25 percent variation with most error on the conservative side. The computed results from the design equations showed that reduction in plate thicknesses can be obtained by the use of stiffeners. The formal design rules and prediction equations have not been widely used or published.

Ahuja[14] was the first to investigate stiffened end-plate moment connections with two rows of bolts on either side of the tension flange. Basically this study was an extension of the work done by Krishnamurthy[7]. The finite element analyses used in the study were based on a hybrid 2D-3D model where the end-plate and bolt shanks and bolt heads were modeled as 3D finite elements and the beam and stiffener components were modeled as 2D finite elements. Only elastic material properties were considered. Using results from the finite element analyses, a feasibility and sensitivity parametric study was conducted to establish pertinent variables (geometry and force related) that govern the connection behavior. The ranges of the variables were restricted to practical ranges. For thirty selected cases, finite element analyses were conducted and the results regressed to develop prediction equations for end-plate behavior. Because of the limitation of elastic material properties, design rules developed from the prediction equations were found to be excessively conservative.

Maxwell et al.[15] studied the end-plate and other connections using various methods: simple bending theory, yield-line theory, the finite difference method and the finite element method. They concluded that the finite element method was the best feasible alternative for analyzing such a problem, because it will significantly reduce the number of full scale tests normally required to establish behavior with this type of investigation, and also the finite element method results are close to experimental results. Based on the finite element method and the experimental tests, they developed prediction equations for ultimate moment of the connections and the moment rotation relationships.

1.3 Objectives

Most end-plate research has been conducted on typical four-bolt, unstiffened, extended end-plate connections. Very limited research has been completed on the behavior of stiffened end-plate connections with multiple bolt rows on each side of the beam tension flange. Although the use of more rows results in smaller bolts, it has not been proven whether a reduction in plate thickness can also be achieved.

The design rules provided in the AISC Manual of Steel Construction [10] and by other researchers are generally limited to end-plate connections using four-bolts. Because heavy wide-flange sections may require greater bolt diameters than can be practically accommodated, multiple rows of bolts must be used in such situations. For this reason, research was undertaken to study the behavior of stiffened end-plate connections with eight bolts (two rows of bolts on either side of the tension flange) at the tension flange.

This study is basically a continuation of the work done by Ahuja [14]. The main objective is to develop a design methodology that can be used to determine end-plate thicknesses and bolt sizes considering material nonlinear behavior. A second objective is to study the bolt forces and the effects of bolts on the stress distribution and deformation of the end-plate.

Based on the review of previous work on end-plate connections, the study is addressed on five fronts:

1. Tee-hanger model development using the finite element method and behavior, mesh refinement, effect of failure criteria, and bolt force behavior.

2. Development of prediction equations for maximum bending stress in the end-plate, maximum deflection in the end-plate, and maximum bolt force considering nonlinear material behavior.

3. Comparison of the analytical results with the tee-hanger test results.

4. Experimental testing of the prototype connection to investigate the actual behavior of the connection and also to investigate if the tee-hanger model used in the analytical study is valid.

5. Development of a design methodology for the stiffened end-plate connection under study.

A computer program originally formulated by Krishnamurthy(7) and further refined by Ahuja(14), was extensively modified to conduct the parametric study needed in this research effort. A parametric study, similar to the previous study, was conducted to evaluate the pertinent geometric and force related variables describing the connection behavior. Limiting the variables to practical ranges, finite element analyses of 25 geometric cases are used to develop the prediction equations. To verify the analytical results, six tee-hanger models were tested and results compared. Also to verify the validity of modeling the tension region of the connection as an equivalent tee-hanger, two full size splice-plate connections were tested and results compared with similar tee-hanger tests and finite element analysis results.

CHAPTER II

MATHEMATICAL MODEL INVESTIGATION

2.1 Introduction

In this Chapter, the mathematical model used to analyze the behavior of a typical stiffened end-plate connection with four bolt rows of two bolts each at the tension flange is explained. The finite element method is used to discretize the tension region of the end-plate connection consisting of beam flange, end-plate, stiffener, bolt head, bolt shank and welds. This portion of the connection will be referred to as the "tee-hanger" model. The development and selection of the finite element model is discussed in Section 2.2, and the preparation of data and mesh generator are explained in Section 2.3. In the computer program developed for the finite element analysis, non-linear material properties are incorporated. Description of the failure criteria used to check the yielding in elements is presented in Section 2.4. The salient features of the finite element program and its flow chart are presented in Section 2.5. Finally, observations as to the adequacy of the mathematical model are discussed in Section 2.6.

2.2 Finite Element Model Development

2.2.1 Basics of Model

The ideal selection of a finite element mesh for any physical problem is a three dimensional (3D) mesh. However, it is not necessarily the best choice, as computer costs associated with the required number of degrees-of-freedom (d.o.f.) in a 3D mesh increases. The primary objective of this study was vested in the accuracy of the plate behavior prediction and so at least a partial three dimensional representation is required. Thus, in the interests of economy and accuracy a "hybrid" 2D-3D model was adopted for the stiffened end-plate connection studied here. The 3D elements are used where most accuracy is needed: the end-plate, bolt heads and bolt shanks. Two dimensional elements are used elsewhere. As the tee-hanger (tension region of stiffened end-plate connection) is symmetrical about the orthogonal planes, only a quarter section is considered in the analysis but with appropriate boundary conditions.

The configuration of the model used in most analyses is shown in Figure 2.1. The most critical part of the model, the end-plate, is idealized using the thirty-three d.o.f. 3D-subparametric element as developed by Levy[13]. For the stiffener, 2D subparametric quadrilateral and triangular elements are used, where as, for the tee-stem, 2D, eight noded rectangular hybrid plane stress elements developed by Turner, et al.[16] are used. The weld connecting the tee-stem with the end-plate is modeled using the aforementioned 3D element. The other welds are modeled using the eight noded rectangular 2D elements.

In standard fabrication practice, the gage of the bolts is much larger than the pitch. More load is therefore transferred to the bolt directly from the tee-stem than through the stiffener. Hence the weld used at the intersection of the beam flange (or tee-stem) and the end-plate is of relatively more importance than the stiffener to end-plate weld. This provides the justification of modeling welds, other than the

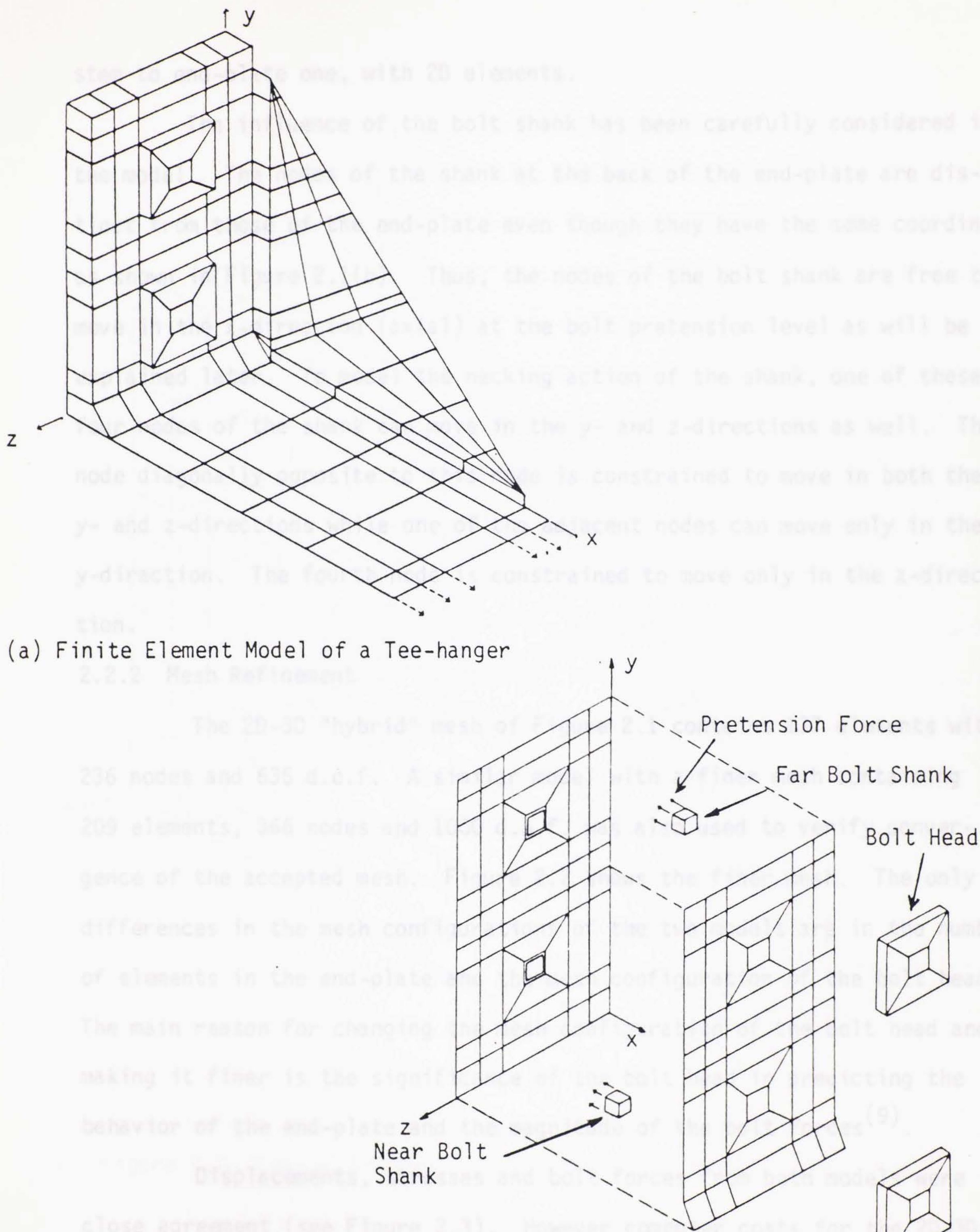

(a) Finite Element Model of a Tee-hanger

(b) Detail of End-Plate Model

Figure 2.1 Typical Configuration of a Coarser "Hybrid" 2D-3D Mesh stem to end-plate one, with 2D elements.

The influence of the bolt shank has been carefully considered in the model. The nodes of the shank at the back of the end-plate are distinct from those of the end-plate even though they have the same coordinates, as shown in Figure 2.1(b). Thus, the nodes of the bolt shank are free to move in the x-direction (axial) at the bolt pretension level as will be explained later. To model the necking action of the shank, one of these four nodes of the shank can move in the y- and z-directions as well. The node diagonally opposite to this node is constrained to move in both the y- and z-directions while one of the adjacent nodes can move only in the y-direction. The fourth node is constrained to move only in the z-direction.

2.2.2 Mesh Refinement

The 2D-3D "hybrid" mesh of Figure 2.1 contains 137 elements with 236 nodes and 636 d.o.f. A similar model with a finer mesh containing 209 elements, 366 nodes and 1000 d.o.f. was also used to verify convergence of the accepted mesh. Figure 2.2 shows the finer mesh. The only differences in the mesh configurations of the two models are in the number of elements in the end-plate and the mesh configuration of the bolt heads. The main reason for changing the mesh configuration of the bolt head and making it finer is the significance of the bolt head in predicting the behavior of the end-plate and the magnitude of the bolt forces[9].

Displacements, stresses and bolt forces from both models were in close agreement (see Figure 2.3). However computer costs for the 2D-3D model with 137 elements were much less than for the fine mesh model. For instance, for a typical problem (results in Figure 2.3), the coarse

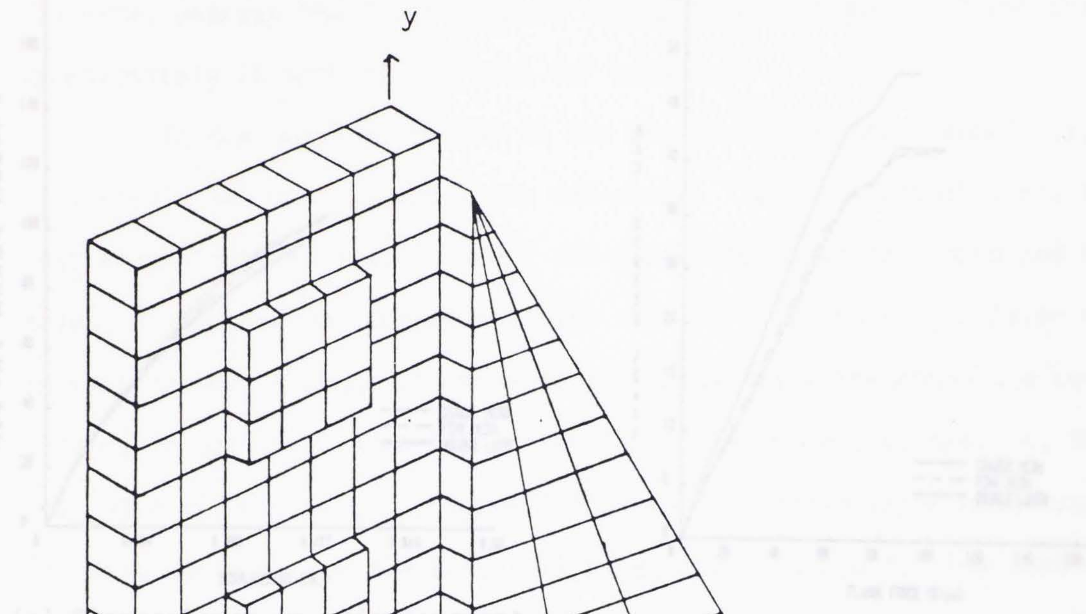

Figure 2.2 Typical Configuration of the Fine "Hybrid" 2D-3D Mesh

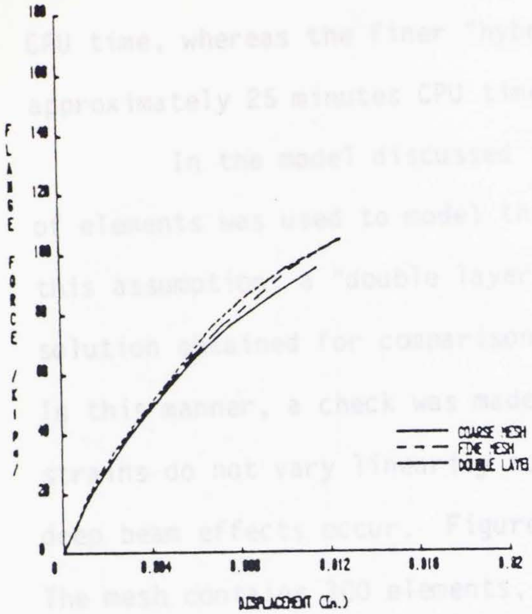

(a) Flange Force vs. Displacement

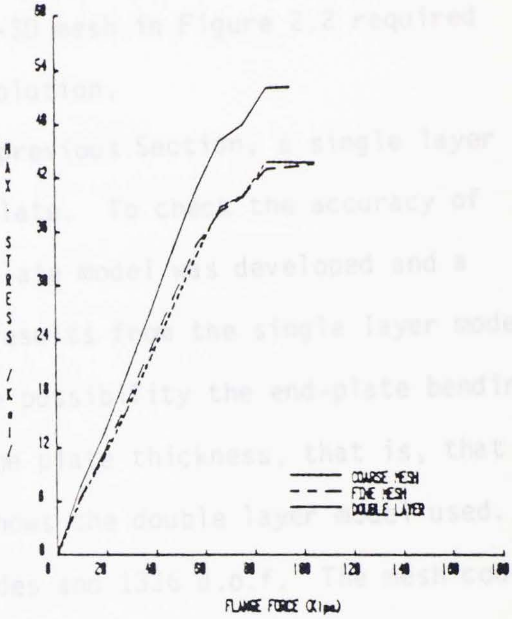

(b) Maximum Stress vs. Flange Force

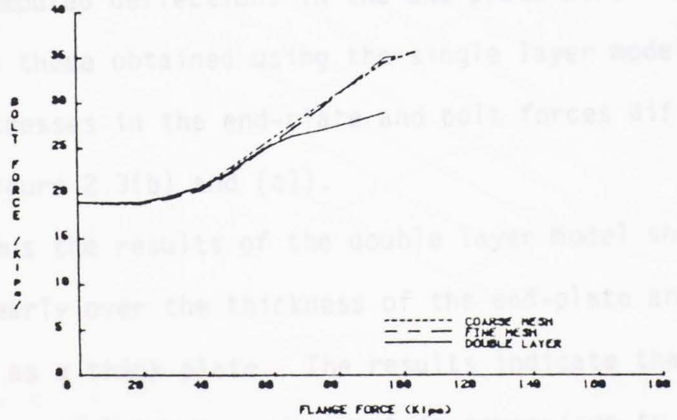

(c) Bolt Force vs. Flange Force

Figure 2.3 Comparison of Results from Various Meshes "hybrid" 2D-3D mesh in Figure 2.1 required approximately 19 minutes of CPU time, whereas the finer "hybrid" 2D-3D mesh in Figure 2.2 required approximately 25 minutes CPU time for solution.

In the model discussed in the previous Section, a single layer of elements was used to model the end-plate. To check the accuracy of this assumption, a "double layer" end-plate model was developed and a solution obtained for comparison with results from the single layer model. In this manner, a check was made on the possibility the end-plate bending strains do not vary linearily across the plate thickness, that is, that deep beam effects occur. Figure 2.4 shows the double layer model used. The mesh contains 300 elements, 478 nodes and 1336 d.o.f. The mesh configuration is the same as used for the fine mesh shown in Figure 2.2, except for layering. The bolt head configurations was the same as used for the 2D-3D "hybrid" fine mesh, but the bolt shank was modeled using two solid elements.

Computed deflections in the end-plate were found to be essentially the same as those obtained using the single layer models (see Figure 2.3(a)). However, stresses in the end-plate and bolt forces differed by as much as 15% (see Figure 2.3(b) and (c)).

Thus the results of the double layer model show that the strain varies linearly over the thickness of the end-plate and the end-plate is not acting as a thick plate. The results indicate that, although the single layer model has a cruder mesh in comparison to the double layer model, its accuracy is about the same as the double layer model. Also, the computing costs and CPU time are very high for a double layer model. For example, for the same problem mentioned previously, the CPU time is 43 minutes.

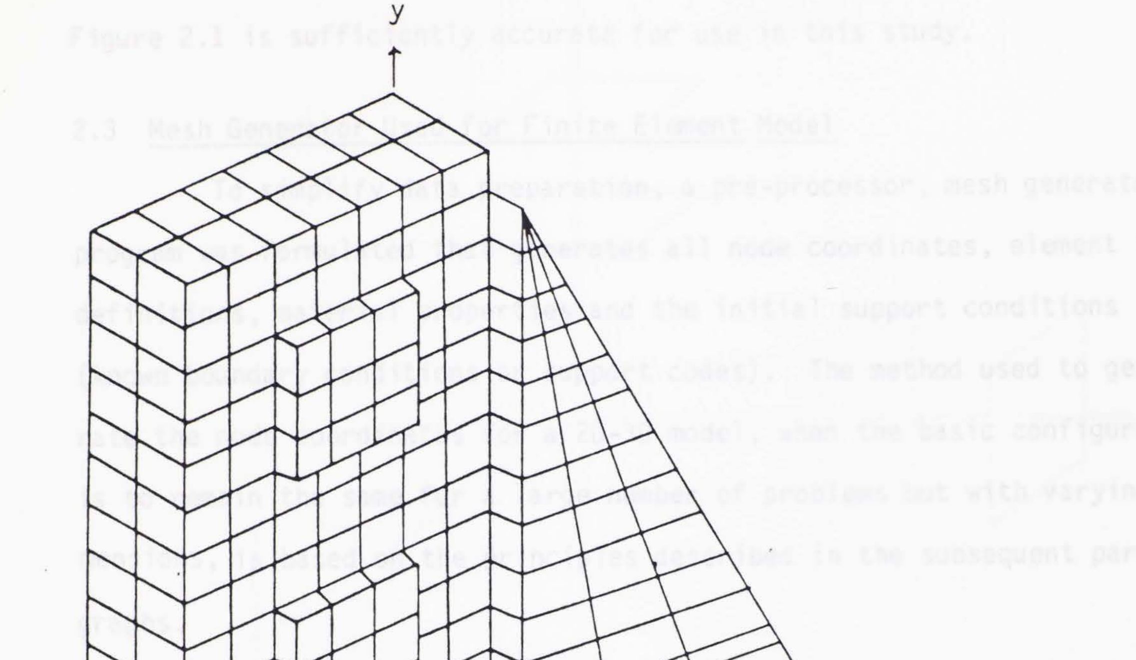

Figure 2.4 Configuration of 2D-3D Mesh with Double Layer of Elements at the End-Plate

Thus, it was concluded that the coarse "hybrid" 2D-3D mesh of Figure 2.1 is sufficiently accurate for use in this study.

2.3 Mesh Generator Used for Finite Element Model

To simplify data preparation, a pre-processor, mesh generator program was formulated that generates all node coordinates, element type definitions, material properties and the initial support conditions (known boundary conditions or support codes). The method used to generate the node coordinates for a 2D-3D model, when the basic configuration is to remain the same for a large number of problems but with varying dimensions, is based on the principles described in the subsequent paragraphs.

Any node may be identified by the x-, y-, z-planes which intersect at that point. For instance, node 36 of Figure 2.5(b) is located at the intersection of the x-plane 2, y-plane 3 and z-plane 3. The planes are located in space in such a manner as to define the bounding surfaces and the slicing planes (see Figure 2.6). Thus a plate parallel to the xy-plane may be sliced by planes xp(1), xp(2), ..., xp(5), and the plate parallel to the yz-plane may be sliced by planes yp(1), yp(2), ..., yp(6), as shown in Figure 2.6. The node numbering is selected so as to yield the least band-width.

Basic data for node-coordinate generation consists of node numbers and plane identifications, as will be illustrated for the mesh shown in Figure 2.6. Intersecting planes at each node are first identified:

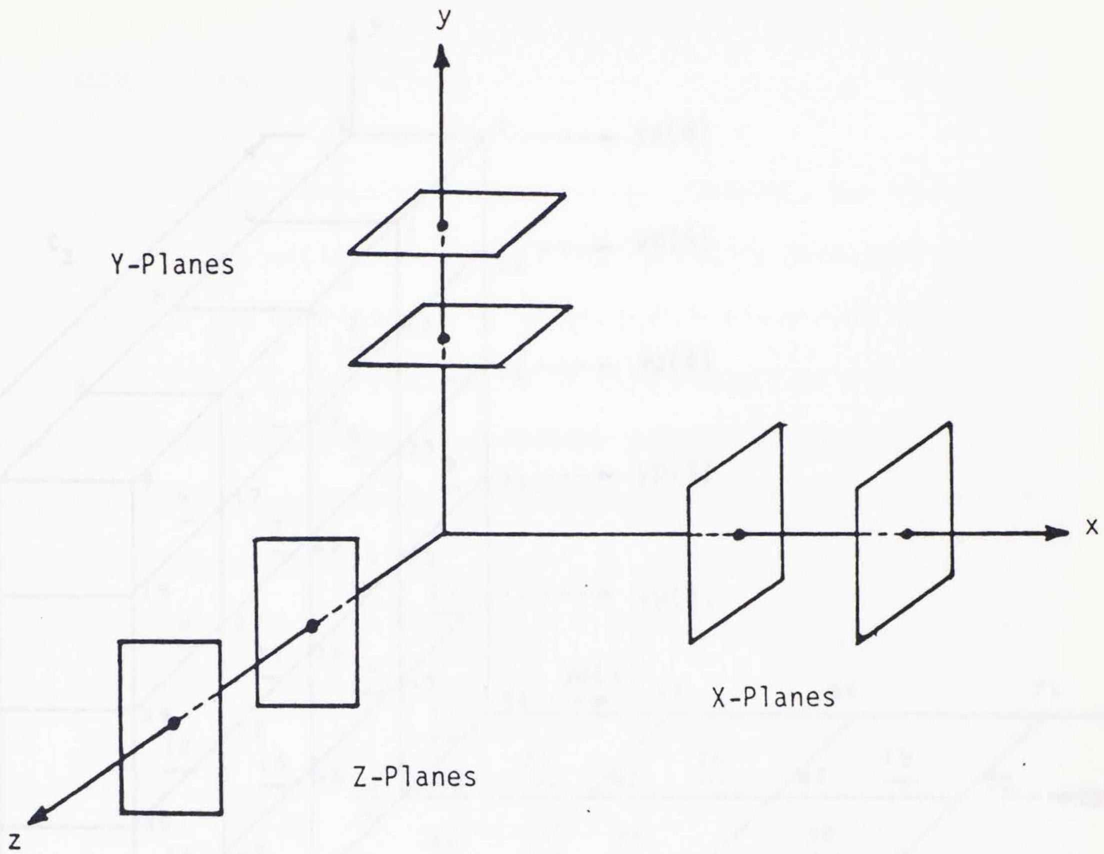

(a) Configuration of Planes

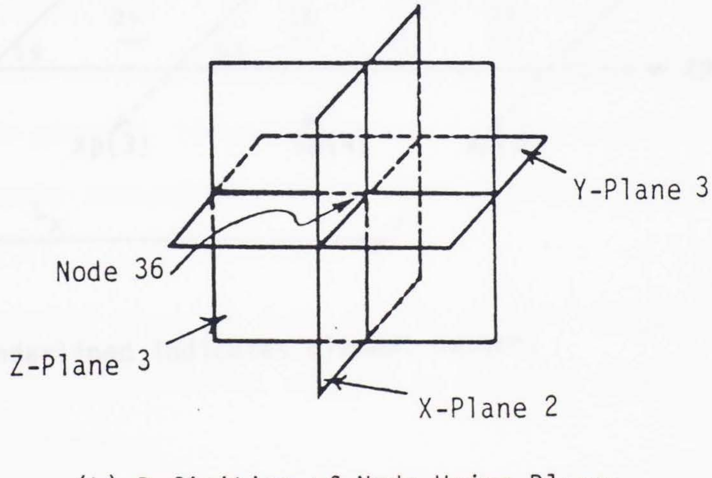

(b) Definition of Node Using Planes

Figure 2.5 Plane Identifications for the Mesh Pre-Processor

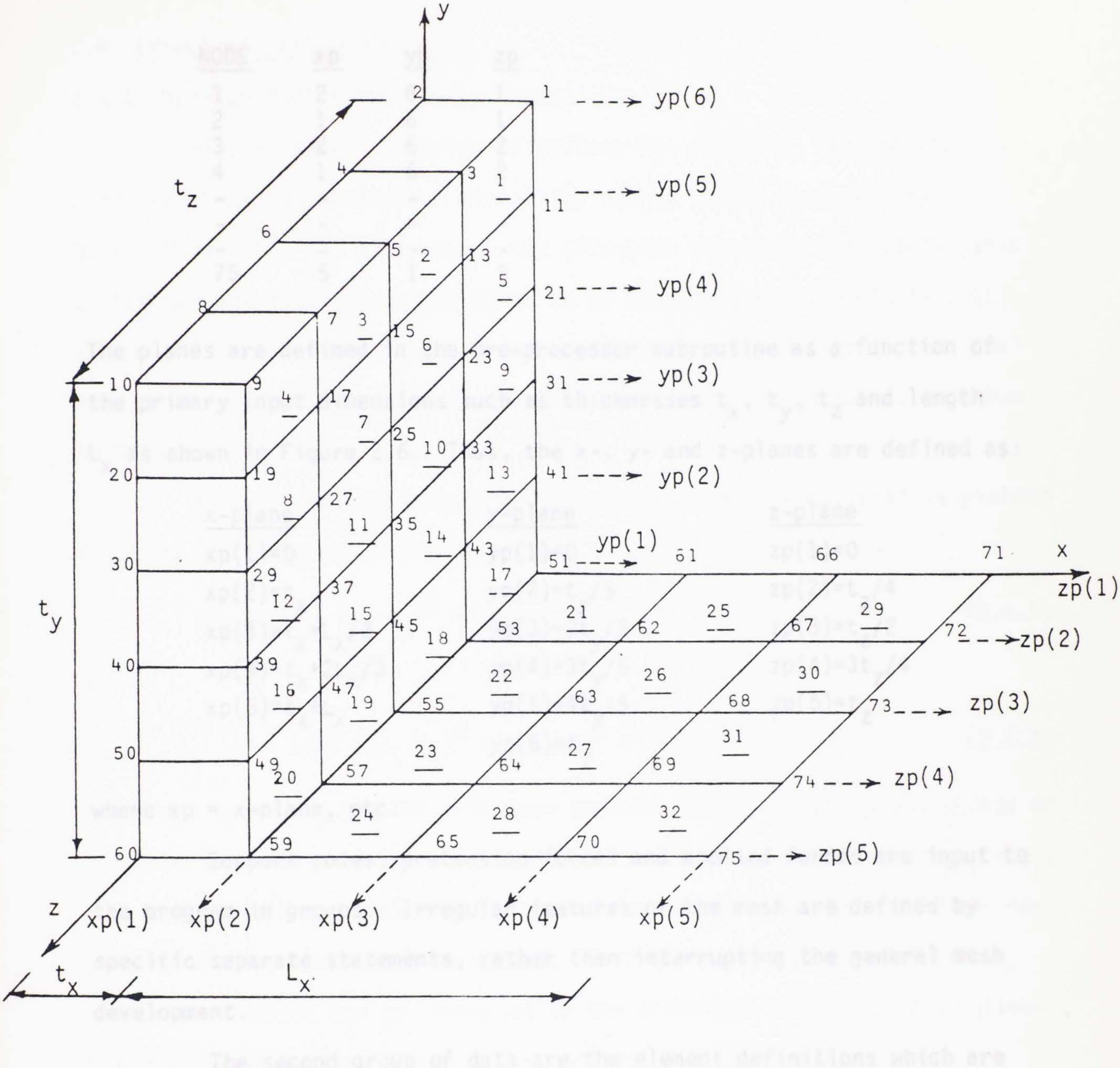

Note: Number underlined indicates element number.

Figure 2.6 Typical Mesh Example with Surfaces and Slicing Planes

NODE	xp	yp	zp
1	2	6	1
2	1	6	1
3	2	6	2
4	1	6	2
-	-	-	-
-	-	-	-
-	-	-	-
75	5	1	5

The planes are defined in the pre-processor subroutine as a function of the primary input dimensions such as thicknesses t_x, t_y, t_z and length L_x as shown in Figure 2.6. Thus, the x-, y- and z-planes are defined as:

x-plane	y-plane	z-plane
xp(1)=0	yp(1)=0	zp(1)=0
$xp(2)=t_x$	$yp(2)=t_y/5$	$zp(2)=t_z/4$
$xp(3)=t_x+L_x/3$	$yp(3)=2t_y/5$	$zp(3)=t_z/2$
$xp(4)=t_x+2L_x/3$	$yp(4)=3t_y/5$	$zp(4)=3t_z/4$
$xp(5)=t_x+L_x$	$yp(5)=4t_y/5$	$zp(5)=t_z$
	$yp(6)=t_y$	

where xp = x-plane, etc.

Support codes, pretension forces and applied forces are input to the program in groups. Irregular features of the mesh are defined by specific separate statements, rather than interrupting the general mesh development.

The second group of data are the element definitions which are all given as input statements, as well as material properties and thickness of plane elements.

2.4 Effect of Failure Criteria

2.4.1 Maximum Distortion Energy Theory

Of the several theories of failure for yielding, the one most used for steel is the maximum distortion energy theory developed by R. Von-Mises[17]. In this study, the effective stress-strain relationship of the various steel plates is taken to be elastic-perfectly plastic, as shown in Figure 2.7(a). The effective stress-strain behavior of the steel bolt material is represented by the bilinear stress-strain curve, as shown in Figure 2.7(b).

Based on the Maximum Distortion Energy Theory a material is yielded when the following relationship holds

$$(\sigma_1-\sigma_2)^2 + (\sigma_2-\sigma_3)^2 + (\sigma_3-\sigma_1)^2 > 2\sigma_y^2 \qquad (2.4.1)$$

or

$$\sigma_{eff} = 1/\sqrt{2}\ \{(\sigma_1-\sigma_2)^2 + (\sigma_2-\sigma_3)^2 + (\sigma_3-\sigma_1)^2\}^{\frac{1}{2}} > \sigma_y \qquad (2.4.2)$$

where σ_1, σ_2 and σ_3 are the principal stresses and σ_y is the yield stress of the material from an uniaxial tensile test. For any element when $\sigma_{eff} > \sigma_y$, then the element has yielded. To extend the analysis in the non-linear region it will be convenient to convert all the stresses to strains. The principal stresses can be converted to the principal strains by the following relationships

$$\sigma_1 = \mu\{(1-\nu)\ \varepsilon_1 + \nu\varepsilon_2 + \nu\varepsilon_3\} \qquad (2.4.3a)$$

$$\sigma_2 = \mu\{\nu\varepsilon_1 + (1-\nu)\ \varepsilon_2 + \nu\varepsilon_3\} \qquad (2.4.3b)$$

$$\sigma_3 = \mu\{\nu\varepsilon_1 + \nu\varepsilon_2 + (1-\nu)\varepsilon_3\} \qquad (2.4.3c)$$

where $\mu = E/\{(1+\nu)(1-2\nu)\}$, ν is the Poisson's ratio, and ε_1, ε_2 and ε_3 are the principal strains. These give

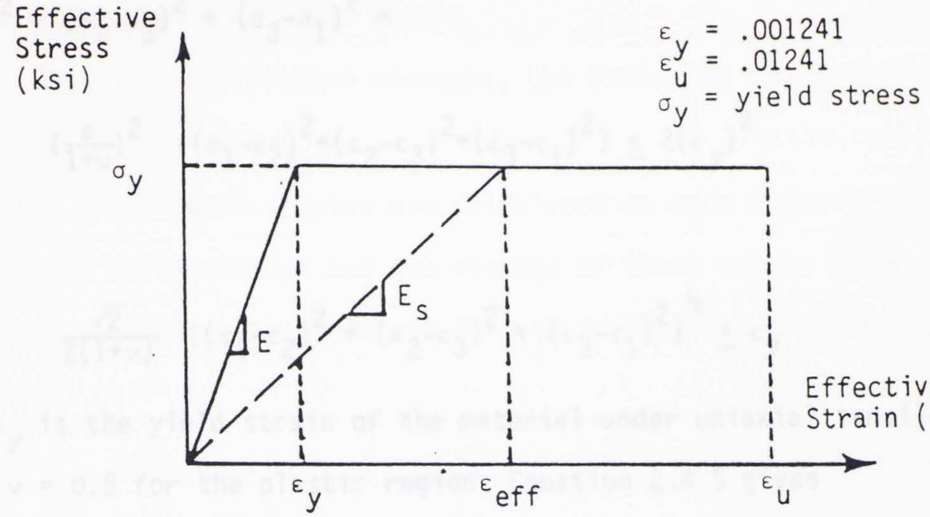

(a) Idealized Stress-Strain Diagram and Secant Modulus for End-Plate

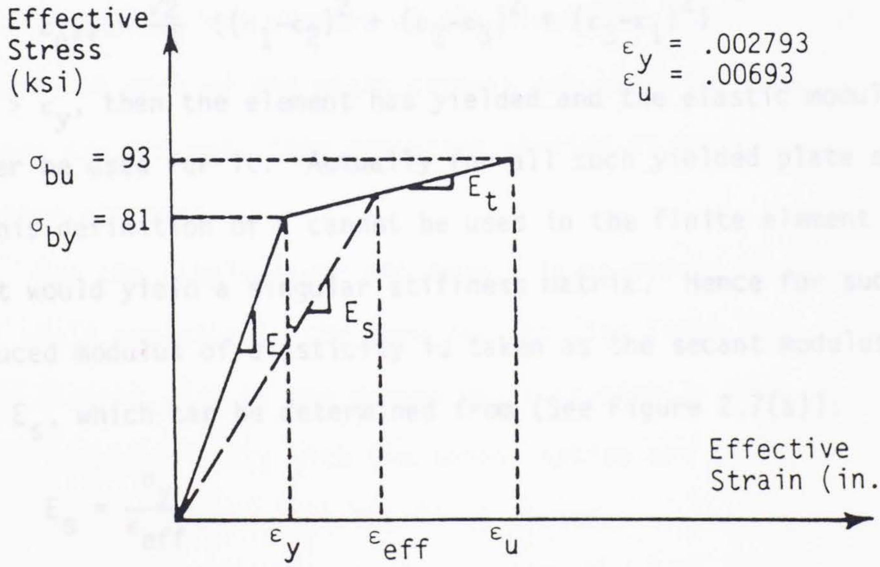

(b) Idealized Stress-Strain Diagram and Secant Modulus for A325 Bolt

Figure 2.7 Idealized Stress-Strain Curves Used

$$(\sigma_1-\sigma_2)^2 + (\sigma_2-\sigma_3)^2 + (\sigma_3-\sigma_1)^2 =$$

$$\{\frac{\varepsilon}{1+\nu}\}^2 \ \{(\varepsilon_1-\varepsilon_2)^2+(\varepsilon_2-\varepsilon_3)^2+(\varepsilon_3-\varepsilon_1)^2\} \leq 2(\varepsilon_y)^2 \tag{2.4.4}$$

or

$$\frac{\sqrt{2}}{2(1+\nu)} \ \{(\varepsilon_1-\varepsilon_2)^2 + (\varepsilon_2-\varepsilon_3)^2 + (\varepsilon_3-\varepsilon_1)^2\}^{\frac{1}{2}} \leq \varepsilon_y \tag{2.4.5}$$

where ε_y is the yield strain of the material under uniaxial tensile test. Taking $\nu = 0.5$ for the plastic region, Equation 2.4.5 gives

$$\frac{\sqrt{2}}{3} \ \{(\varepsilon_1-\varepsilon_2)^2 + (\varepsilon_2-\varepsilon_3)^2 + (\varepsilon_3-\varepsilon_1)^2\}^{\frac{1}{2}} \leq \varepsilon_y \tag{2.4.6}$$

Thus, the effective strain, ε_{eff} in any element of the end-plate is calculated in terms of the principal strains of the element, as follows:

$$\varepsilon_{eff} = \frac{\sqrt{2}}{3} \ \{(\varepsilon_1-\varepsilon_2)^2 + (\varepsilon_2-\varepsilon_3)^2 + (\varepsilon_3-\varepsilon_1)^2\}^{\frac{1}{2}} \tag{2.4.7}$$

If $\varepsilon_{eff} > \varepsilon_y$, then the element has yielded and the elastic modulus, E, can no longer be used for it. Actually for all such yielded plate elements, E=0. This definition of E cannot be used in the finite element method since it would yield a singular stiffness matrix. Hence for such elements, the reduced modulus of elasticity is taken as the secant modulus of elasticity, E_s, which can be determined from (See Figure 2.7(a)):

$$E_s = \frac{\sigma_y}{\varepsilon_{eff}} \tag{2.4.8}$$

In each cycle, the elastic moduli of the yielded elements (i.e., when $\varepsilon_{eff} > \varepsilon_y$) is reset to their secant values. This was the reason for not choosing the stress relation for the failure criterion, because for a yielded element ε_{eff} would have always been equal to ε_y and then secant modulus would always be equal to one.

To check for yielded elements, the following two options are considered:

1. Principal strains are calculated at each eight corner of each end-plate 3D solid element and the average of these values taken as ε_1, ε_2 and ε_3 for each respective element for use in Equation 2.4.7 to compute ε_{eff}.

2. Principal strains are calculated at the centroid of each end-plate element by finding the Jacobian of each solid element directly at the centroid from the shape functions of the eight corner nodes. Then, these principal strains are used for each respective element in Equation 2.4.7 to compute ε_{eff}.

The first option is reasonable if the strain stays more or less constant throughout the element or the element is small enough so that the strains at each of the eight corners are about the same. If these conditions are not met, then computing strains at the centroid seems to be a better approach.

For the single layer and double layer models studied here, both options yield essentially the same results (See Table 2.1). This shows that the element size of the meshes was sufficiently fine to check yielding. The computer costs with the second option are considerably less (about 30 percent) than with the first option.

2.4.2 Maximum Principal Strain Theory (St. Venant)

The results were also checked using the St. Venant failure criterion. Like the Von-Mises failure criterion the principal strains were used for determining yielding of the element. Based on St. Venant theory

Table 2.1
Comparison of Different Failure Criterion Including Layering Options

	Von-Mises Criterion				St. Venant Criterion	
	Single Layer		Double Layer		Single Layer	
F/F_{max}	δ_c/δ_r	δ_a/δ_r	δ_c/δ_r	δ_a/δ_r	δ_c/δ_r	δ_a/δ_r
0.09	1.00	0.99	0.96	0.94	1.00	0.99
0.36	1.00	1.00	1.03	1.02	1.00	1.00
0.64	1.00	1.00	1.03	1.03	1.01	1.00
0.91	1.00	0.99	1.11	1.11	1.13	1.12
1.00	1.00	0.99	-	-	1.15	1.15
F/F_{max}	σ_c/σ_r	σ_a/σ_r	σ_c/σ_r	σ_a/σ_r	σ_c/σ_r	σ_a/σ_r
0.09	1.00	0.99	1.18	1.18	1.00	0.99
0.36	1.00	0.99	1.19	1.17	1.00	0.99
0.64	1.00	0.99	1.22	1.20	1.01	1.00
0.91	1.00	0.98	1.22	1.19	1.02	1.00
1.00	1.00	0.98	-	-	1.02	1.00
F/F_{max}	τ_c/τ_r	τ_a/τ_r	τ_c/τ_r	τ_a/τ_r	τ_c/τ_r	τ_a/τ_r
0.09	1.00	1.00	1.00	1.00	1.00	1.00
0.36	1.00	0.99	1.01	1.01	1.00	0.99
0.64	1.00	1.01	0.97	0.98	0.98	0.98
0.91	1.00	1.01	0.86	0.88	0.90	0.91
1.00	1.00	1.02	-	-	0.91	0.93

Note - See nomenclature in Appendix A for definitions of terms the effective strain, ε_{eff}, at any point on the end-plate is approximately equal to the maximum of the three principal strains (ε_1, ε_2 and ε_3). The secant modulus of elasticity, E_s, of the yielded material is then determined from Equation 2.4.8. The rest of the procedure is the same as for the previous criterion.

The two options discussed in the previous Subsection were also considered for this failure criterion and the results obtained are very close to the results obtained by using the maximum Distortion Energy Theory (See Table 2.1).

Figure 2.8 shows the results of an experimental specimen (TH-1) analyzed by using both failure criteria to determine element yielding.

2.4.3 Selection of Failure Criterion

By comparing the results of both failure criterion it was found that both the Von-Mises and the St. Venant criterion for checking the yielding give about the same results. As will be shown subsequently, use of the Von-Mises criterion resulted in predictions closer to experimental values. Further, the criterion also used about 1 to 2 minutes less CPU computer time than when the St. Venant criterion was used. Thus, the Von-Mises criterion was selected for determining yielding in an element for all further calculations.

2.5 Finite Element Program

The complete finite element program was written in the FORTRAN language and implemented on the University of Oklahoma's IBM-380 Model D computer. The program is written specifically for the purpose of analyzing bolted end-plate connections considering non-linear material behavior and takes into account the pretension force applied to the bolts. It also

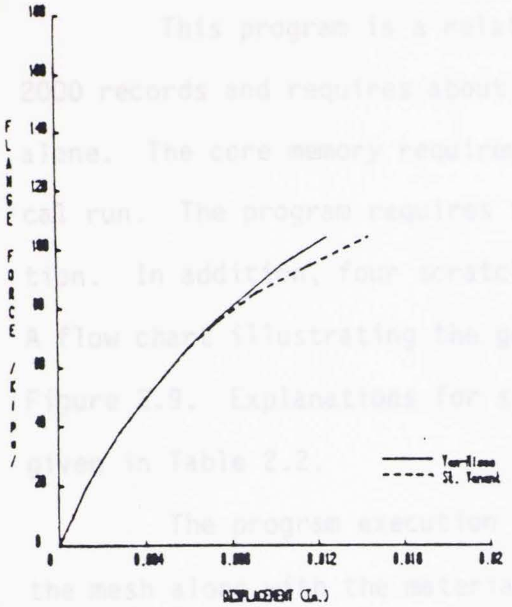

(a) Flange Force vs. Displacement

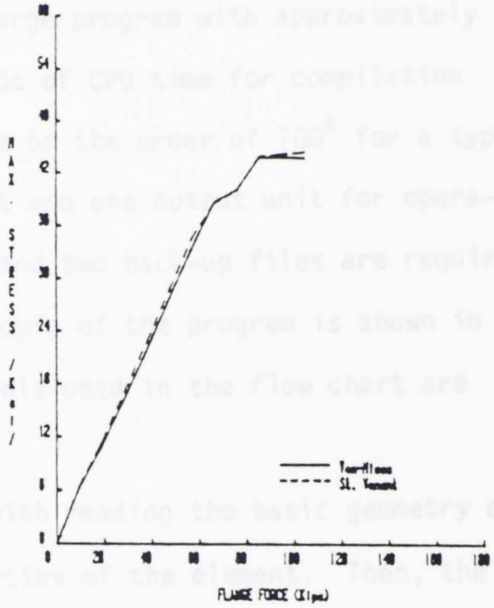

(b) Maximum Stress vs. Flange Force

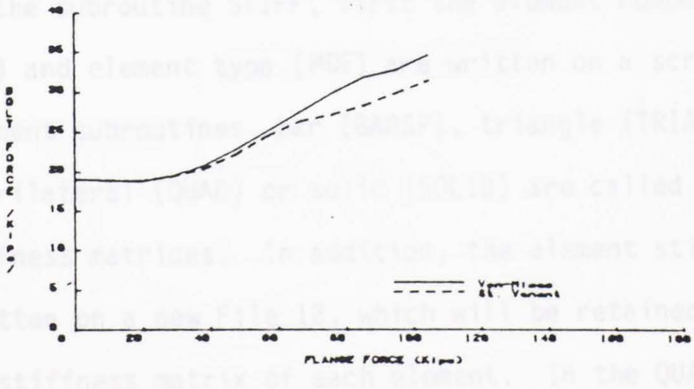

(c) Bolt Force vs. Flange Force

Figure 2.8 Comparison of Results using Different Failure Criteria considers the possibility of plate separation.

This program is a relatively large program with approximately 2000 records and requires about 8 seconds of CPU time for compilation alone. The core memory requirements are of the order of 700^k for a typical run. The program requires two input and one output unit for operation. In addition, four scratch files and two back-up files are required. A flow chart illustrating the general logic of the program is shown in Figure 2.9. Explanations for some symbols used in the flow chart are given in Table 2.2.

The program execution begins with reading the basic geometry of the mesh along with the material properties of the element. Then, the main program calls the pre-processor subroutine for generating node coordinates, element definitions and material properties of the elements. Data is processed and all the elements are identified with their appropriate boundary conditions. The main program then calls the subroutine STIFF to calculate the system stiffness matrix.

In the subroutine STIFF, first the element number (MM), d.o.f. numbers (MID) and element type (MDF) are written on a scratch File 9. Then the element subroutines, bar (BARSP), triangle (TRIAN), rectangle (RECT), quadrilateral (QUAD) or solid (SOLID) are called to calculate the element stiffness matrices. In addition, the element stiffness matrices are also written on a new File 12, which will be retained so as to store the elastic stiffness matrix of each element. In the QUAD subroutine, the displacement-stress transformation matrices (DB) of the 4 corner nodes of the element are also written on Files 9 and 12 before the element stiffness matrix is written. Similarly, in the SOLID subroutine, the displacement-

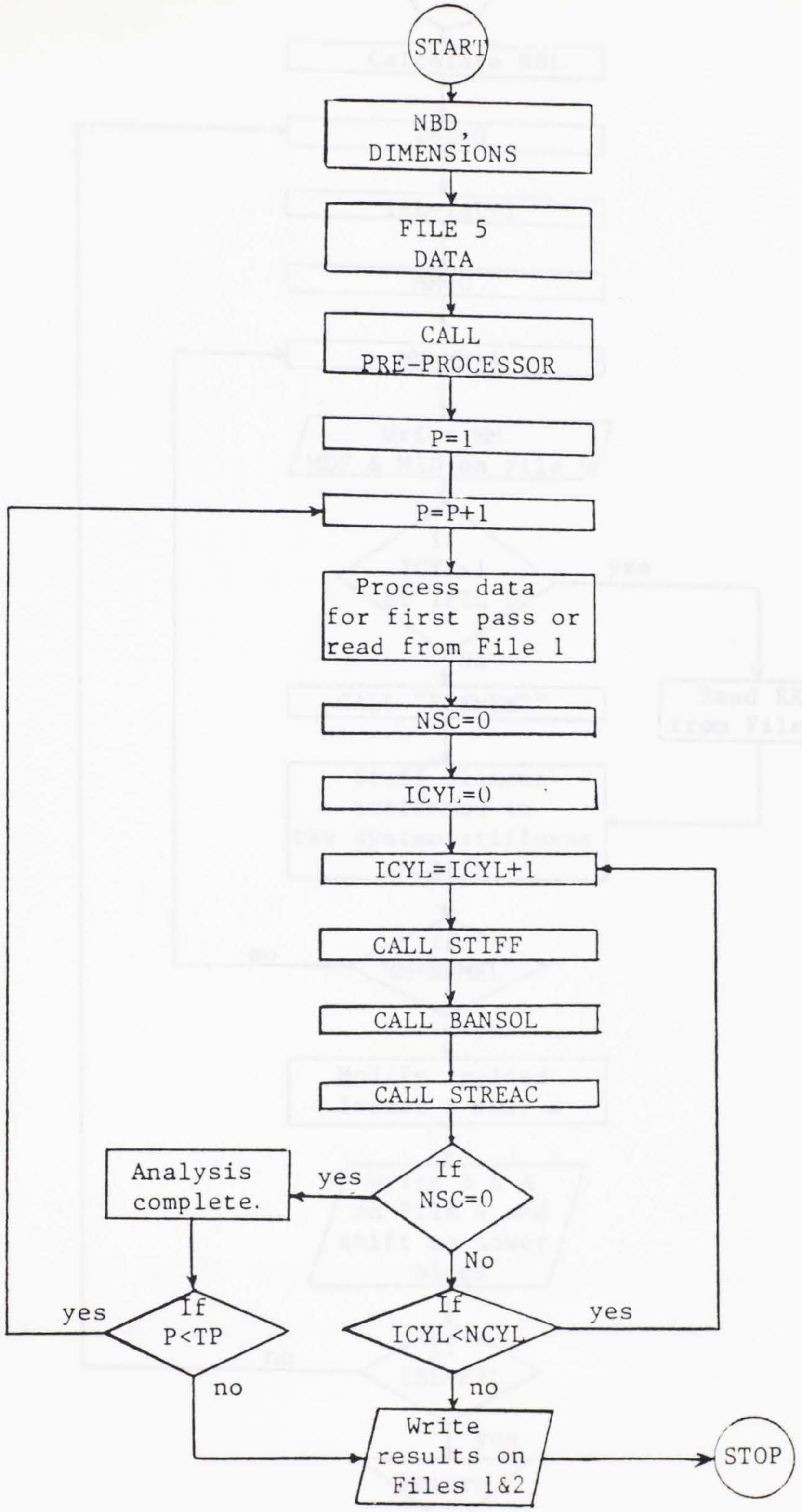

(a) MAIN Routine

Figure 2.9 Macro Flow Chart for Finite Element Program

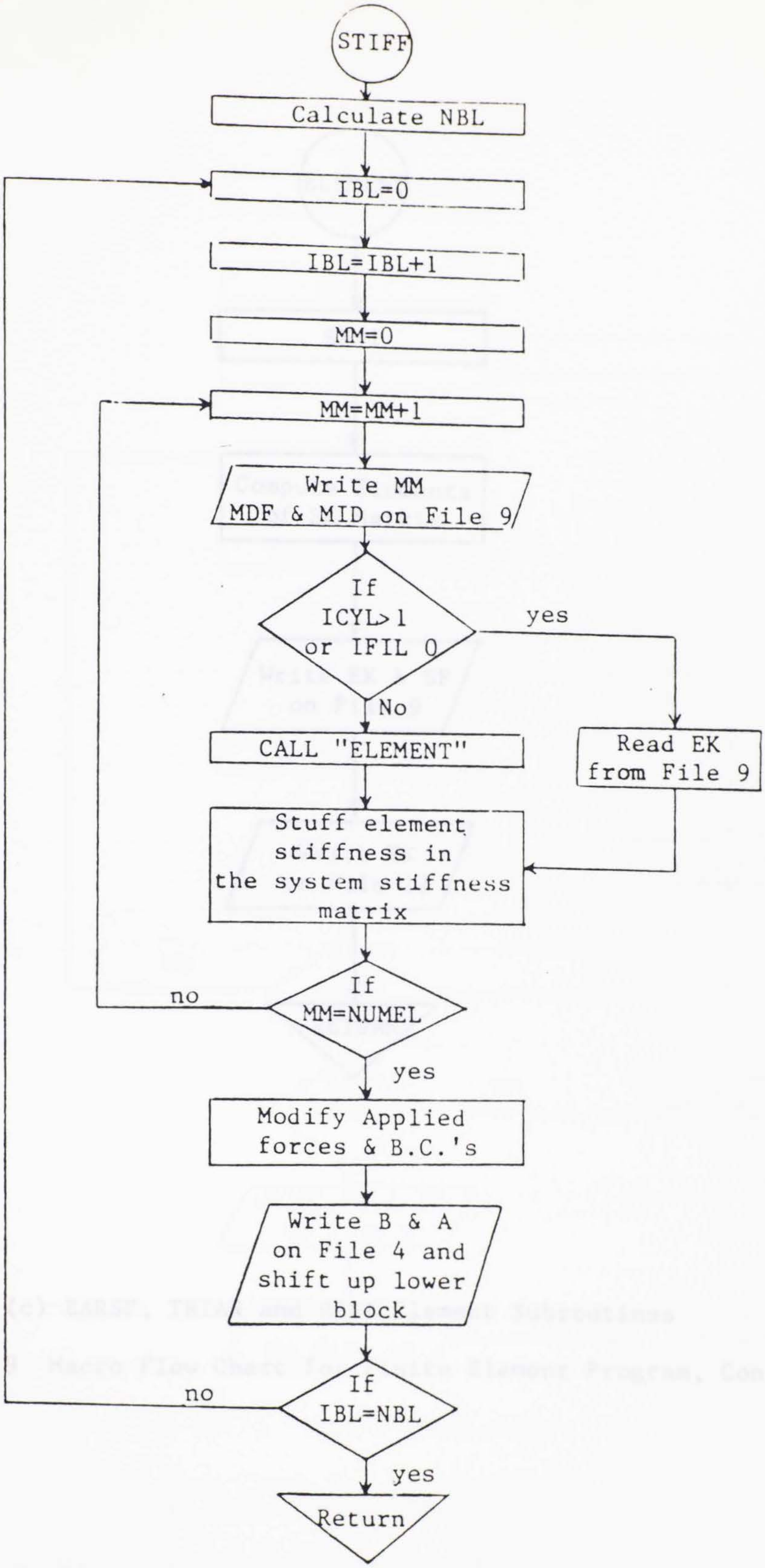

(b) STIFF Subroutine

Figure 2.9 Macro Flow Chart for Finite Element Program, Cont.

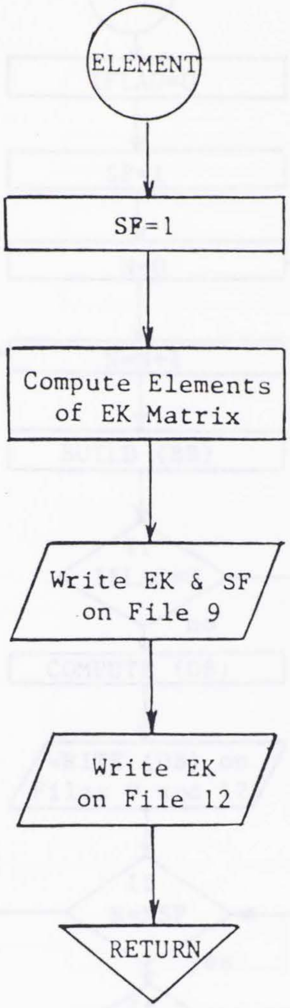

(c) BARSP, TRIAN and REST Element Subroutines

Figure 2.9 Macro Flow Chart for Finite Element Program, Cont.

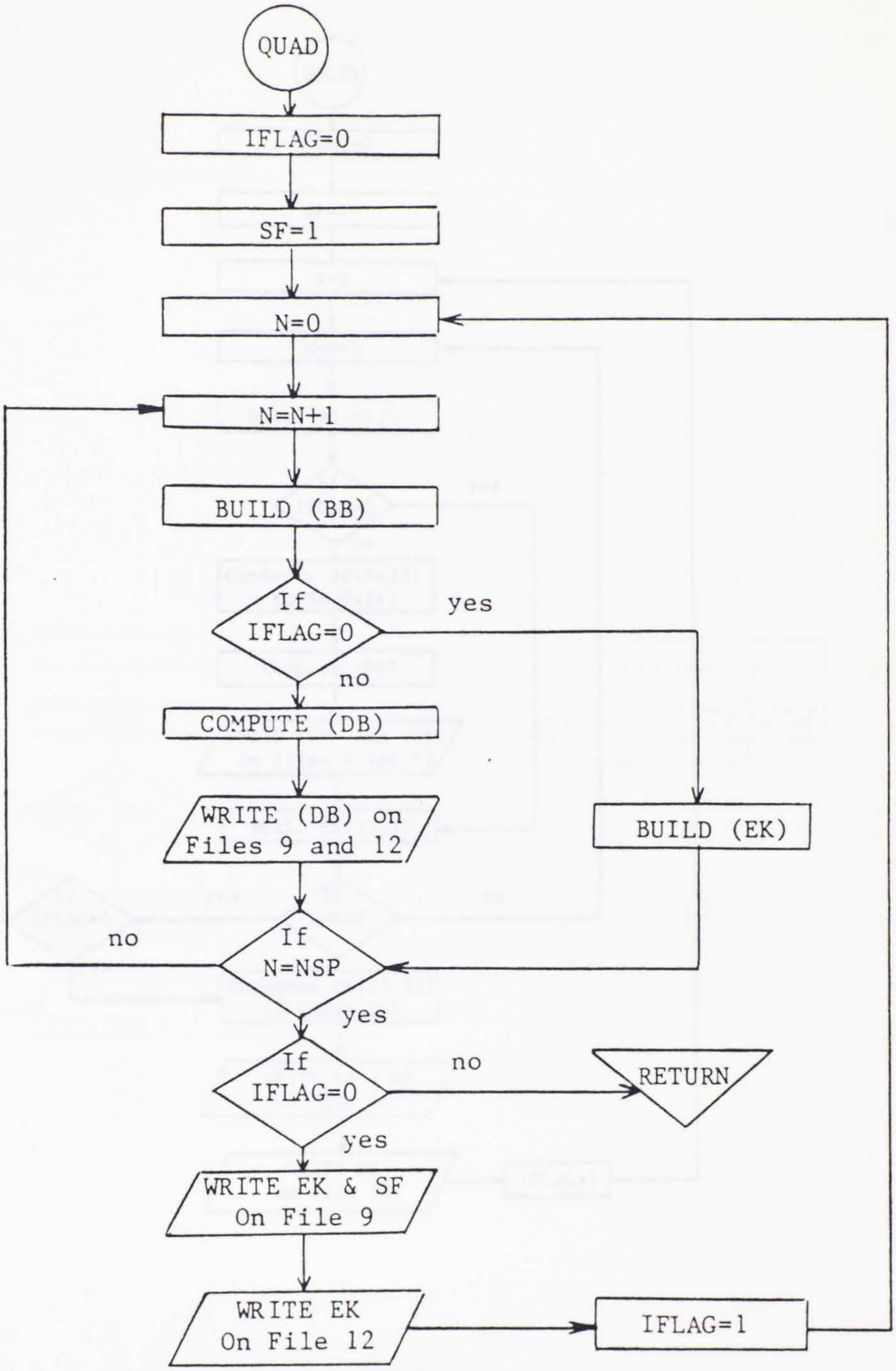

(d) QUAD Element Subroutine

Figure 2.9 Macro Flow Chart for Finite Element Program, Cont.

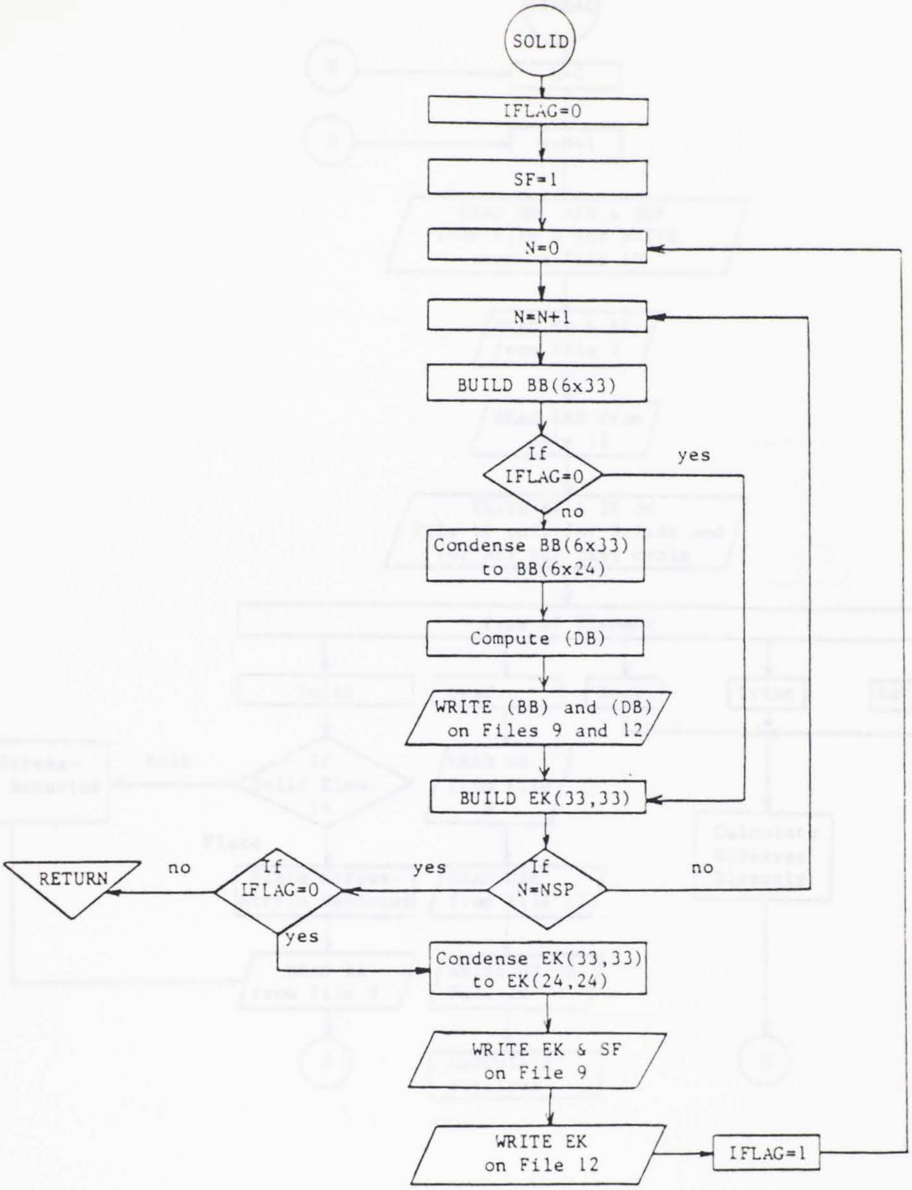

(e) SOLID Element Subroutine

Figure 2.9 Macro Flow Chart for Finite Element Program, Cont.

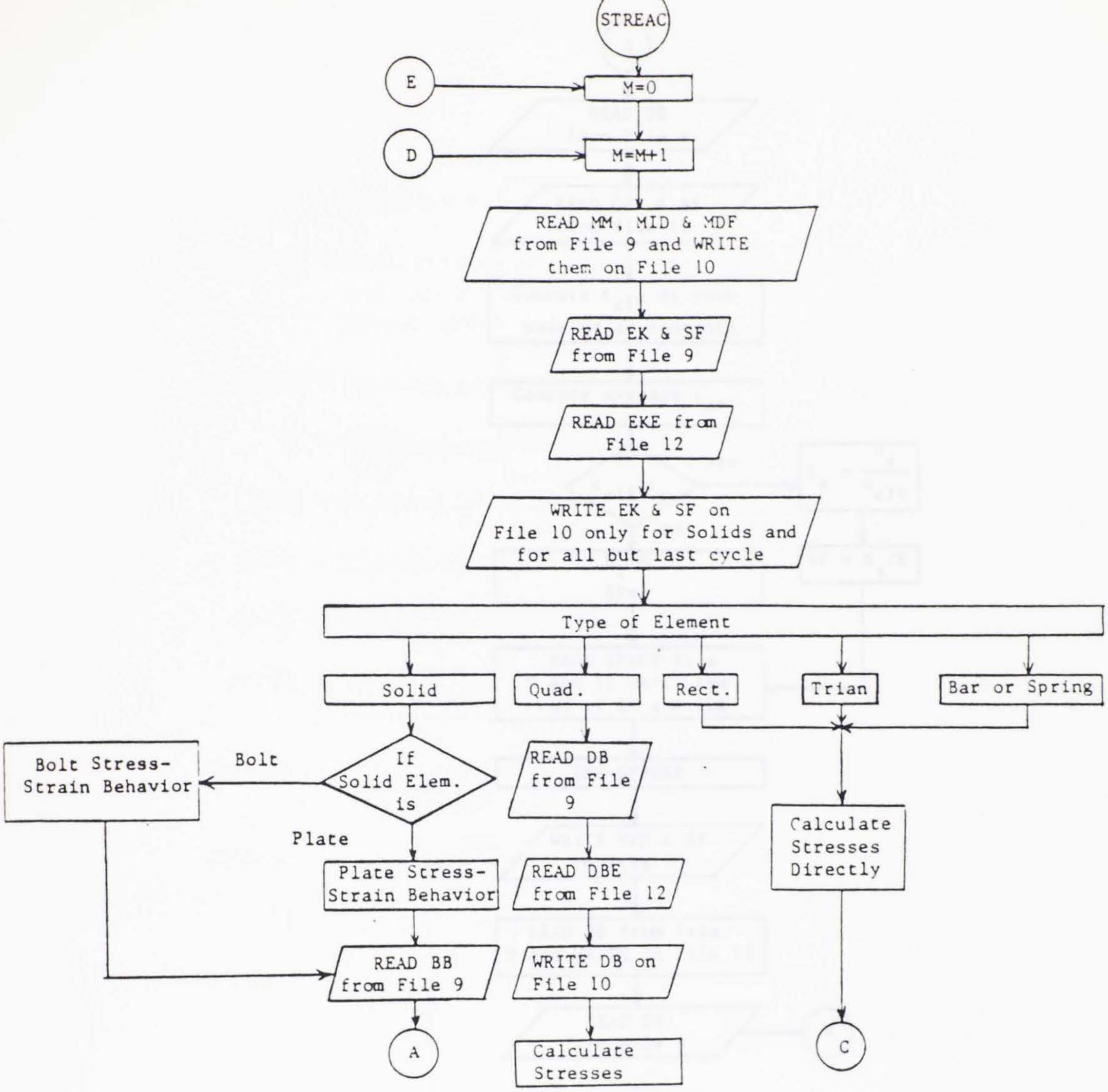

(f) STREAC Subroutine

Figure 2.9 Macro Flow Chart for Finite Element Program, Cont.

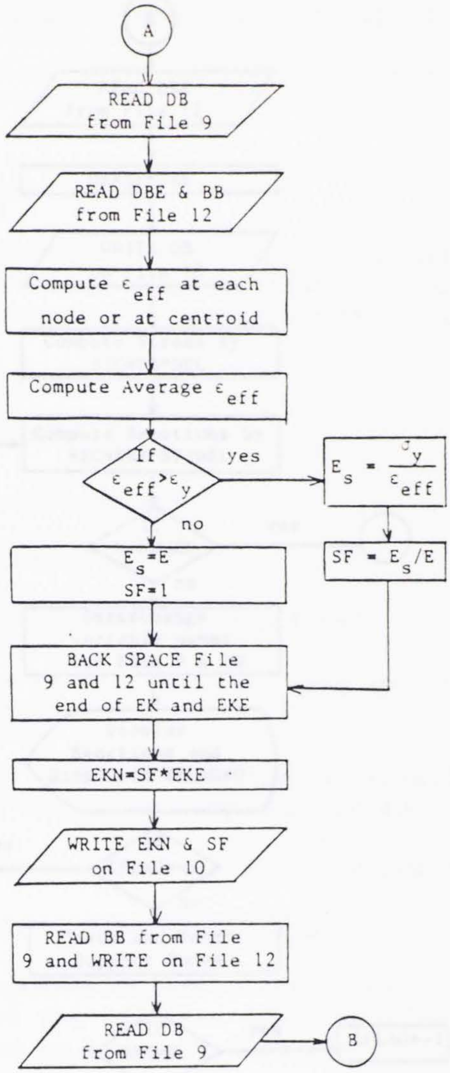

(f) STREAC Subroutine, Cont.

Figure 2.9 Macro Flow Chart for Finite Element Program, Cont.

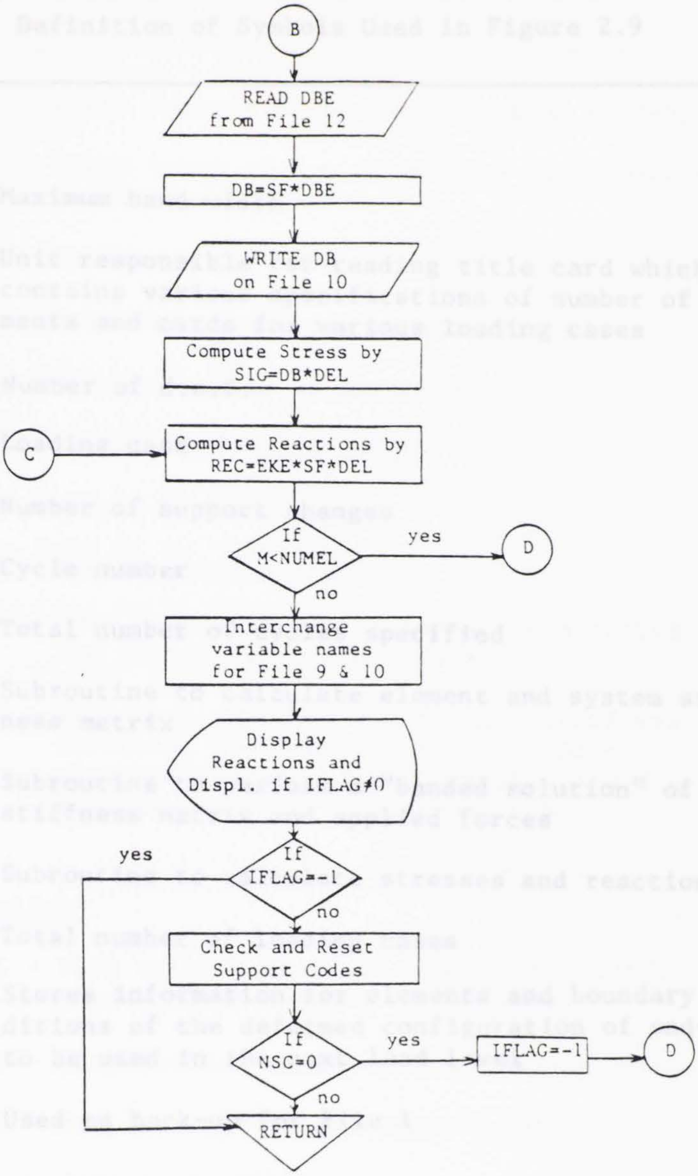

(f) STREAC Subroutine, Cont.

Figure 2.9 Macro Flow Chart for Finite Element Program, Cont.

Table 2.2 Definition of Symbols Used in Figure 2.9

(a) MAIN Routine

NBD	- Maximum band width
File 5	- Unit responsible for reading title card which also contains various specifications of number of elements and cards for various loading cases
NDOF	- Number of d.o.f.
P	- Loading case
NSC	- Number of support changes
ICYL	- Cycle number
NCYL	- Total number of cycles specified
STIFF	- Subroutine to calculate element and system stiffness matrix
BANSOL	- Subroutine to perform a "banded solution" of the stiffness matrix and applied forces
STREAC	- Subroutine to calculate stresses and reactions
TP	- Total number of loading cases
File 1	- Stores information for elements and boundary conditions of the deformed configuration of end-plate to be used in the next load level
File 2	- Used as back-up for File 1

(b) STIFF Subroutine

IBD	- Half of band-width
NBL	- Total number of blocks into which system stiffness matrix is divided
IBL	- Block number
MM	- Element number

Table 2.2 Definition of Symbols Used in Figure 2.9, Cont.

MDF	-	Total degrees of freedom for that element
MID	-	Keeps track of d.o.f. numbers associated with a particular element
ICYL	-	Cycle number
IFIL	-	Code for generating or using data
NUMEL	-	Maximum number of elements
EK	-	Element stiffness matrix
B	-	Boundary force vector
A	-	System stiffness matrix
File 4	-	Unit that contains boundary force vector and system stiffness matrix
File 9	-	Unit that contains the element stiffness matrices, modification factors, displacement-strain transformations and displacement-stress transformations.

(c) Element Subroutines

IFLAG	-	Flag to keep track of number of passes. Stress computations skipped in 1st pass
BB	-	Displacement-strain transformation
DB	-	Displacement-stress transformation
EK	-	Same as in STIFF
NSP	-	Number of corner nodes
DBE	-	Elastic displacement - stress transformation
EKE	-	Elastic element stiffness matrix
File 9	-	Same as in STIFF
File 12	-	Unit that contains the elastic element stiffness matrices and elastic displacement-stress transformation.

Table 2.2 Definition of Symbols Used in Figure 2.9, Cont.

(d) STREAC Subroutine

MID - Same as in STIFF

EK - Same as in STIFF

NUMEL - Same as in STIFF

MM - Same as in STIFF

NSC - Same as in MAIN

DB - Same as in "Element"

DBE - Same as in "Element"

BB - Same as in "Element"

NSC - Number of support changes

ε_{eff} - Effective strain

ε_y - Yield strain

σ_y - Yield stress

E - Modulus of elasticity

E_s - Modified modulus of elasticity

SF - Modification factor for element stiffness matrix

EKN - Modified element stiffness matrix

EKE - Same as in "Element"

SIG - Nodal stress

REC - Nodal reaction

DEL - Nodal deflection

File 9 - Same as in STIFF

Table 2.2 Definition of Symbols Used in Figure 2.9, Cont.

File 10 -	Temporary unit similar to File 9 except contains modified element stiffness matrices, updated modification factors and modified displacement-stress transformations
File 12 -	Same as in "Element"
IFLAG -	Flag to keep track of number of passes. Stress computations are for last pass

strain transformation matrices (BB) and the displacement-stress transformation matrices (DB) evaluated at the corner nodes (or at the centroid when a yield check is made at the centroid) of the element are also written on Files 9 and 12 before the element stiffness matrix is written.

After the element stiffness matrices have been obtained, they can be stuffed into the system stiffness matrix by using compatibility relationships between element nodes. Similarly, the load vector for each loaded element (concentrated nodal loads only are considered) is stuffed into the system load vector. The resulting stiffness matrix will be symmetric and banded and of size: total d.o.f. (NDOF) x half band-width (IBD). Thus it will contain (2*IBD-1) x NDOF non-zero elements. The economy of core storage can be achieved by storing only the NDOF x IBD portion of the system matrix, which is a rectangular matrix. But, since the end-plate model yields a large system of equations, even this method of storage is inadequate, and an alternative procedure had to be developed. This problem was solved in the subroutine STIFF by dividing the system stiffness matrix into many blocks and having two blocks in the computer core at a time, while the remaining portions are kept in the peripheral storage, in File 4. Thus, in the subroutine STIFF two blocks are used with the lower one being moved up as the upper one is read in from File 4. Determination of the block size and number of blocks is automated. The block size is computed as NBD-3*(maximum node difference + 1) and the number of blocks required to subdivide the system stiffness matrix is computed from NBL = 1+(NDOF-1)/NBD. In a "Do" loop for NBL, elements associated with the d.o.f. in a certain block are stored in that block. Also, modifications are made in the load vector for the changes made in the boundary conditions of the back nodes of the end-plate.

The main routine then calls the subroutine BANSOL to obtain the solution of the system stiffness equilibrium equation for nodal displacements. The modified Gauss elimination method is used for the solution of the banded equations, stored in blocks. Finally, the program calls the subroutine STREAC to calculate the stresses and reactions.

In the subroutine STREAC, the element number, d.o.f. numbers and element type are read from File 9 and are written on scratch File 10. Then, the strain-displacement matrices and stress-displacement matrices are read from File 9 and elastic stress-displacement matrices are read from File 12. Following these, the element stiffness matrix is read from File 9 and the elastic stiffness matrix is read from File 12. As mentioned in the previous Section, the element stiffness matrix of those elements whose effective strain exceeds the yield strain will have to be modified. The effective strain for each element is calculated using Equation 2.4.7, where principal strains are calculated (using strain-displacement matrices) first at each corner node and then average value used to check the yielding. In case of the yield check at the centroid, the effective strain is calculated directly at the centroid only. If an element is yielded, then the element stiffness matrix is adjusted by an appropriate scaling factor (SF) which is found from the following equation:

$$SF = \frac{E_s}{E} \qquad (2.5.1)$$

For a yielded element i, the new element stiffness matrix is then

$$(K)^i_{New} \quad = \quad SF\ (K)^i_{Elastic} \qquad (2.5.2)$$

From Equation 2.5.2, it can be seen that the elastic element stiffness matrices are needed to compute the modified element stiffness matrices in the non-linear analyses. This is the reason for the creation of scratch File 12. If an element is not yielded, then the program proceeds. The updated element stiffness matrix will then be written on File 10 for further computations. When an element is yielded, the stress-displacement matrices $(DB)^i$, also needs to be adjusted in the same manner as the element stiffness matrix, i.e.,

$$(DB)^i_{New} = SF\ (DB)^i_{Elastic} \tag{2.5.3}$$

The updated stress-displacement matrices and strain-displacement matrices are written on File 10. Finally, the stresses, $\{\sigma\}^i$, and reactions, $\{Rec\}^i$, for each element are calculated from the deflection vector, $\{\delta\}^i$, for the element, i.e., from

$$\{\sigma\}^i = (DB)^i_{New}\ \{\delta\}^i \tag{2.5.4}$$

$$\{Rec\}^i = (K)^i_{New}\ \{\delta\}^i \tag{2.5.5}$$

Thus, the new scratch File 10 has the updated information regarding the stiffness matrices and appropriate transformation matrices of the elements. At this stage, the variable names of Files 9 and 10 are interchanged for the next cycle. At this point, the new File 9 has the same information as the old File 10 (except for the modified matrices) and File 12 still has all the elastic element stiffness matrices and elastic stress-displacement matrices for further modifications and adjustments.

A typical analysis sequence is as follows: The pretension caused by bolt tightening is first applied as forces at the bolt-end nodes and displacements of the bolt nodes and the back of the end-plate are determined. The resulting bolt elongations and displacements are applied as specified displacements for the subsequent external loadings, thus simulating the bolt tightening process and the subsequent interaction with the other components. When the pretension load is first applied, the back of the end-plate is assumed to be in contact with the support, and the actual deformed shape is determined by an automatic trial and error procedure. At the end of each cycle analysis, the displacements and reactions of the nodes at the back of the end-plate are checked. Nodes tending to move away from the support are released; previously released nodes which moved into the support region are constrained. This process of analysis and checking support modifications is repeated until no changes occur.

The program stops automatically, when the scaling factor (SF) in any element is equal or less than 0.1.

2.6 Conclusions

To conduct the feasibility and sensitivity study and to develop the required prediction equations, analyses of a number of cases are needed. From the discussion in Section 2.2, it was concluded that the 2D-3D "hybrid" mesh with 137 elements, 236 nodes and 636 d.o.f. is suitable for the parametric study. It costs less than a more finer mesh model and gives about the same accuracy in results. From the discussion in Section 2.3, it was found that both the Von-Mises and the St. Venant criterion for determining element yielding give about the same results and the Von-Mises criterion was selected. It was also found that it is less expensive to calculate the principal strains at the centroid of the element and this method was adopted.

In summary the 2D-3D "hybrid" mesh of Figure 2.1 and the Von-Mises criterion with the principal strains calculated at the centroid of the element was used for all analyses of the parametric study.

CHAPTER III

PARAMETRIC STUDY

3.1 Introduction

A parametric study was conducted to determine the influence of various parameters on the behavior of eight bolt, stiffened end-plate connections. Parameters describing the geometry of the connection and the applied force were chosen as independent variables and the maximum displacement in the end-plate, maximum normal stress on the end-plate surface, and the axial force in the near bolts were taken as dependent variables. The finite element methodology described in the previous chapter was used to conduct the study.

In this Chapter, independent variables, dependent variables, selection of cases and development of the predicting equations for the dependent variables are presented. Independent and dependent variables are discussed in Sections 3.2 and 3.3, respectively. Selection of cases is explained in Section 3.4. Finally the development of the prediction equations is presented in Section 3.5.

3.2 Independent Variables

From limitations of time and resources, the number of variables to be independently varied in the parametric study was kept to a minimum. These pertinent geometric variables of the tee-hanger model were identified as follows (see Figure 3.1):

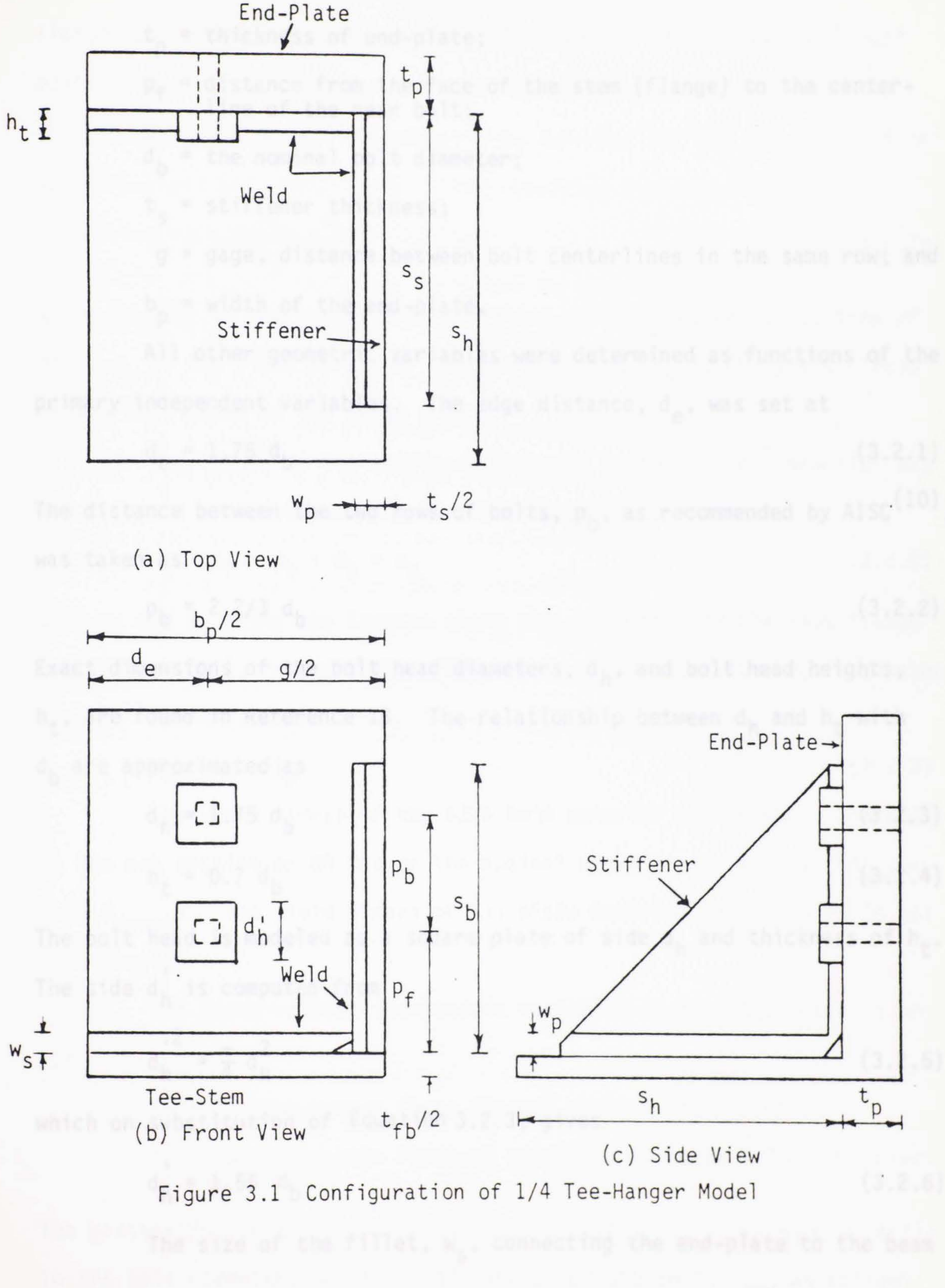

Figure 3.1 Configuration of 1/4 Tee-Hanger Model

t_p = thickness of end-plate;

p_f = distance from the face of the stem (flange) to the centerline of the near bolt;

d_b = the nominal bolt diameter;

t_s = stiffener thickness;

g = gage, distance between bolt centerlines in the same row; and

b_p = width of the end-plate.

All other geometric variables were determined as functions of the primary independent variables. The edge distance, d_e, was set at

$$d_e = 1.75\ d_b \tag{3.2.1}$$

The distance between the two rows of bolts, p_b, as recommended by AISC[10], was taken as

$$p_b = 2\ 2/3\ d_b \tag{3.2.2}$$

Exact dimensions of the bolt head diameters, d_h, and bolt head heights, h_t, are found in Reference 18. The relationship between d_h and h_t with d_b are approximated as

$$d_h = 1.75\ d_b \tag{3.2.3}$$

$$h_t = 0.7\ d_b \tag{3.2.4}$$

The bolt head is modeled as a square plate of side d_h' and thickness of h_t. The side d_h' is computed from

$$d_h'^2 = \frac{\pi}{4} d_h^2 \tag{3.2.5}$$

which on substitution of Equation 3.2.3, gives

$$d_h' = 1.55\ d_b \tag{3.2.6}$$

The size of the fillet, w_s, connecting the end-plate to the beam flange was computed to develop the yield capacity of the six equivalent bolts, i.e.,

$$2(w_s/\sqrt{2})\ b_p\ \sigma_y = 6A_b\ \sigma_{by} \tag{3.2.7a}$$

or

$$w_s = 3\sqrt{2}\left(\frac{A_b}{b_p}\right)\left(\frac{\sigma_{by}}{\sigma_y}\right) \tag{3.2.7b}$$

where $(w_s/\sqrt{2})$ is the throat size of fillet weld, A_b is the gross area of bolt, σ_y is the yield stress of the tee-stem and σ_{by} is the yield stress of the bolt based on the gross area.

The length of the stiffener (assumed to be of a 45^o profile) was set so as to extend beyond the far bolt location, as follows:

$$s_b = p_f + p_b + d_b = s_s \tag{3.2.8}$$

with s_b and s_s being the lengths along the end-plate and the beam flange (see Figure 3.1), respectively. The length of the tee-stem, s_h, was taken as (see Figure 3.1(a))

$$s_h = s_s + t_p \tag{3.2.9}$$

The yield stress of the A325 bolt material was taken as 118 ksi on the net section or 88 ksi on the nominal diameter of the bolt ($A_{net} \approx 0.75\ A_{gross}$). The yield stress of all plate material was taken as 36 ksi (A36 steel).

The force related independent variables in the study were taken as:

F = the tee-hanger (beam flange) applied force, and

P_t = the pretension force as specified in Table 1.23.5 of Reference 10.

The pretension force, P_t, could be omitted because it is related directly to the bolt diameter, d_b, and yield stress of the bolt, σ_{by}, as follows:

$$P_t \approx 0.7(\frac{\pi}{4}\, d_b^2)\ \sigma_{by} \qquad (3.2.10)$$

The six independent geometric variables were reduced to five dimensionless parameters. The normalizing variable for the geometric related parameters was chosen as b_p. The resulting dimensionless parameters associated with the geometry are then:

$\pi_1 = t_p/b_p$, the plate thickness parameter (3.2.11a)

$\pi_2 = p_f/b_p$, the bolt pitch parameter (3.2.11b)

$\pi_3 = d_b/b_p$, the bolt diameter parameter (3.2.11c)

$\pi_4 = t_s/b_p$, the stiffener thickness parameter (3.2.11d)

$\pi_5 = g/b_p$, the bolt gage parameter (3.2.11e)

The force related parameter is not nondimensionalized and is chosen as

$\psi_6 = F$, the force parameter (force units) (3.2.11f)

After numerous attempts, it was found that two more parameters were needed to improve the results of the predicting equations, (refer to Appendix B). These were chosen as the bending parameters in the two directions (1/length units), as follows:

$$\psi_7 = \frac{p_e^3}{b_p\ t_p^3} \qquad (3.2.12a)$$

$$\psi_8 = \frac{g_e^3}{p_f\ t_p^3} \qquad (3.2.12b)$$

where p_e, the effective bolt pitch, and g_e, the effective bolt gage, are found from the following equations:

$$p_e = p_f - (d_b/4) - w_s \qquad (3.2.13a)$$

and

$$g_e = g/2 - (d_b/4) - (t_s/4) \qquad (3.2.13b)$$

3.3 Dependent Variables

Three quantities of primary concern are the maximum deflection of the end-plate, maximum bending stress in the end-plate and the maximum bolt force. From previous studies on tee-stubs[12], it was found that the maximum deflection, δ_x, occurred at the back of the tee-stub along the stem centerline, and that the critical stress was the plate bending stress, σ_b, also occurring at the same location. The change of axial force, T_n, in the near bolt as the flange force is increased is also of primary interest. Hence, five dependent parameters were chosen as follows:

1) The parameter, ψ_a, for maximum deflection δ_x was defined as,

$$\psi_a = (\delta_x)_{max} \tag{3.3.1}$$

2) The parameter, ψ_{by}, for maximum stress σ in the y-direction was chosen as,

$$\psi_{by} = (\sigma_y)_{max} \tag{3.3.2}$$

3) The parameter, ψ_{bx}, for maximum stress σ in the x-direction was chosen as,

$$\psi_{bx} = (\sigma_x)_{max} \tag{3.3.3}$$

4) The parameter, ψ_{c1}, for the near bolt force T_n was defined as,

$$\psi_{c1} = T_n \tag{3.3.4}$$

5) And the parameter, ψ_{c2}, for the modified near bolt force T_{nm} (discussed in Chapter IV, Section 4.4) was defined as,

$$\psi_{c2} = T_{nm} \tag{3.3.5}$$

3.4 Cases Considered for Analysis

The parametric study was limited to practical ranges of the various geometric and force parameters. It is important in any moment resisting connection that the first failure not occur in the bolts, since if this occurs the nature of the collapse is sudden. Thus, bolt size sets an upper limit on the area of the beam flange. Unless the end-plate is very stiff, assuming that the far row of bolts contributes the same as the inner row may be unconservative. Therefore, as a starting point, it was assumed that the outer row of bolts contributes only half as much as the inner row or an equivalent of only six bolts is available to develop the beam flange force. The corresponding tee-stem or beam flange area limits for various bolt diameters are shown in Table 3.1. A maximum bolt diameter of 1½ in. was considered in the study.

To establish limits for the parametric study, ranges of the various geometric parameters were established based on usual detailing practice and are shown in Table 3.2. Also, a limitation was placed on the combination of bolt size and end-plate thickness (Table 3.3). The distances between bolt rows used in the study are tabulated in Table 3.3. Based on the ranges given in Tables 3.1 through 3.3, the first five independent geometric parameters (π-terms) are assigned "Low" (L), "Intermediate" (I) and "High" (H) values as shown in Table 3.4.

The parametric study is organized into four categories based on the plate thickness parameter (π_1):

1) Low values of π_1
2) Intermediate values of π_1
3) High values of π_1
4) Special values of π_1

Table 3.1 Flange Area (A36) to Develop Bolts (A325)-8 Bolt Stiffened Connection

Bolt Dia. (in.)	5/8	3/4	7/8	1	1 1/8	1 1/4	1 3/8	1 1/2
P_{bolt} (kips)	13.5	19.4	26.5	34.6	43.7	54.0	65.3	77.7
6 P_{bolt} (kips)	81.0	116.4	159.0	207.6	262.2	324.0	391.8	466.2
A_{flg} (in.^{2})	3.375	4.850	6.625	8.650	10.925	13.500	16.325	19.425

Notes:
1. A325 bolts and A36 steel
2. F_b = 24ksi
3. Inside:Outside bolt force = 1:0.5
4. $A_{flg} = 6\ P_{bolt}/24$

Table 3.2 Practical Ranges for Various Geometric Parameters

Parameter	Low	Intermediate	High
t_p	1/2"	1 3/4"	3"
p_f	1 1/8"	1 3/4"	2 1/2"
d_b	5/8"	1"	1 1/2"
t_s	5/16"	1/2"	1"
g	3 1/2"	5 1/2"	7 1/2"
b_p	6"	10"	16"

Table 3.3 Practical Ranges for End Plate Thickness Corresponding to Various Bolt Diameters

Bolt Diameter d_b (in.)	Minimum t_p (in.)	Maximum t_p (in.)	Minimum Distance Between Bolts, $p_b = 2\ 2/3\, d_b$ (in.)
5/8	1/2	1 1/4	1 2/3
3/4	1/2	1 1/2	2
7/8	5/8	1 3/4	2 1/3
1	5/8	2	2 2/3
1 1/8	3/4	2 1/4	3
1 1/4	1	2 1/2	3 1/3
1 1/2	1	3	4

Table 3.4
Range of Geometric Dimensionless Variables

π	Definition	Low		Intermediate		High		Special		Extreme	
		π	section (b_p)	π	section (b_p)	π	section (b_p)	π	section (b_p)	π	section (b_p)
π_1	t_p/b_p	0.0622	W12x45 (8.045")	0.1747	W27x102 (10.015")	0.2880	W10x112 (10.415")	0.1905	W33x152 (15.745")	0.0861	W10x30 (5.810")
π_2	p_f/b_p	0.1611	W16x36 (6.985")	0.2078	W21x93 (8.420")	0.2400	W10x112 (10.415")	0.1588	W33x152 (15.745")	0.1936	W10x30 (5.810")
π_3	d_b/b_p	0.0895	W16x36 (6.985")	0.1168	W21x93 (8.420")	0.1440	W10x112 (10.415")	0.0953	W33x152 (15.745")	0.1076	W10x30 (5.810")
π_4	t_s/b_p	0.0358	W16x36 (6.985")	0.0411	W12x96 (12.160")	0.0801	W12x152 (12.480")	0.0635	W33x152 (15.745")	0.0430	W10x30 (5.810")
π_5	g/b_p	0.4950	W16x50 (7.070")	0.5342	W16x77 (10.295")	0.5789	W24x162 (12.955")	0.4763	W33x152 (15.745")	0.6024	W10x30 (5.810")

In each category, the value of π_1 is held constant and the values of π_2 through π_5 are varied through low, intermediate and high levels one at a time. Thus, thirty-six cases are generated and are tabulated in Tables 3.5 through 3.7. Four additional cases are formulated using lowest and maximum practical values of the flange width and are tabulted in Table 3.8 as "Extreme" (E) and "Special" (S) cases, respectively. A summary of the cases considered is shown in Figure 3.2. (This Figure also shows the distribution of the data used for the regression analysis).

From Tables 3.5 through 3.8, it can be seen that the total number of cases to be analyzed are forty. Of those forty cases, six cases are not practically feasible, as they did not comply with the limitations of Tables 3.1 through 3.3, and were removed from the study. Nine pairs of cases are identical and were not reanalyzed. Finite element analyses were made for the remaining twenty-five cases.

Maximum deflection $(\delta_x)_{max}$ at the back of the plate on the outside surface, maximum bending stress in the y-direction $(\delta_y)_{max}$ maximum bending stress in the x-direction $(\delta_x)_{max}$, near bolt force (T_n) and modified near bolt force (T_{nm}) were obtained from the finite element analyses results for the twenty-five cases. Data from the various analyses is found in Appendix C.

3.5 Predicting Equations

The Computer Package SPSS[19] was used to develop the predicting equations for the deflection parameter, ψ_a; the maximum bending stress parameter in the y-direction, ψ_{by}; the maximum bending stress parameter in the x-direction, ψ_{bx}; the near bolt force parameter, ψ_{c1}; and the modified near bolt force parameter, ψ_{c2}. The predicting equations were sought

Table 3.5
Cases Chosen for Parametric Study (Low Values of π_1)

Case	π Values π_1 π_2 π_3 π_4 π_5	π_1 (t_p)	π_2 (p_f)	π_3 (d_b)	π_4 (t_s)	π_5 (g)	b_p (in)	Description
L1	L L L I L	0.0622 (0.4665")	0.1611 (1.2083")	0.0895 (0.6713")	0.0411 (0.3083")	0.4950 (3.7125")	7.5	
L2	L I L I L	"	0.2078 (1.5585")	"	"	"	"	Effects of p_f on t_p
L3	L H L I L	"	0.2400 (1.8000")	"	"	"	"	
L4*	L H L I L	"	0.2400 (1.8000")	0.0895 (0.6713")	"	"	"	
L5	L H I I L	"	"	0.1168 (0.876")	"	"	"	Effects of d_b on t_p
L6	L H H I L	"	"	0.1440 (1.080")	"	"	"	
L7	L I L L L	"	"	0.0895 (0.6713")	0.0358 (0.2684")	"	"	
L8*	L I L I L	"	"	"	0.0411 (0.0308")	"	"	Effects of t_s on t_p
L9	L I L H L	"	"	"	0.0801 (0.6008")	"	"	
L10*	L I L I L	"	"	"	0.0411 (0.3083")	0.4950 (3.7125")	"	
L11	L I L I I	"	"	"	"	0.5342 (4.0065")	"	Effects of g on t_p
L12	L I L I H	"	"	"	"	0.5789 (4.3418")	"	

* Repetitive Cases
L = low, I = intermediate, H = high

Table 3.6
Cases Chosen for Parametric Study (Intermediate Values of π_1)

Case	π Values π_1 π_2 π_3 π_4 π_5	π_1 (t_p)	π_2 (p_f)	π_3 (d_b)	π_4 (t_s)	π_5 (g)	b_p (in)	Description
I1	I L I I I	0.1747 (1.7473")	0.1611 (1.6110")	0.1168 (1.1680")	0.0411 (1.4110")	0.5342 (5.3420")	10.0	
I2	I I I I I	"	0.2078 (2.0780")	"	"	"	"	Effect of p_f on t_p
I3**	I H I I I	"	0.2400 (2.4000")	"	"	"	"	
I4**	I I L I I	"	0.2078 (2.0780")	0.0895 (0.8950")	"	"	"	
I5*	I I I I I	"	"	0.1168 (1.1680")	"	"	"	Effect of d_b on t_p
I6	I I H I I	"	"	0.1440 (1.4400")	"	"	"	
I7	I I I L I	"	"	0.1168 (1.1680")	0.0358 (0.3579")	"	"	
I8*	I I I I I	"	"	"	0.0411 (0.4110")	"	"	Effect of t_s on t_p
I9	I I I H I	"	"	"	0.0801 (0.8010")	"	"	
I10	I I I I L	"	"	"	0.0411 (0.4110")	0.4950 (4.9500")	"	
I11*	I I I I I	"	"	"	"	0.5342 (5.3420")	"	Effect of g on t_p
I12	I I I I H	"	"	"	"	0.5789 (5.7890")	"	

* Repetitive Cases
** Impractical Cases

L = low, I = intermediate, H = high

Table 3.7
Cases Chosen for Parametric Study (High Values of π_1)

Case	π Values π_1 π_2 π_3 π_4 π_5	π_1 (t_p)	π_2 (p_f)	π_3 (d_b)	π_4 (t_s)	π_5 (g)	b_p (in)	Description
H1**	H L H H H	0.288 (2.8805")	0.1611 (1.6110")	0.1440 (1.4400")	0.0801 (0.8010")	0.5789 (5.789")	10.0 "	
H2	H I H H H	"	0.2078 (2.0780")	"	"	"	"	Effect of p_f on t_p
H3	H H H H H	"	0.2400 (2.4000")	"	"	"	"	
H4**	H H L H H	"	0.2400 (2.4000")	0.0895 (0.8950")			"	
H5	H H I H H	"	"	0.1168 (1.1680")	"	"	"	Effect of d_b on t_p
H6*	H H H H H	"		0.1440 (1.4400")		"	"	
H7	H H H L H	"	"	0.1440 (1.4400")	0.0358 (0.3579")	"	"	
H8	H H H I H	"	"	"	0.0411 (0.4110")	"	"	Effect of t_s on t_p
H9*	H H H H H	"	"	"	0.0801 (0.8010")	"	"	
H10	H H H H L	"	"	"	0.0801 (0.8010")	0.4950 (4.9500")	"	
H11	H H H H I	"	"	"	"	0.5342 (5.3420")	"	Effect of g on t_p
H12*	H H H H H	"	"	"	"	0.5789 (5.7890")	"	

* Repetitive Cases
** Impractical Cases

L = low, I = intermediate, H = high

Table 3.8

Cases Chosen for Parametric Study (Special Cases)

Case	π Values π_1 π_2 π_3 π_4 π_5	π_1 (t_p)	π_2 (p_f)	π_3 (d_b)	π_4 (t_s)	π_5 (g)	Section (b_p)	Description
S1	S S S S S	0.1908 (3.0051")	0.1588 (2.5011")	0.0953 (1.5010)	0.0635 (1.0001")	0.4763 (7.5017")	15.75	special case
S2**	H S S S S	0.2400 (3.78")	"	"	"	"	"	highest b_p
E1	E E E E E	0.0861 (0.4951")	0.1936 (1.1132")	0.1076 (0.6187)	0.043 (0.2474)	0.6024 (3.4638)	5.75	Extreme case
E2**	L E E E E	0.0622 (0.3577")	"	"	"	"	"	lowest b_p

* Repetitive Cases

** Impractical Cases

L = low, I = intermediate, H = high, S = special, E = extreme

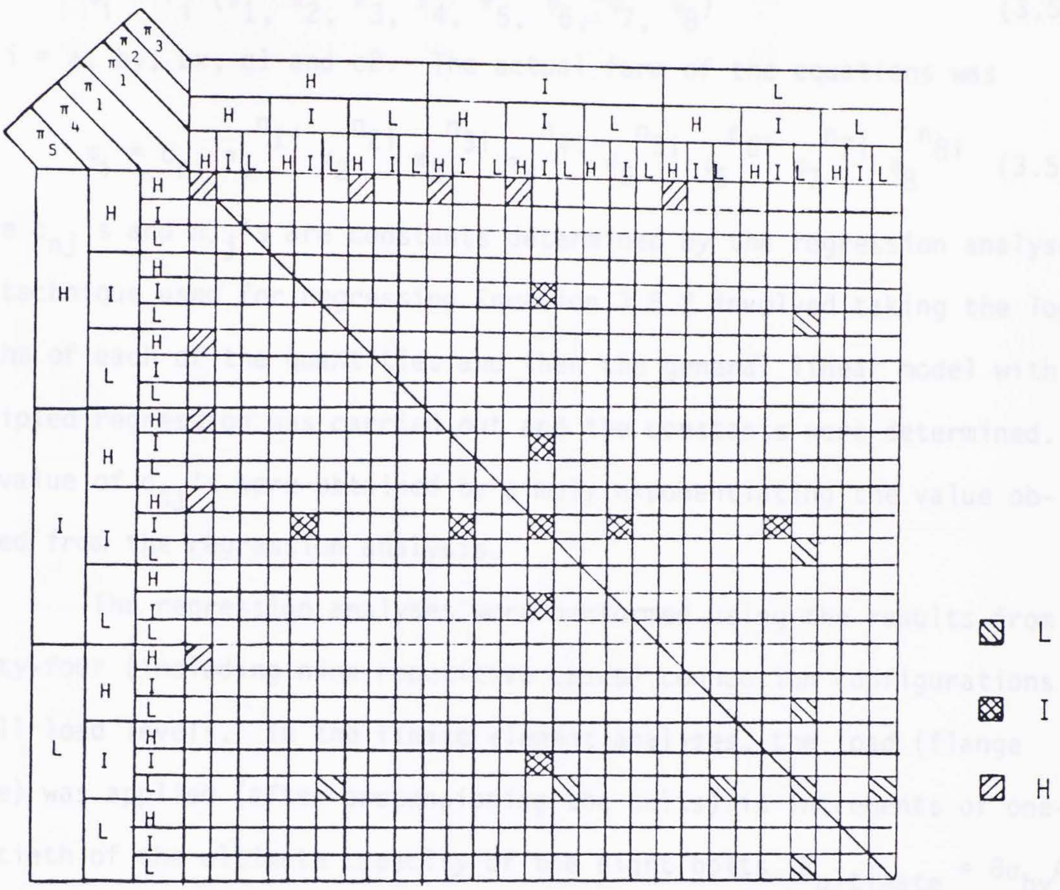

Figure 3.2 Distribution of Cases Selected for Parametric Study

in the following general relationship

$$\psi_i = f_i\ (\pi_1,\ \pi_2,\ \pi_3,\ \pi_4,\ \pi_5,\ \psi_6,\ \psi_7,\ \psi_8) \tag{3.5.1}$$

for i = a, by, bx, c1 and c2. The actual form of the equations was

$$\psi_i = c_{ni}\ \pi_1^{n_{1i}}\ \pi_2^{n_{2i}}\ \pi_3^{n_{3i}}\ \pi_4^{n_{4i}}\ \pi_5^{n_{5i}}\ \psi_6^{n_{6i}}\ \psi_7^{n_{7i}}\ \psi_8^{n_{8i}} \tag{3.5.2}$$

where c_{nj}'s and n_{ij}'s are constants determined by the regression analyses. The technique used for regressing Equation 3.5.2 involved taking the logarithm of each of the quantities and then the general linear model with multipled regression was carried out and the constants were determined. The value of c_{nj}'s were obtained by simply exponentiating the value obtained from the regression analysis.

The regression analyses were performed using the results from thirty-four (including nine repetitive cases) connection configurations at all load levels. In the finite element analyses, the load (flange force) was applied (after pretensioning the bolts) in increments of one-twentieth of the ultimate capacity of the eight bolts ($F_{ultimate} = 8\sigma_{by}A_b$), until failure occurred. Connection failure, as defined in Section 2.5 of Chapter II, was taken when the ratio of the secant modulus and the elastic modulus of the plate material is equal to or less than 0.1 or when the bolt strain reaches the ultimate value, $\varepsilon_u = 0.00693$. It was assumed that end-plate deflections at zero load (pretension only) were zero.

The best fit equations that were found are given in Figure 3.3. The corresponding values of R^2 are indicated in Table 3.9, the closer R^2 is to unity the better correlation between the predicted and observed values. Also, the maximum unconservative error and the maximum conservative error for the five regression Equations 3.5.3 through 3.5.7 are tabulated in Table 3.9. Figures 3.4 through 3.8 present the comparison of

$$\psi_a = (\delta_x)_{max} = (1.04\times10^{-5})\left(\frac{t_p}{b_p}\right)^{1.460}\left(\frac{p_f}{b_p}\right)^{0.143}\left(\frac{d_b}{b_p}\right)^{-0.053}\left(\frac{t_s}{b_p}\right)^{-0.096}\left(\frac{g}{b_p}\right)^{-2.767}\left(\frac{p_e^{3}}{b_p t_p^{3}}\right)^{0.227}\left(\frac{g_e^{3}}{p_f t_p^{3}}\right)^{0.805}(F)^{1.364} \qquad (3.5.3)$$

$$\psi_{by} = (\sigma_y)_{max} = (27.964)\left(\frac{t_p}{b_p}\right)^{2.124}\left(\frac{p_f}{b_p}\right)^{1.224}\left(\frac{d_b}{b_p}\right)^{0.596}\left(\frac{t_s}{b_p}\right)^{0.045}\left(\frac{g}{b_p}\right)^{-3.76}\left(\frac{p_e^{3}}{b_p t_p^{3}}\right)^{0.062}\left(\frac{g_e^{3}}{p_f t_p^{3}}\right)^{1.030}(F)^{0.800} \qquad (3.5.4)$$

$$\psi_{bx} = (\sigma_x)_{max} = (167.688)\left(\frac{t_p}{b_p}\right)^{4.737}\left(\frac{p_f}{b_p}\right)^{3.154}\left(\frac{d_b}{b_p}\right)^{0.161}\left(\frac{t_s}{b_p}\right)^{0.290}\left(\frac{g}{b_p}\right)^{-8.189}\left(\frac{p_e^{3}}{b_p t_p^{3}}\right)^{-0.084}\left(\frac{g_e^{3}}{p_f t_p^{3}}\right)^{2.056}(F)^{1.260} \qquad (3.5.5)$$

$$\psi_{c1} = T_n = (.0781)\left(\frac{t_p}{b_p}\right)^{-4.606}\left(\frac{p_f}{b_p}\right)^{-1.810}\left(\frac{d_b}{b_p}\right)^{1.116}\left(\frac{t_s}{b_p}\right)^{-0.306}\left(\frac{g}{b_p}\right)^{5.612}\left(\frac{p_e^{3}}{b_p t_p^{3}}\right)^{0.038}\left(\frac{g_e^{3}}{p_f t_p^{3}}\right)^{-1.544}(F)^{0.223} \qquad (3.5.6)$$

$$\psi_{c2} = T_m = (.0534)\left(\frac{t_p}{b_p}\right)^{-4.904}\left(\frac{p_f}{b_p}\right)^{-1.720}\left(\frac{d_b}{b_p}\right)^{1.037}\left(\frac{t_s}{b_p}\right)^{-0.326}\left(\frac{g}{b_p}\right)^{5.909}\left(\frac{p_e^{3}}{b_p t_p^{3}}\right)^{0.014}\left(\frac{g_e^{3}}{p_f t_p^{3}}\right)^{-1.627}(F)^{0.186} \qquad (3.5.7)$$

Figure 3.3 Best Fit Equations from Regression Analysis

Table 3.9
Relative Measurements of the Prediction Equations

Equation	R^2	Conservative % error	Unconservative % error
$\psi_a = (\delta_x)_{max}$	0.961	46	41
$\psi_{by} = (\sigma_y)_{max}$	0.934	32	40
$\psi_{bx} = (\sigma_x)_{max}$	0.902	64	47
$\psi_{c1} = T_n$	0.979	16	14
$\psi_{c2} = T_{nm}$	0.988	10	11

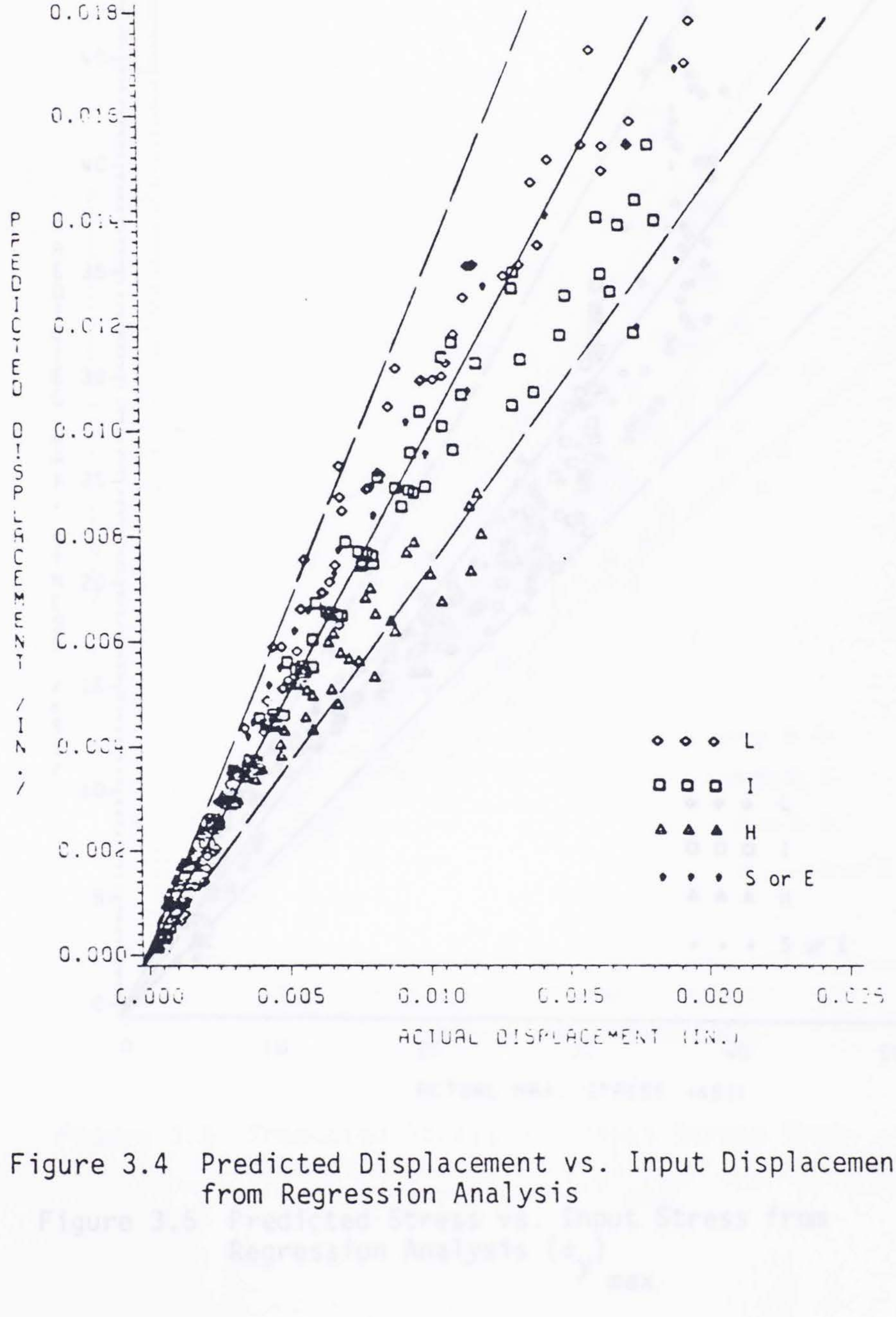

Figure 3.4 Predicted Displacement vs. Input Displacement from Regression Analysis

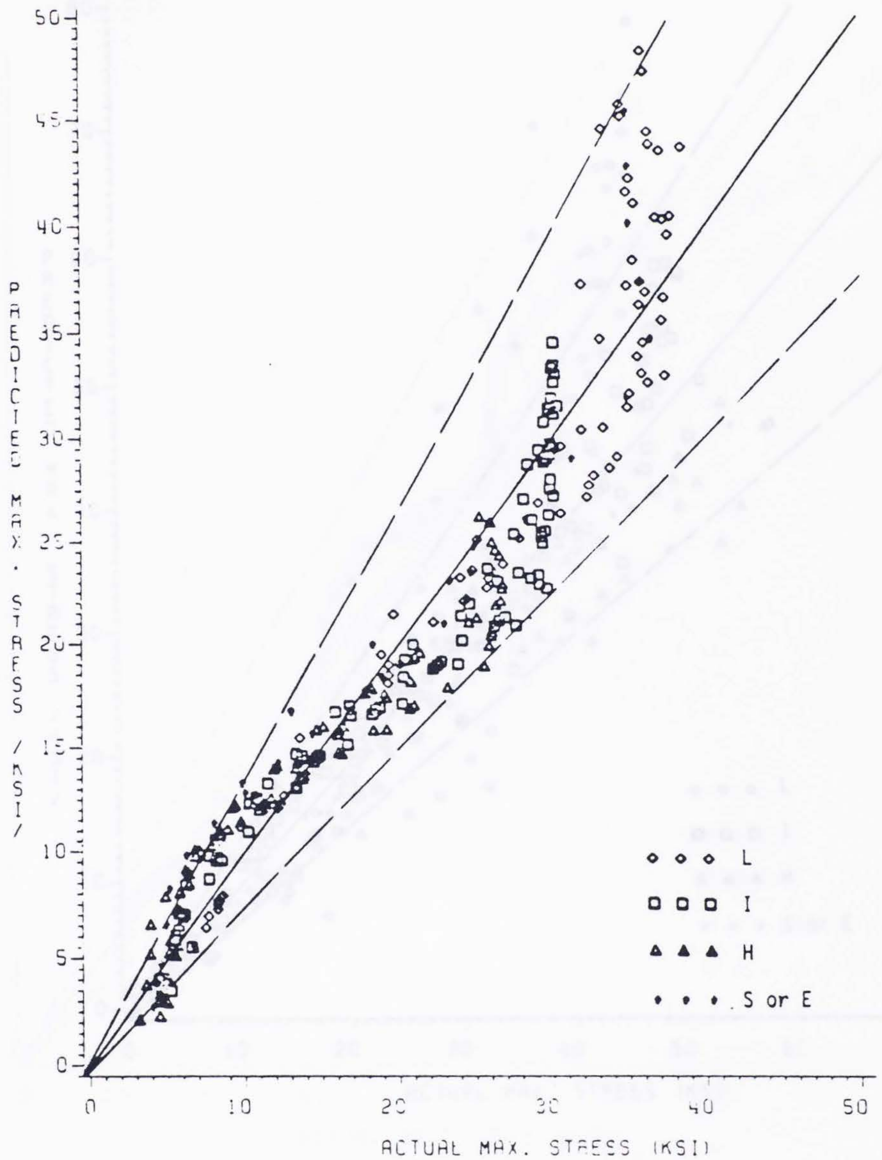

Figure 3.5 Predicted Stress vs. Input Stress from Regression Analysis $(\sigma_y)_{max}$

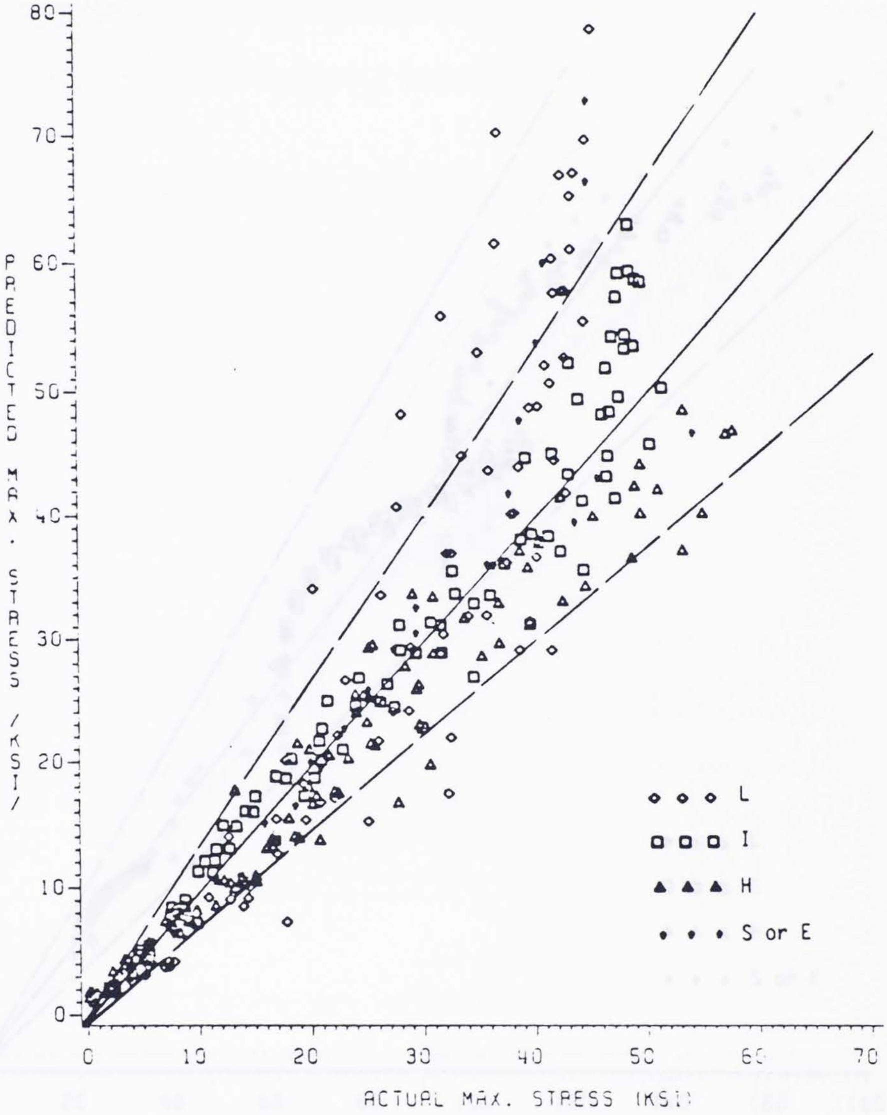

Figure 3.6 Predicted Stress vs. Input Stress from Regression Analysis $(\sigma_x)_{max}$

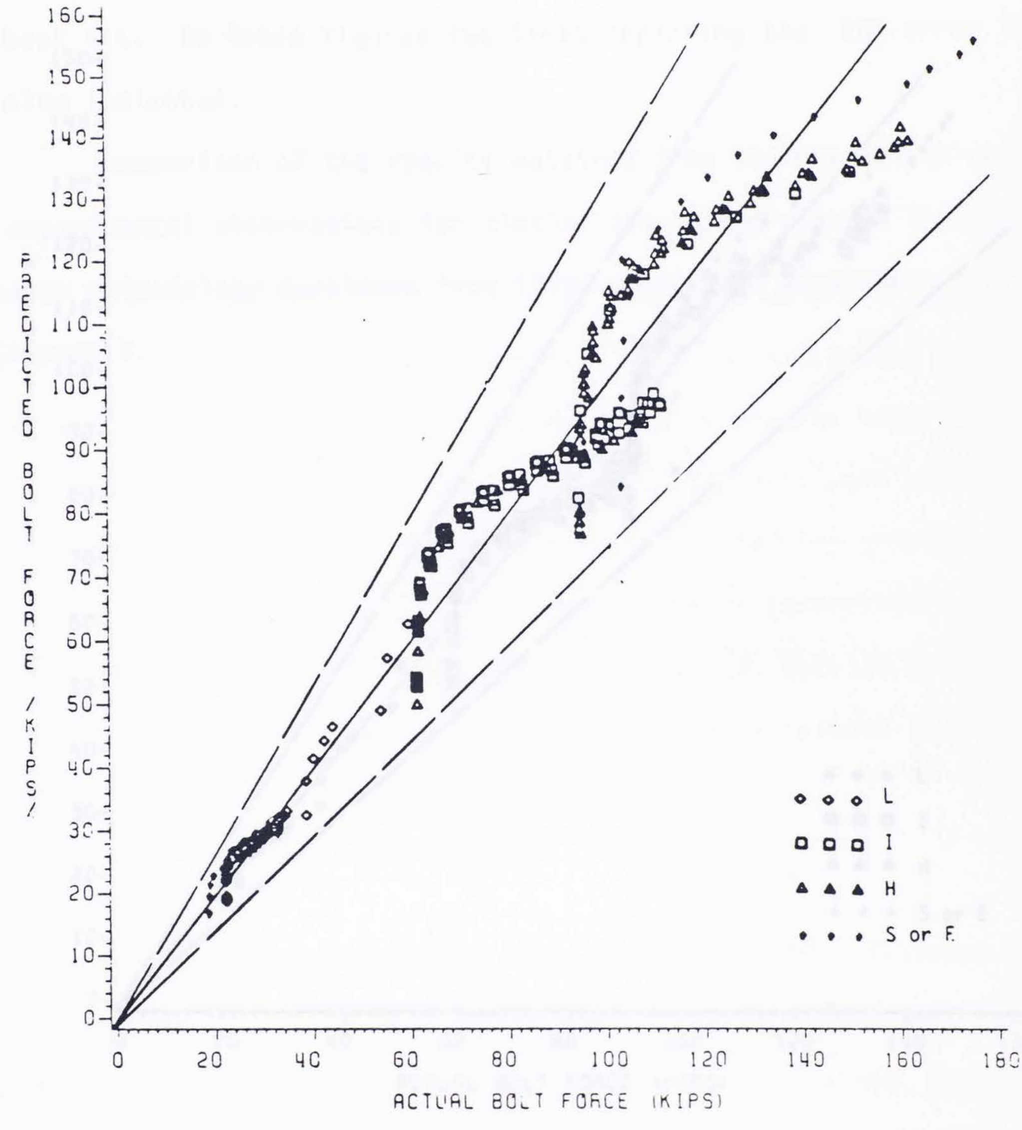

Figure 3.7 Predicted Near Bolt Force vs. Input Near Bolt Force from Regression Analysis

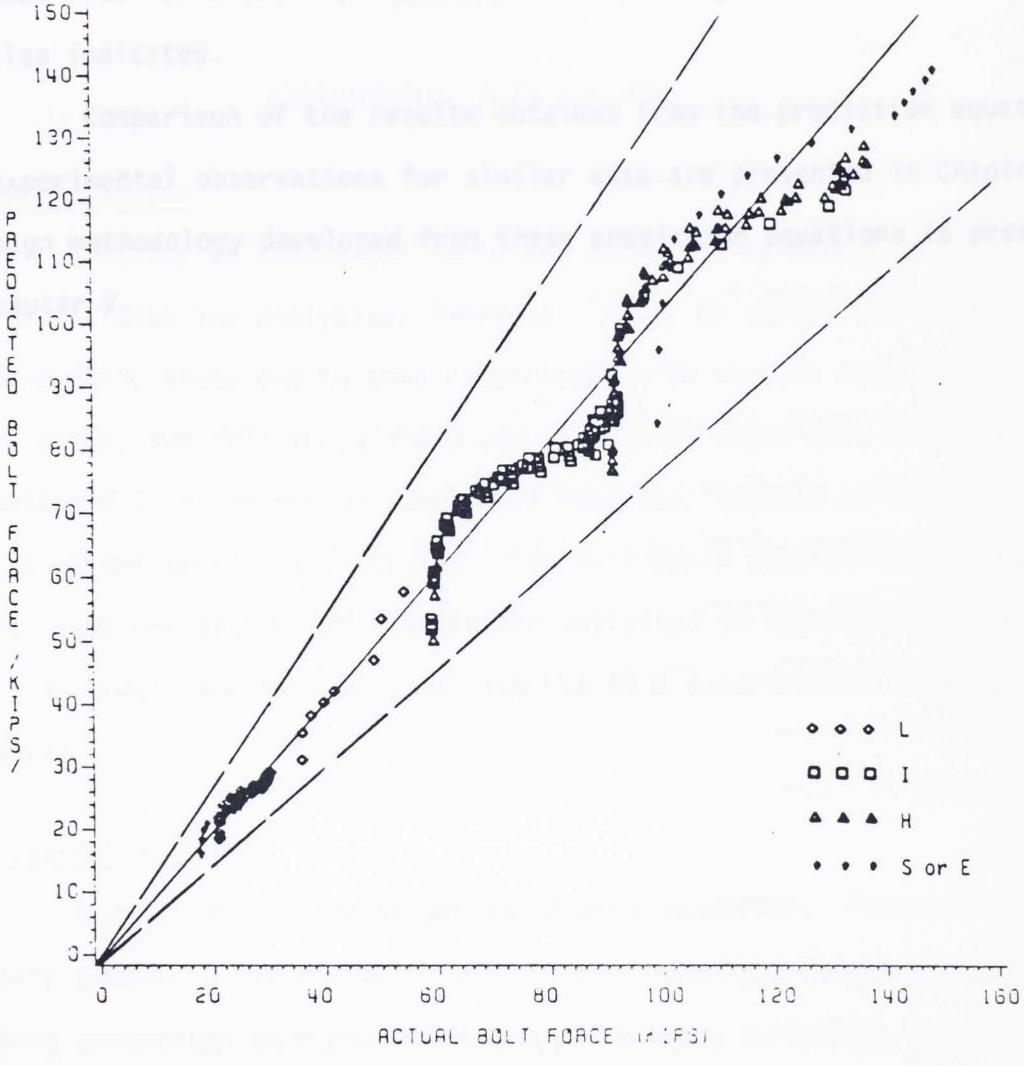

Figure 3.8 Predicted Modified Near Bolt Force vs. Input Modified Near Bolt Force from Regression Analysis

the values obtained from the predicting equations and those input from the finite element analyses for the five dependent parameters. Values on the line drawn with a slope of one-vertical and one-horizontal is defined as the best fit. In these figures two lines depicting the 25% error limits are also indicated.

Comparison of the results obtained from the prediction equations and experimental observations for similar data are presented in Chapter IV. A design methodology developed from these prediction equations is presented in Chapter V.

CHAPTER IV

EXPERIMENTAL VERIFICATION

4.1 Introduction

A series of tee-hanger tests was conducted to obtain data necessary to evaluate the analytical findings. Also, to verify the results of the parametric study and to make comparisons with results from the tee-hanger tests, two full-scale end-plate connection tests were conducted. In Section 4.2, selection of tee-hanger geometry, testing procedure, and results of the tests are discussed. The full-scale connection test procedure, instrumentation and results are explained in Section 4.3. In Section 4.4, comparison of analytical results with experimental results is presented.

4.2 Tee-hanger Tests

A total of six tee-hanger tests were conducted. Although there are many geometric factors which affect the connection behavior, the test specimen geometries were developed using four main variables, namely bolt pitch, bolt gage, end-plate width and end-plate thickness. Stiffener thickness and bolt diameter were kept the same for all six specimens. Eight 5/8 in. diameter A325 bolts were used in each test. Stiffener thickness for all tests was 1/2 in.

4.2.1 Selection of Specimen Geometry

From Table 3.2, the practical range of end-plate thickness corresponding to 5/8 in. diameter bolts is between 1/2 in. and 1 in. Bolt pitch corresponding to 5/8 in. diameter bolts is usually between 1 1/8 in. and 1 5/8 in., and bolt gage is usually between 3 1/2 in. and 5 1/2 in. Thus, combinations of end-plate thickness of 1/2 in., 3/4 in. and 1 in.; bolt pitch of 1 1/8 in. and 1 5/8 in.; bolt gage of 3 1/2 in. and 5 1/2 in.; and end-plate width of 6 in. and 8 in. were selected to develop a possible test configuration matrix. The total number of combinations is 12 as shown in Table 4.1.

The combinations selected from the table for testing were the four cases at the corners and the two cases in the middle. These cases are marked TH-1 through TH-6 in Table 4.1. Case TH-2, at the top right corner is the case with the widest gage and the thinnest end-plate; the case at the bottom left is the narrowest gage and thickest end-plate (TH-3). These are the most flexible and stiffest cases, respectively. The flexibility of the other cases (TH-1, TH-4, TH-5 and TH-6) is between these cases.

4.2.2 Testing Procedure and Instrumentation

Each test specimen consisted of two tee-stubs connected to each other by four rows of two bolts as shown in Figure 4.1. The specimens were loaded using a 200 kip capacity universal type testing machine under pure tension, developed by means of applying load to the tee-hanger stems as shown in Figure 4.1. Load was applied in increments until the capacity of the machine was reached (Test TH-2) or failure occurred. The failure criterion was either rupture of the bolts or excessive deformation of the end-plate.

Table 4.1
Tee-hanger Configurations Using
5/8 in. Diameter Bolts

t_p		1/2"		1/2"		1/2"		1/2"
p_f		1 1/8"		1 5/8"		1 1/8"		1 5/8"
g	TH-1	3 1/2"		3 1/2"		5 1/2"	TH-2	5 1/2"
b_p		6"		6"		8"		8"
t_p		3/4"		3/4"		3/4"		3/4"
p_f		1 1/8"		1 5/8"		1 1/8"		1 5/8"
g		3 1/2"	TH-5	3 1/2"	TH-6	5 1/2"		5 1/2"
b_p		6"		6"		8"		8"
t_p		1"		1"		1"		1"
p_f		1 1/8"		1 5/8"		1 1/8"		1 5/8"
g	TH-3	3 1/2"		3 1/2"		5 1/2"	TH-4	5 1/2"
b_p		6"		6"		8"		8"

Table 4.2
Summary of Tee-Hanger Test Results

	Max. Applied Force (kips)		Mode of Failure	
Test	F.E.M.	Experimental	F.E.M.	Experimental
TH-1	123.5+	160	Bolt	Bolt
TH-2	104.5+	140	Plate	Plate
TH-3	199.5+	200+	Bolt	Bolt
TH-4	190+	195	Bolt	Plate
TH-5	152+	170	Bolt	Bolt
TH-6	142.5+	-	Bolt	N.A.

Note: Plate failure is based on excessive deformation.

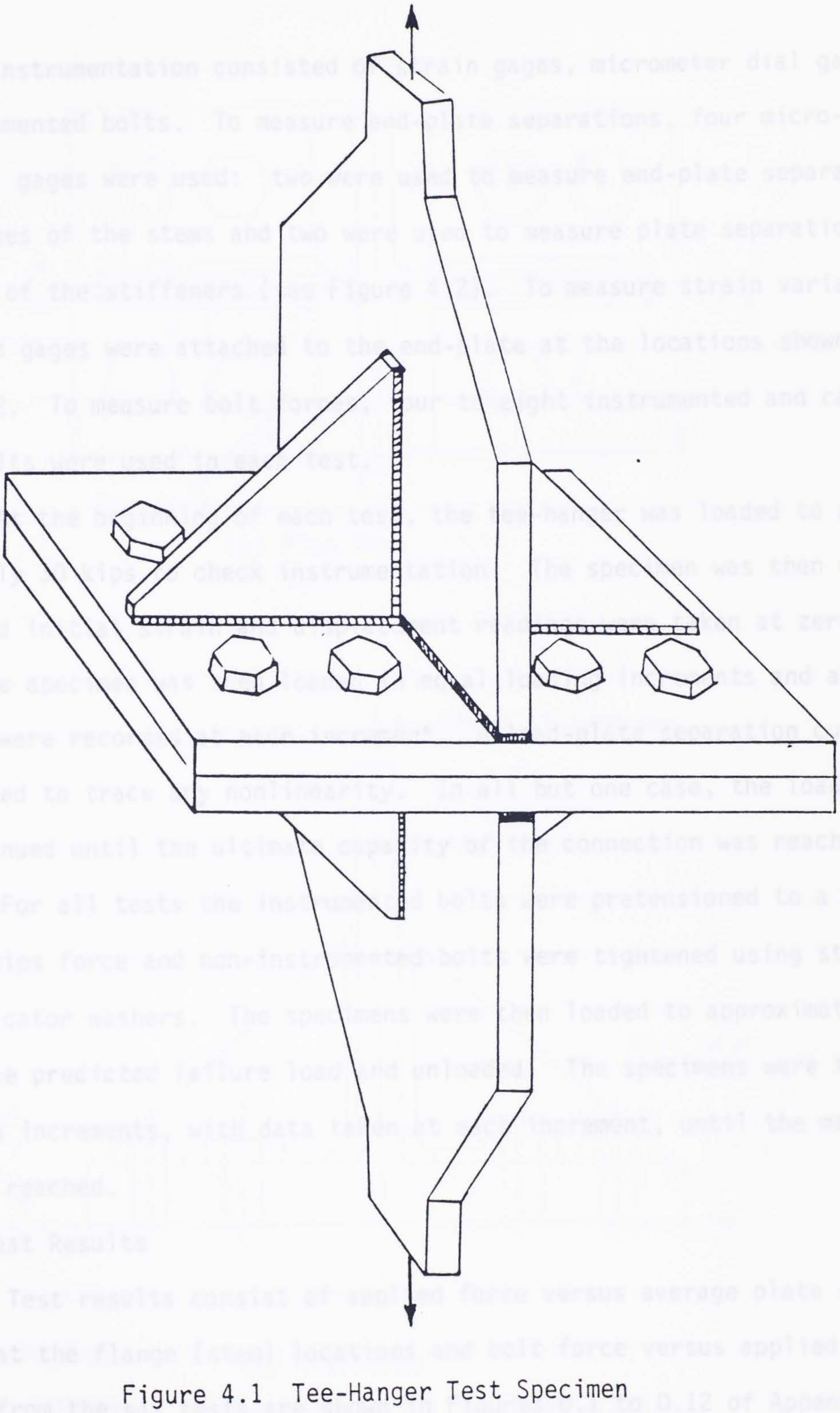

Figure 4.1 Tee-Hanger Test Specimen

Instrumentation consisted of strain gages, micrometer dial gages and instrumented bolts. To measure end-plate separations, four micrometer dial gages were used: two were used to measure end-plate separation at the edges of the stems and two were used to measure plate separation at the edges of the stiffeners (see Figure 4.2). To measure strain variation, six strain gages were attached to the end-plate at the locations shown in Figure 4.2. To measure bolt forces, four to eight instrumented and calibrated bolts were used in each test.

At the beginning of each test, the tee-hanger was loaded to approximately 30 kips to check instrumentation. The specimen was then unloaded and initial strain and displacement readings were taken at zero load. The specimen was then loaded in equal loading increments and all readings were recorded at each increment. A load-plate separation curve was plotted to trace any nonlinearity. In all but one case, the loading was continued until the ultimate capacity of the connection was reached.

For all tests the instrumented bolts were pretensioned to a measured 19 kips force and non-instrumented bolts were tightened using standard load indicator washers. The specimens were then loaded to approximately 30% of the predicted failure load and unloaded. The specimens were then loaded in increments, with data taken at each increment, until the maximum load was reached.

4.2.3 Test Results

Test results consist of applied force versus average plate separation at the flange (stem) locations and bolt force versus applied force. Results from the six tests are shown in Figures D.1 to D.12 of Appendix D. On each of these plots, the results of finite element analyses are also

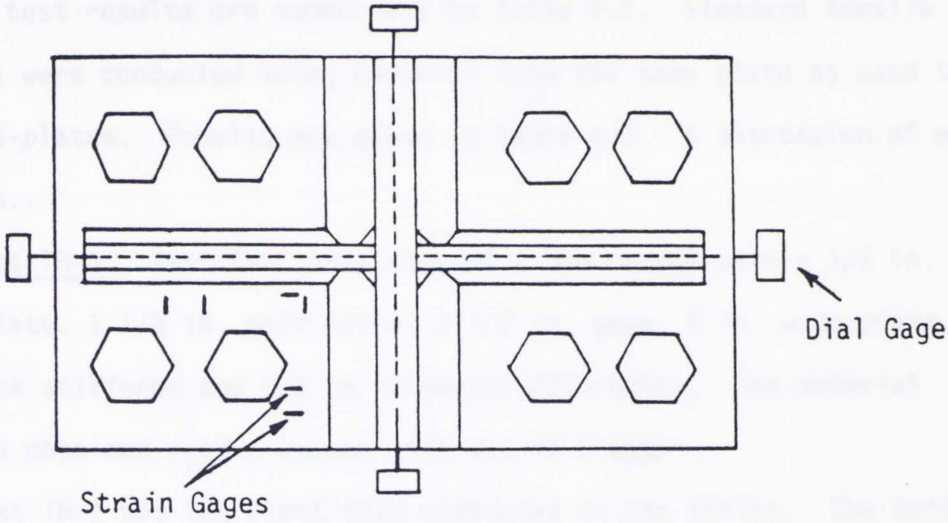

(a) Plan View

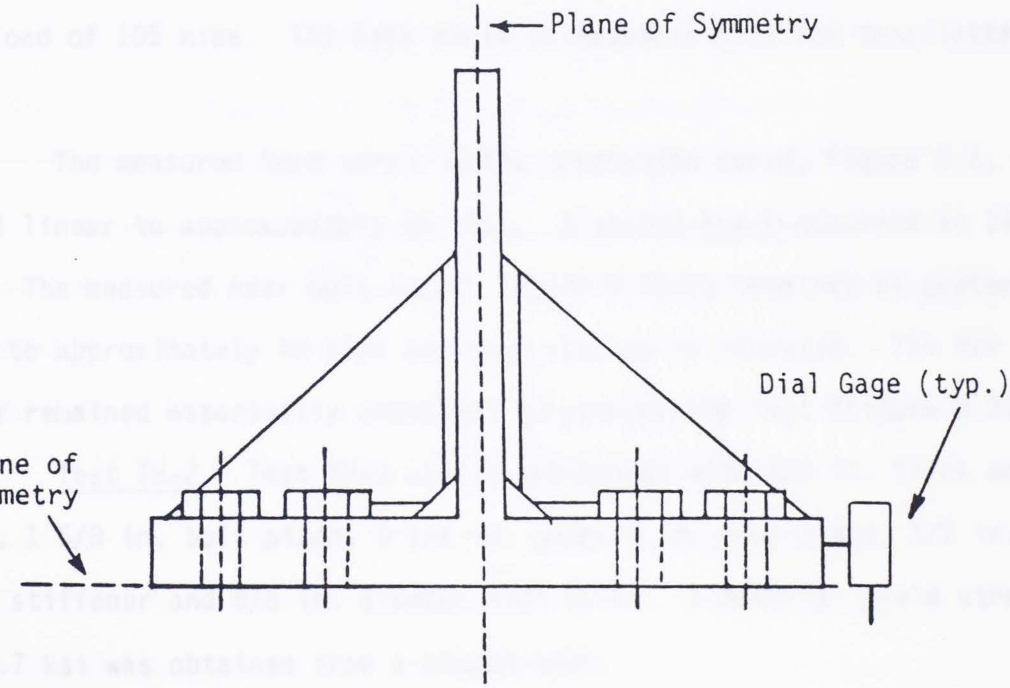

(b) Elevation

Figure 4.2 Tee-Hanger Test Instrumentation shown. The test results are summarized in Table 4.2. Standard tensile coupon tests were conducted using material from the same plate as used to make the end-plates. Results are given in Table 4.3. A discussion of each test follows..

Test TH-1. Test TH-1 consisted of a tee-hanger with a 1/2 in. thick end-plate, 1 1/8 in. bolt pitch, 3 1/2 in. gage, 6 in. wide plate, 1/2 in. thick stiffener and 5/8 in. diameter A325 bolts. The material yield stress obtained from a coupon test was 43.5 ksi.

Test TH-1 was the first test conducted in the series. The failure mode of the initial test was by rupture of the near bolts at a load of 160 kips. It appeared upon examination of the data that the instrumentation was not properly working. The test was then repeated to a maximum load of 105 kips. The data shown in Appendix D is for this latter test.

The measured load versus plate separation curve, Figure D.1, remained linear to approximately 80 kips. A second break occurred at 100 kips. The measured near bolt force, Figure D.2(a), remained at pretension force to approximately 40 kips and then started to increase. The far bolt forces remained essentially unchanged throughout the test (Figure D.2(b)).

Test TH-2. Test TH-2 used a tee-hanger with 1/2 in. thick end-plate, 1 5/8 in. bolt pitch, 5 1/2 in. gage, 8 in. wide plate, 1/2 in. thick stiffener and 5/8 in. diamter A325 bolts. A material yield stress of 38.7 ksi was obtained from a coupon test.

The experimental load versus plate separation curve shown in Figure D.3 is linear to approximately 40 kips. A second break occurred at approximately 95 kips. At 110 kips the plate separation was 0.016 in.

Table 4.3 Coupon Test Results

Test	Thickness (in.)	Yield Stress (ksi)	Ultimate Stress (ksi)	Elongation 2 in. %
TH-1	0.5	43.5	65.9	N.A.*
TH-2	0.5	38.7	70.1	58.0
TH-3	1.0	45.4	66.5	65.0
TH-4	1.0	43.1	73.9	73.1
TH-5	0.75	44.9	72.5	43.9
TH-6	0.75	37.7	65.2	64.4
EP-3	0.75	38.7	65.96	53.0
EP-4	1.0	40.28	69.05	56.0

*Not available

Table 4.4 Prototype Configuration

Test	Section	M_p (k.ft)	$F = \frac{M_p}{d-t_f}$ (k)	d_b (in.)	t_s (in.)	P_f (in.)	g (in.)	t_s (in.)	b_p (in.)
EP3	W24x100	840	434	7/8	3/4	1 3/8	5½	5/8	12
EP4	W24x100	840	434	7/8	1	1 3/8	5½	5/8	12

and from white wash flaking off of the specimen it was clear that the end-plates had significantly yielded. At 114 kips the plate separation was 0.022 in. and a "yield" plateau had formed, Figure D.3. At this load level, the measured near bolt forces remained unchanged, Figure D.4(a), possibly due to instrumentation failure. Far bolt forces did not change significantly to this load level, Figure D.4(b).

The instrumentation was then removed and loading continued until rupture of the near bolts occurred at 140 kips.

Test TH-3. A 1 in. thick end-plate was used for the tee-hanger of Test TH-3 with the 1 1/8 in. bolt pitch, 3 1/2 in. gage, 6 in. plate width, 1/2 in. thick stiffener and 5/8 in. diameter A325 bolts. From a coupon test, the material yield stress was found to be 45.4 kips.

For this test load was applied to 165 kips with data taken at all increments. At 165 kips, the dial gages were removed and loading continued until the capacity of the machine was reached, 200 kips.

Figure D.5 shows the experimental load versus plate separation curve. The curve remains nearly linear to 165 kips. The plate separation was approximately 0.006 in. at this load.

The near bolt force versus the applied load is plotted in Figure D.6(a). The near bolt force stayed at the pretension level to 60 kips of applied load and then started to increase. Far bolt forces did not significantly change as load was applied. From the condition of the specimen at the 200 kip load level, it is believed that the ultimate failure mode would be bolt rupture without significant plate yielding.

Test TH-4. Test TH-4 consisted of a tee-hanger with a 1 in. thick end-plate, 1 5/8 in. bolt pitch, 5 1/2 in. gage, 8 in. end-plate width, 1/2 in. thick stiffener and 5/8 in. diamter A325 bolts. The material yield stress from a coupon test was found to be 43.1 ksi.

From Figure D.7, the first break from linearity in the load versus plate separation curve, occurred at approximately 150 kips, the second at approximately 160 kips, and the third near 180 kips. The maximum applied load was 195 kips.

As seen in Figure D.8(a), the near bolt force stayed at the pretension level to 40 kips and then started to increase very slightly. At 170 kips, the plate separation was about 0.013 in. and started to increase rapidly. When the load was increased to 195 kips, the near bolts ruptured.

Test TH-5. Test TH-5 consisted of a 3/4 in. thick end-plate with 1 5/8 in. bolt pitch, 3 1/2 in. gage, 1/2 in. thick stiffener, 6 in. plate width and 5/8 in. bolt diameter. The material yield stress obtained from a coupon test was 44.9 ksi.

The measured load versus plate separation curve, Figure D.9, remained linear to approximately 130 kips. A second break occurred at 140 kips and a third at 150 kips.

The measured near bolt force, Figure D.10(a), remained at the pretension force to approximately 80 kips load and then started to increase. Little change was found in the far bolt force, Figure D.10(b).

Instrumentation was removed at the 150 kips level and loading was continued to approximately 170 kips when the near bolts ruptured. The end-plates were severely yielded at this load level.

Test TH-6. This test was made up of a 3/4 in. thick end-plate with 1 1/8 in. bolt pitch, 5 1/2 in. gage, 1/2 in. thick stiffener, 8 in. plate width and 5/8 in. bolt diameter. A material yield stress of 37.7

ksi was obtained from a coupon test. The specimen was not loaded to failure.

The experimental load versus plate separation curve shown in Figure D.11 is linear to 70 kips. The near bolt force, Figure D.12(a) remained unchanged from the pretension level to an applied force of approximately 60 kips at which time the force began to increase rapidly. The far bolt forces remained unchanged, Figure D.12(b).

4.3 Prototype Testing

To further evaluate the analytical results, two full end-plate connection tests were conducted (with four more planned as part of the total research effect). A W24x100, A36 steel, section was used to conduct the tests. The setup is shown in Figure 4.3. Each beam segment had end-plates welded to the ends allowing two tests per beam segment by simply rotating the sections. Test EP-1 was conducted with 3/4 in. thick end-plates and Test EP-2 with 1 in. thick end-plates. For both tests 7/8 in. diameter A325 bolts were used and end-plate width was 12 in., bolt pitch 1 3/8 in., gage 5 1/2 in. and stiffener thickness 5/8 in. Details are summarized in Table 4.4.

The test set-up, instrumentation, testing procedure, results and comparisons with analytical predictions are described in the following Subsections.

4.3.1 Test Set-up and Loading

Each test specimen consisted of two W24x100 beam sections 11 ft. long with the end-plates at each end. The sections were bolted together and tested at an effective span of 20 ft. under pure bending moment, developed by a symmetric two-point loading applied through a W33x130 spreader beam, as shown schematically in Figure 4.3. The pure moment region was 10 ft. in length to avoid effects of local stress concentration at load and reaction locations. The load was applied using a 750 kips capacity hydraulic ram supported by an H-shaped load frame which in turn was bolted to a stiff reaction floor. The supports for the test beam were also supported by the reaction floor. To monitor the applied load, a load cell was interposed between the ram and the spreader beam. An extensive system of lateral bracing was provided to permit loading of the specimen to failure without lateral buckling or torsional twisting of the specimen.

For each test, the specimen was loaded to approximately 30% of the predicted failure load and then unloaded. The specimen was then unloaded. The specimen was then loaded in increments until the maximum load was reached. The tests were terminated when a definite yield plateau was developed in both the vertical load versus vertical deflection and plate separation curves and when the measured bolt strains were rapidly increasing per load increment.

4.3.2 Instrumentation

Each specimen was instrumented to measure and record the following quantities: (1) plate separation, (2) plate strains, (3) beam strains, (4) vertical deflections, and (5) bolt strains.

The plate separation at the beam tension flange was measured by means of caliper gages. A spring was inserted between the two legs of the caliper to keep the tips pressed against the two end-plate faces. A strain gage was mounted on the standard caliper spring and the modified caliper was calibrated prior to use. Three caliper gages were used, one at the plane of the beam section webs and one near each edge of the end-plates.

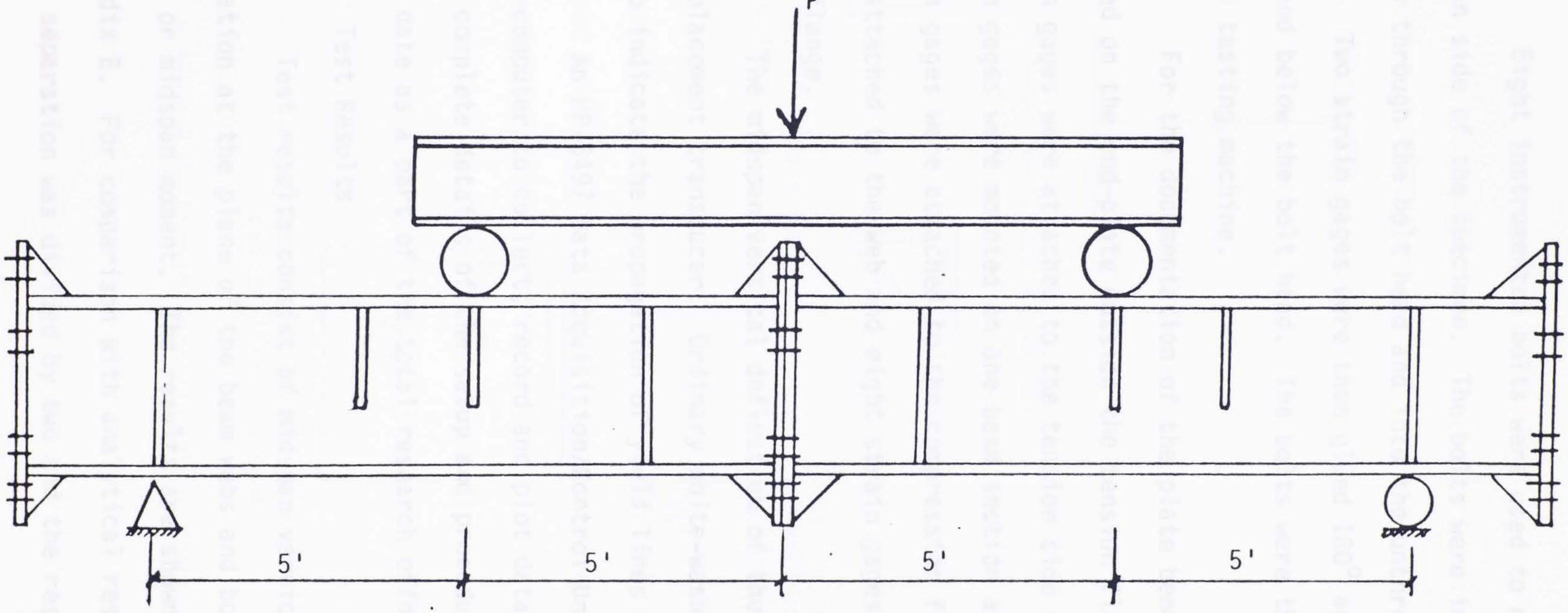

Figure 4.3 Prototype Test Set-up

Eight instrumented bolts were used to measure bolt strains at the tension side of the specimen. The bolts were instrumented by first boring a hole through the bolt head and into the unthreaded portion of the bolt shank. Two strain gages were then glued 180^{0} apart on the inside of the hole and below the bolt head. The bolts were then calibrated using a universal testing machine.

For the documentation of the plate bending, six strain gages were mounted on the end-plate outside the tension flange. Three additional strain gages were attached to the tension side stiffener. Twenty-five strain gages were mounted on one beam section as shown in Figure 4.4. Six strain gages were attached to the compression flange, eleven strain gages were attached to the web and eight strain gages were attached to the tension flange.

The midspan vertical deflection of the beam was measured using a displacement transducer. Ordinary white-wash was painted on the specimen to indicate the propagation of yield lines and deformation lines.

An HP-3497 Data Acquisition/Control Unit was used with an HP-85 micro-computer to collect, record and plot data as the tests progressed. (More complete details of the setup and procedure will be provided at a later date as a part of the total research effort).

4.3.3 Test Results

Test results consist of midspan vertical displacement, plate separation at the plane of the beam webs and bolt force versus applied force or midspan moment. The results are shown in Figures E.1 to E.6 of Appendix E. For comparison with analytical results, the total measured plate separation was divided by two and the result was plotted versus

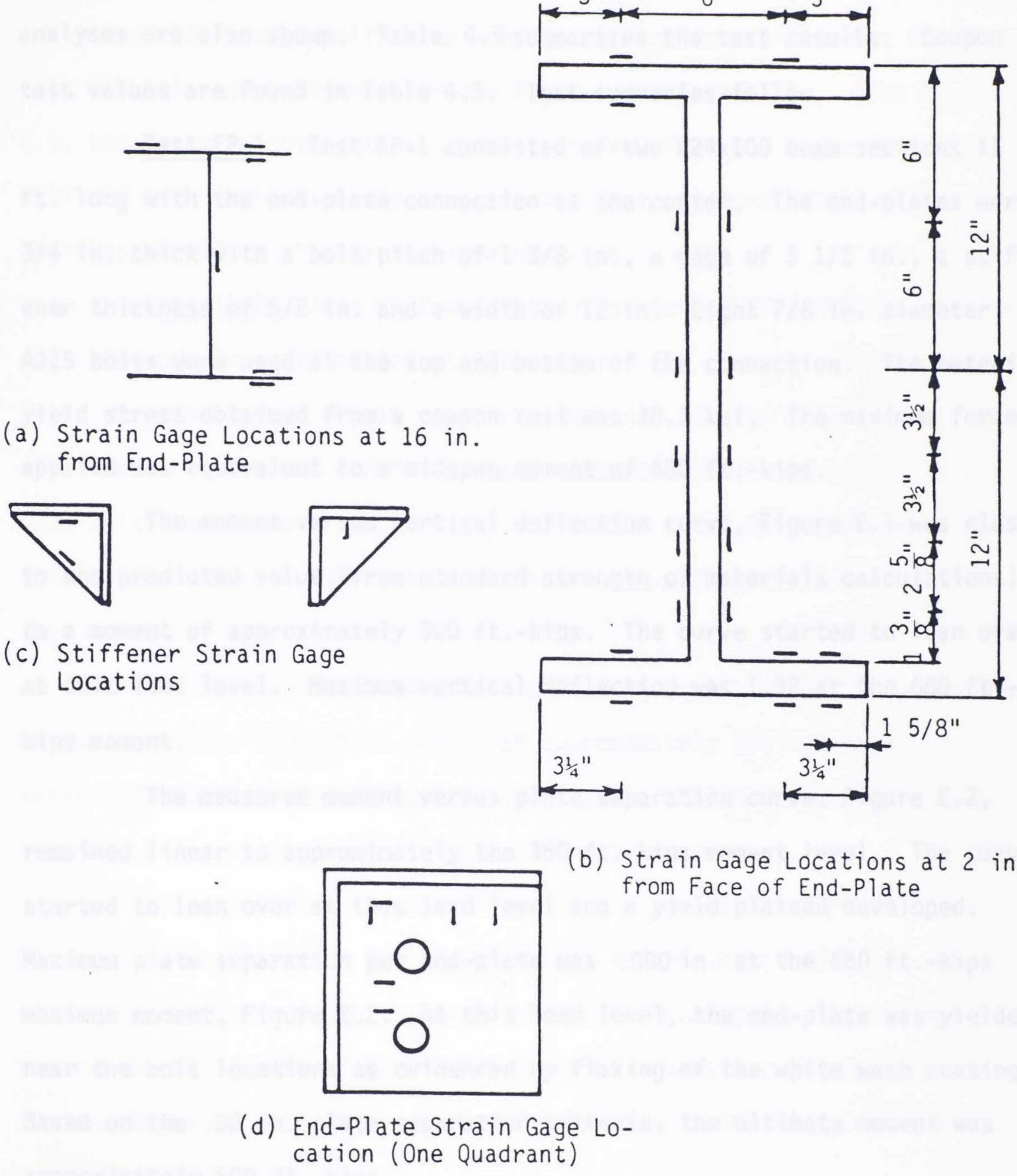

(a) Strain Gage Locations at 16 in. from End-Plate

(b) Strain Gage Locations at 2 in. from Face of End-Plate

(c) Stiffener Strain Gage Locations

(d) End-Plate Strain Gage Location (One Quadrant)

Figure 4.4 Strain Gage Locations for Prototype Testing midspan moment. On each of these plots, the results of finite element analyses are also shown. Table 4.5 summarizes the test results. Coupon test values are found in Table 4.3. Test summaries follow.

Test EP-1. Test EP-1 consisted of two W24x100 beam sections 11 ft. long with the end-plate connection at the center. The end-plates were 3/4 in. thick with a bolt pitch of 1 3/8 in., a gage of 5 1/2 in., a stiffener thickness of 5/8 in. and a width of 12 in. Eight 7/8 in. diameter A325 bolts were used at the top and bottom of the connection. The material yield stress obtained from a coupon test was 38.7 ksi. The maximum force applied was equivalent to a midspan moment of 680 ft.-kips.

The moment versus vertical deflection curve, Figure E.1 was close to the predicted value (from standard strength of materials calculations) to a moment of approximately 300 ft.-kips. The curve started to lean over at this load level. Maximum vertical deflection was 1.32 at the 680 ft.-kips moment.

The measured moment versus plate separation curve, Figure E.2, remained linear to approximately the 350 ft.-kips moment level. The curve started to lean over at this load level and a yield plateau developed. Maximum plate separation per end-plate was .080 in. at the 680 ft.-kips maximum moment, Figure E.2. At this load level, the end-plate was yielded near the bolt locations as evidenced by flaking of the white wash coating. Based on the .02 in. plate separation criteria, the ultimate moment was approximately 500 ft.-kips.

For this test, only four instrumented bolts were used. All were placed adjacent to the tension flange (near bolts). The four instrumented bolts were pretensioned to a measured 39 kips. For pretensioning of the non-instrumented bolts standard load-indicator washers were used. Figure E.4 shows the average bolt force for the two inside (relative to the tension flange) near bolts and for the two outside near bolts. From Figure E.4, the force in both sets of bolts increased from the beginning of the test and were increasing rapidly when the test was terminated. Both sets of bolts showed relatively the same behavior.

Test EP-2. Test EP-2 was made up of two W24x100 beam 11 ft. long with the end-plate connection at the center. The connection consisted of 1 in. end-plates with a bolt pitch of 1 3/8 in., a gage of 5 1/2 in., a stiffener thickness of 5/8 in. a plate width of 12 in. and 7/8 in. diameter A325 bolts were used. A material yield stress of 40.28 ksi was obtained from a coupon test. The maximum applied force was equivalent to a mid-span moment of 750 ft.-kips.

The moment versus vertical deflection curve, Figure E.4, was close to the predicted curve to a moment of approximately 350 ft.-kips. The curve started to lean over at this load level. Maximum vertical deflection was 1.45 in. at the 750 ft.-kips moment level.

The experimental moment versus plate separation curve shown in Figure E.5 was linear to the approximately 400 ft.-kips level and then started to soften. A short yield plateau was developed. The maximum plate separation reached at the 750 ft.-kips moment was .04 in. per end-plate. Based on the .02 in. plate separation criteria, the ultimate moment was 637 ft.-kips.

For this test, four instrumented bolts were also used at the near bolts locations of the tension area. These bolts were pretensioned to a measured 39 kips. The non-instrumented bolts were tightened using load-

Table 4.5
Summary of Prototype Test Results

Test	Flange Force (kips)				Mode of Failure	
	Max. Applied Force (kips)		Force @ 0.02 in. Plate Separation (kips)			
	F.E.M.	Experimental	F.E.M.	Experimental	F.E.M.	Experimental
EP-1	296.3+	350	255	258	Bolt	Plate
EP-2	370.4+	387	370.4	328.8	Bolt	Plate

Note: Plate failure is based on excessive deformation.

Table 4.6
Comparison of Experimental and Predicted Flange Forces

Test	Experimental Flange Force		Predicted Flange Force				
	Maximum (kips)	At 0.02 in. (kips)	$(\delta_x)_{max}$ [1] (kips)	$(\sigma_x)_{max}$ [2] (kips)	$(\sigma_y)_{max}$ [2] (kips)	T_n [3] (kips)	T_{nm} [3] (kips)
TH-1	160	*	211.5	116.6	80.9	98.2	183.3
TH-2	140	110	153.4	121.3	103.1	71.4	104.4
TH-3	200+	*	485.8	328.4	158.0	133.7	238.3
TH-4	195	180	352.0	317.7	177.8	113.6	165.4
TH-5	170	*	309.2	174.8	98.9	136.4	227.1
TH-6	-	-	248.1	218.1	150.3	84.7	120.7
EP-1	350	258.0	207.0	229.2	170.9	196.3	357.4
EP-2	387	328.8	331.0	410.2	250.2	226.2	405.9

Note: * - Not reached
1 - $(\delta_x)_{max} = 0.02$ in.
2 - $(\sigma_y)_{max} = 36$ ksi, or $(\sigma_x)_{max} = 36$ ksi
3 - Ultimate bolt strength used for T_n or T_{nm}, Equations (3.5.6) and (3.5.7)

indicator washers. Figure E.6 shows average bolt force versus midspan moment. Both sets of near bolts showed increasing force from the beginning of the tests. The outside near bolts showed a more rapid increase, however, both bolts showed similar levels when the test was terminated.

4.4 Comparison of Experimental and Analytical Results

The data resulting from the tee-hanger tests consisted of plate separation, bolt forces, and end-plate strains at various load levels. The data resulting from the prototype testing consisted of plate separation, bolt forces, end-plate strains at critical locations, flange and web strains adjacent to the connection, and vertical deflections of the beam at midspan. In the following paragraphs, first the test results (plate separations and bolt forces only) are compared with results from finite element analyses of the test specimens, then test results are compared with the results of the predicting equations.

Figures D.1, D.3, D.5, D.7, D.9 and D.11 depict the measured and computed plate separations for the six tee-hanger specimens. Figures E.2 and E.5 show the measured and computed plate separation versus moment for the prototype specimens. Correlation between the finite element analyses and experimental results are considered very good since the differences are within 20% for the tee-hanger tests and within 10% for the prototype tests.

Figures D.2, D.4, D.6, D.8, D.11 and D.12 illustrate the measured and computed bolt forces for the six tee-hanger specimens. In all cases, excellent agreement was found between predicted and measured far bolt forces. Excellent agreement was also obtained for near bolt forces at low loads. However, at higher loads significant differences were found. On investigation, it was determined that the near bolt force from the finite element analyses includes effects due to tensile force and bending force, however, in the experiments the bolt force is due only to axial deformation. Thus, in order to compare the measured and the analytical near bolt forces, the near bolt forces from the finite element analyses must be modified by excluding effects due to bending of the bolt. This was done by simply calculating the average elongation of the bolt shank in the near bolt from the nodal deflection and converting to force.

By removing the bending effect from the near bolt force, the results of the finite element analysis were shifted toward the experimental results. The results are shown in Figures D.2(a), D.4(a), D.6(a), D.8(a), D.10(a) and D.12(a). The modified results are within 25% of the experimental results.

Figures E.3 and E.6 show comparison of bolt forces form tests and finite element analyses (without modification) for the prorotype specimens. The measured bolt forces were closer to the analytical bolt forces than for the tee-hanger tests.

In general, the agreement between the results of finite element analyses and the experimental results vary from fair to excellent.

Experimental flange (or tee-stem) forces and forces calculated using the predicting equations are compared in Table 4.6. It is noted that the geometries used in the tee-hanger tests fall outside the limits of the parametric study (Table 3.4) used to develop the predicting equations. If only modified bolt force and plate separation are considered the predicted results for Test EP-1 and EP-2 are in excellent agreement with the test results when the complexity of the problem is considered. At 0.02 in.

separation, the ratio of experimental to predicted flange forces are 1.25 and 0.99 for tests EP-1 and EP-2, respectively. The ratios of maximum force to failure flange force based on the modified bolt force equation are 0.98 and 0.96 for Tests EP-1 and EP-2, respectively.

CHAPTER V

PROPOSED DESIGN METHODOLOGY

5.1 Introduction

The predicting equations developed from regression analyses of finite element results (Chapter III) have been shown to adequately explain the behavior of stiffened end-plate moment connections with eight bolts in four rows at the beam tension flange (Chapter IV). These equations will now be used to develop a design procedure. The procedure is explained in Section 5.2 and a design example is presented in Section 5.3. A slightly less accurate, but considerably simplified procedure is proposed in Section 5.4.

5.2 Design Methodology

Using Equations 3.5.3 to 3.5.7 of Figure 3.3, a design procedure for determining required end-plate thickness and bolt diameter can be developed assuming all other variables are known. The steps are as follows:

1. Calculate the beam flange force, F_u, from the factored beam moment, M_u:

$$F_u = M_u/d\text{-}t_{fb} \tag{5.2.1}$$

in which d = beam depth and t_{fb} = thickness of beam flange.

2. Estimate the required bolt force for 6.8 equivalent bolts from:

$$T_u = F/6.8 \tag{5.2.2}$$

The constant 6.8 is based on the assumptions that the near bolts contribute their full strength and the far bolts only the pretension force (evaluated at 0.7 $A_b F_y$).

3. Select bolt size. Note if Table I-A of the AISC manual[10] is used to select the bolt size, T_u from Equation 5.2.2 must be divided by 2.0 to account for the factor of safety implied in Table I-A.

4. Select pitch, p_f, and gage, g. The selected pitch and gage must be within the ranges defined in Tables 3.2 and 3.3.

5. Select stiffener thickness, t_s, approximately equal to the beam web thickness, t_w, and end-plate thickness, b_p, approximately equal to the beam flange width, b_f.

6. Calculate the effective pitch, b_e, and effective gage, g_e, from

$$p_e = p_f - (d_b/4) - w_s \tag{5.2.3}$$

$$g_e = g/2 - (d_b/4) - (t_s/4) \tag{5.2.4}$$

in which d_b = bolt diameter and w_s = estimated length of the fillet weld leg at the beam flange.

7. Using the limiting deflection criterion given in Appendix F, 0.02 in., compute a required end-plate thickness from Equation 3.5.3 which can be rearranged as:

$$t_p = (9.00\times10^{-4}) \frac{(p_e)^{.416}(g_e)^{1.476}(b_p)^{.664}(F)^{.834}}{(p_f)^{.405}(g)^{1.691}(d_b)^{.0324}(t_s)^{.059}(\delta_x)_{max}^{\;.611}} \tag{5.2.5}$$

Taking δ = .02 in., the above equation reduces to

$$t_{p1} = (9.82\times10^{-3}) \frac{(p_e)^{.416}(g_e)^{1.476}(b_p)^{.664}(F)^{.834}}{(p_f)^{.405}(g)^{1.691}(d_b)^{.0324}(t_s)^{.059}} \qquad (5.2.6)$$

8. Taking the maximum bending stress in the end-plate equal to σ_y, compute a required end-plate thickness, t_p, from Equation 3.5.4 which can be rearranged as:

$$t_p = (18.019) \frac{(p_f)^{.168}(p_e)^{.161}(d_b)^{.517}(t_s)^{.039}(g_e)^{2.682}}{(b_p)^{.253}(g)^{3.264}(\sigma_y)_{max}^{.368}} (F)^{.694} \qquad (5.2.7)$$

Taking $(\sigma_y)_{max}$ = 36 ksi the above equation reduces to

$$t_{p2} = (0.803) \frac{(p_f)^{.168}(p_e)^{.161}(d_b)^{.517}(t_s)^{.039}(g_e)^{2.682}}{(b_p)^{.253}(g)^{3.264}} (F)^{.694} \qquad (5.2.8)$$

9. From the end-plate thicknesses, t_{p1} and t_{p2}, choose the larger as the trial thickness, t_p.

10. Using the end-plate thickness chosen in Step 9, compute the maximum force in the near bolt, T_n, from Equation 3.5.7, which can be rearranged as:

$$T_n = (0.0534) \frac{(d_b)^{1.037}(g)^{5.909}(p_e)^{.042}(F)^{.186}}{(t_p)^{.065}(b_p)^{.01}(t_s)^{.326}(p_f)^{.093}(g_e)^{4.881}} , \qquad (5.2.9)$$

11. If the bolt force determined in Step 10 is less than or equal to the capacity of the bolt previously selected, the bolt size determined in Step 3 and end-plate thickness determined in Step 9 are acceptable. If not, choose a larger bolt size and repeat Steps 4 to 11.

5.3 Design Example

To illustrate the various steps described above, calculations are presented for the maximum moment and beam section of Test EP-2 as reported in Chapter IV.

Example: Determine bolt size and end-plate thickness for a W24x100 A36 beam with M_u = 637 ft.-kips. For a W24x100, d = 24.00 in., t_w = 0.468 in., b_f = 12.00 in. and t_{fb} = 0.775.

Step 1. Calculate flange force (Equation 5.2.1):

F_u = (637x12)/(24-0.775) = 329.1 kips

Step 2. Estimate required bolt force (Equation 5.2.2):

T_u = 329.1/6.8 = 48.4 kips

Step 3. Choose 7/8 in. A325 bolts. Working load for this bolt is 26.5 kips from Table I-A, AISC Manual(10).

Step 4. Choose pitch, p_f = 1 3/8 in. (as recommended on p. 4-111 of Reference 10), and gage, g = 5 1/2 in.

Step 5. Choose stiffener thickness, t_s = 1/2 in. and end-plate width, b_p = 12 in.

Step 6. Calculate p_e and g_e from Equation 5.2.3 and 5.2.4. Assume w_s = 3/16 in. (minimum fillet with full penetration weld).

p_e = 1.375 - 0.875/4 - 0.1875 = 0.969 in.

g_e = 5.5/2 = 0.875/4 = 0.50/4 = 2.41 in.

Step 7. Calculate plate thickness to limit maximum deflection (Equation 5.2.6).

$$t_{pl} = \frac{(9.82\times10^{-3})(0.969)^{0.416}(2.41)^{1.476}(12.0)^{0.664}(329.1)^{0.834}}{(1.375)^{0.405}(5.5)^{1.691}(0.875)^{0.0324}(0.500)^{0.059}} = 1.197 \text{ in.}$$

Step 8. Calculate plate thickness based on a maximum stress in the end-plate of 36 ksi (Equation 5.2.8).

$$t_{p2} = \frac{(0.803)(1.375)^{0.168}(0.969)^{0.161}(0.875)^{0.517}(0.500)^{0.039}(2.41)^{2.682}}{(12.0)^{0.253}(5.5)^{3.264}} \times$$

$$(329.1)^{0.694} = 0.925 \text{ in.}$$

Step 9. Take t_p = 1.197 in. and select 1 1/8 in. thick end-plate.

Step 10. Calculate the maximum bolt force from Equation 5.2.9.

$$T_n = \frac{(0.0534)(0.875)^{1.037}(5.5)^{5.909}(0.969)^{0.042}(329.1)^{0.186}}{(1.125)^{0.065}(12.0)^{0.010}(0.50)^{0.326}(1.375)^{0.093}(2.41)^{4.881}} = 52.0 \text{ kips}$$

Step 11. Since T_n = 52.0 kips is less than the factored bolt capacity, 2 x 26.5 = 53.0 kips, the connection is adequate.

Use PL 12x 1 1/8 A36 w/8-7/8 in. diameter A325 bolts.

The above design example uses identical dimensions to those specified for Test EP-2. The design moment is the applied moment at the measured plate separation of 0.02 in. (Table 4.5). The resulting design requires an end-plate thickness of 1 1/8 in., a 1 in. thick end-plate was used in the test.

Using the maximum moment which was applied in the test, 750 ft.-kips, the equivalent flange force is 387.5 kips. Using Equation 5.2.8 for maximum stress (Step 8), the required end-plate thickness for this force is 1.04 in. It is noted that the design is based on an end-plate yield stress of 36 ksi and the measured yield stress of the material used in the test is 40.28 ksi.

5.4 Design Methodology using Simplified Equations

Equations 5.2.6, 5.2.7 and 5.2.9 are relatively complex for routine design use. Hence, an attempt was made to develop simplified equations with sufficient accuracy so that conservative solutions are obtained without undue costs. The parameters which most effect connection behavior have been identified as the flexibility parameters (Section 3.2). The parameters are defined in terms of end-plate width and thickness (b_p and t_p), and effective gage and pitch (g_e and p_e). Regression analysis using similar procedures to those described in Section 3.2 were used to obtain predicting equations for plate separation, bending stresses and near bolt force as a function of the above geometric terms and the flange force, F. The R^2 values for these four predicting equations were close to those obtained from the regression analyses described in Section 3.2.

The resulting predicting equation for plate separation is

$$(\delta_x)_{max} = (2.858\text{x}10^{-6}) \left(\frac{p_e^{\,3}}{t_p^{\,4}}\right)^{0.133} \left(\frac{g_e^{\,3}}{t_p^{\,4}}\right)^{0.365} (F)^{1.367} \tag{5.4.1}$$

with R^2 equal to 0.955. Taking $(\delta_x)_{max}$ = 0.02 in. and rearranging, the required plate thickness based on plate separation is

$$t_{p1} = (0.0117)\ (p_e)^{0.200} (g_e)^{0.550} (F)^{0.686} \tag{5.4.2}$$

The predicting equation for $(\delta_y)_{max}$ was found to be (R^2 = 0.914)

$$(\sigma_y)_{max} = (0.2657) \left(\frac{p_e^{\,3}}{t_p^{\,4}}\right)^{0.088} \left(\frac{g_e^{\,3}}{t_p^{\,4}}\right)^{0.241} (F)^{0.750} \tag{5.4.3}$$

With $(\sigma_y)_{max}$ = 36 ksi, the required plate thickness is

$$t_{p2} = (0.0240)\,(p_e)^{0.200}(g_e)^{0.550}(F)^{0.594} \qquad (5.4.4)$$

The modified near bolt force predicting equation (R^2 = 0.942) was found to be

$$T_{nm} = (24.0)\left(\frac{p_e^{\,3}}{t_p^{\,4}}\right)^{-0.0198}\left(\frac{g_e^{\,3}}{t_p^{\,4}}\right)^{-0.152}(F)^{0.202} \qquad (5.4.5)$$

Rearranging for design

$$T_n = \frac{(24.0)(t_p)^{0.687}(F)^{0.202}}{(p_e)^{0.059}\,(g_e)^{0.456}} \qquad (5.4.6)$$

The design procedure outlined in Section 5.2 remains the same except Equation 5.4.2 replaces Equation 5.2.6 in Step 7, Equation 5.4.4 replaces Equation 5.2.8 in Step 8, and Equation 5.4.6 replaces Equation 5.2.9 in Step 10.

To illustrate the use of these new equations, the example in Section 5.3 is reworked:

<u>Design Example</u>:

Steps 1 through 6 remain the same.

Step 7. Calculate plate thickness to limit maximum deflection (Equation 5.2.4)

$$t_{p1} = (0.0117)\,(0.969)^{.200}(2.41)^{.550}(329.1)^{.686} = 1.00 \text{ in.}$$

Step 8. Calculate plate thickness based on a maximum stress in the end-plate of 36 ksi (Equation 5.4.4)

$$t_{p2} = (0.0240)\,(0.969)^{.200}(2.41)^{.550}(329.1)^{.570} = 1.05 \text{ in.}$$

Step 9. Select 1 in. thick end-plate

Step 10. Calculate the maximum bolt force from Equation 5.4.6

$$T_n = (24.0)\,\frac{(1.00)^{.6872}(329.1)^{.202}}{(0.969)^{.059}(2.41)^{.456}} = 51.9 \text{ kips}$$

Step 11. Since T_n = 51.9 kips is less than the factored bolt capacity, 2x26.5 = 53.0 kips, the connection is adequate.

Use PL 12x1 A36 W/8-7/8 in. diameter A325 bolts.

As noted previously, this example is based on Test EP-2 which used a 1 in. thick end-plate. The design moment corresponds to a measured plate separation of 0.02 in. For the maximum applied moment of 750 ft.-kips (flange force of 387.5 kips), the required plate thickness for maximum stress (Step 8) is 1.12 in.

CHAPTER VI

CONCLUSIONS AND RECOMMENDATIONS

6.1 Summary

This study is the second phase of a research project to develop a design methodology for the stiffened end-plate moment connections having two rows of pretensioned high-strength bolts on either side of the beam flange. The effective stress-strain behavior of steel plate is represented as elastic-perfectly plastic bilinear behavior and of the bolt is represented as bilinear behavior. This geometric configuration results in a highly indeterminate problem as the bolt forces cannot be determined directly. Thus it was decided to conduct an analytical study, modeling the connection as an assemblage of finite elements with the objective of developing prediction equations using regression analysis of finite element results for the connection behavior.

In the analysis it was assumed (which was later verified experimentally) that the tension beam flange and the plate around it act as a (stiffened) tee-hanger. A length of the beam flange equal to the stiffener length (measured along the tee-stem) plus the beam flange thickness are chosen as adequate for inclusion in the analysis domain. One-quarter of a symmetric section of this tension region is analyzed using eight-noded isoparametric brick element for the end-plate elements so that transverse geometry, such as separate bolts at specified gages can be closely represented in the input, and transverse variations of deformations and stresses of the end-plate can be determined in the solution. All other elements are 2-D elements. The effect of bolt heads and welds are incorporated in the analysis. The bolt shank is modeled so that the necking action of the shank can be considered. The boundary conditions of the plate are modeled by an iterative procedure. To consider the inelastic steel behavior in each cycle, the elastic moduli of the yielded elements (i.e., when effective strain exceeds the yield strain for steel) is reset to their secant values.

Information from sufficient cases is gathered from the analytical effort to conduct a feasibility and sensitivity study so as to select certain parameters from the pertinent geometry (end-plate thickness and width; bolt pitch, gage and diameter; and stiffener thickness) and force related variables (flange force and bolt pretension force) governing the connection behavior. The ranges of the parameters have been restricted to practical ranges with thirty-four cases identified for the study. Finite element analyses were carried out for these selected cases and results regressed to yield prediction equations for maximum deflection in the end-plate, maximum bending stresses (in x- and y-directions) in the end-plate, near bolt force and modified near bolt force. For verification, the same analytical results were compared to experimental results from tee-hanger and prototype end-plate tests. Based on comparison of experimental and analytical results, it was concluded that the prediction equations developed adequately explain the connection behavior. Finally, the predicting equations were used to develop a design methodology.

6.2 Conclusions

From the mathematical model investigation it was concluded that the 2D-3D "hybrid" mesh with 137 elements, 236 nodes and 636 d.o.f. (using a single layer of elements in the end-plate) is suitable for the parametric study. It costs less than a more finer mesh model and gives sufficiently accurate results. Both Von-Mises and St. Venant criterion for determining element yielding give about the same results and the Von-Mises criterion was selected. It was found that it is less expensive to calculate the principal strains at the centroid of the element and this method was adopted.

The prototype end-plate connection tests validate the tee-hanger model used in the study. The prediction equations developed from the finite element analyses have been shown to adequately explain the behavior of stiffened end-plate moment connections based on comparisons with six tee-hanger tests and two full-scale tests. Both from analytical and experimental results it is seen that the far bolt remains more or less at pretension level. Thus the ultimate load of the connection can be taken equal to approximately 6.8 equivalent ultimate bolt capacity. The failure criterion limiting the end-plate separation equal to 0.02 in. was found to be adequate in the two prototype tests.

The design procedure was checked with prototype test specimens and the results indicated that the plate thickness obtained from the maximum deflection prediction equation is more conservative than that obtained from the bending stress (y-direction) prediction equation. But there is not a very significant difference between the answers.

Comparing the results with the previous study conducted by

Ahuja[14] it was found that the prediction equation developed considering linear material behavior give very conservative plate thickness (for EP-2 Test about 200% difference). Thus, it is necessary to consider nonlinear material behavior for the end-plate and bolts to develop any design equations.

6.3 Recommendations

The proposed design methodology must be validated with more tests of full beam end-plate connections with different sizes. The present study was restricted to the pure moment condition. Thus a study with combined moment and shear loadings is recommended. Also it may be worthwhile to investigate the behavior of the connections under the cyclic loadings.

REFERENCES

1. Douty, R.T. and W. McGuire, "High Strength Bolted Moment Connections", Journal of the Structural Division, ASCE, Vol. 91, No. ST2, April, 1965, pp. 101-128.

2. ________, Manual of Steel Construction, Seventh ed., American Institute of Steel Construction, New York, NY, 1969.

3. Kato, B. and W. McGuire, "Analysis of T-Stub Flange-to-Column Connections", Journal of the Structural Division, ASCE, Vol. 99, No. ST5, May, 1973, pp. 865-888.

4. Nair, R.S., P.C. Birkemoe and W.H. Munse, "High Strength Bolts Subject to Tension and Prying", Journal of the Structural Division, ASCE, Vol. 100, No. ST2, February, 1974, pp. 351-372.

5. Fisher, J.W. and J.H.A. Struik, Guide to Design Criteria for Bolted and Riveted Joints. New York: John Wiley and Sons, 1974, Chapters 16-18.

6. Mann, A.P. and Morris, L.J., "Limit Design of Extended End-Plate Connections", Journal of the Structural Division, ASCE, Vol. 105, No. ST3, March, 1979, pp. 511-526.

7. Kennedy, N.A., S. Vinnakota and A.N. Sherbourne, "The Split-Tee Analogy in Bolted Splices and Beam-Column Connections", Joints in Structural Steelwork, Proceedings of the International Conference on Joints in Steelwork, held at Middlesbrough, Cleveland, United Kingdom Pentach Press, London, England, 1981, pp. 2.138-2.157.

8. Zoetemeijer, P., "A Design Method for the Tension Side of Statically Loaded, Bolted Beam-to-Column Connections", Heron, Vol. 20, No. 1, The Netherlands, 1974, pp. 1-59.

9. Krishnamurthy, N., "Fresh Look at Bolted End-Plate Behavior and Design", Engineering Journal, American Institute of Steel Construction, Vol. 15, No. 2, Second Quarter, 1978, pp. 39-49.

10. ________, Manual of Steel Construction, Eighth ed., American Institute of Steel Construction, Chicago, IL, 1980.

11. Krishnamurthy, N. and Krishna, V. Radha, "Behavior of Splice-Plate Connections with Multiple Bolt Rows", Report No. CE-MBMA-97/7609-1, Dept. of Civil Engineering, Alabama University, Birmingham, Alabama, Feb., 1981.

12. Krishnamurthy, N., "Analytical Investigation of Bolted Stiffened Tee Stubs", Report #CE-MBMA-1902, Dept. of Civil Engineering, Vanderbilt University, Nashville, Tennessee, December 1978, (submitted to the Metal Building Manufacturers Association).

13. Levy, S., "3-D Isoparametric Finite Element Program", Report No. 71-C-191, General Electric Company, Schenectady, N.Y., June 1971.

14. Ahuja, V., "Analysis of Stiffened End-Plate Connections Using the Finite Element Method", A Thesis submitted to the Graduate Faculty in Partial Fulfillment of the Requirements for the Degree of Master of Science, School of Civil Engineering and Environmental Science, University of Oklahoma, Norman, Oklahoma, 1982.

15. Maxwell, S.M., W.M. Jenkins and J.H. Howlett, "Theoretical Approach to the Analysis of Connection Behavior", Joints in Structural Steelwork, Proceedings of the International Conference on Joints in Steelwork, held at Middlesbrough, Cleveland, United Kingdom Pentach Press, London, England, 1981, pp. 2.49-2.70.

16. Turner, M.H., et al, "Stiffness and Deflection Analysis of Complex Structures", Journal of Aeronautical Science, No. 23, September 1956, pp. 815-824.

17. Ugural, A.C. & S.K. Fenster, Advanced Strength and Applied Elasticity. New York, NY: Elsevier, 1975.

18. ________, Steel Connections/Details and Relative Costs, The Steel Committee of Northern California.

19. Nie, N.H., et al., Statistical Package for the Social Sciences (SPSS). Second edition, New York, NY: McGraw-Hill, Inc., 1975.

20. Isaacson, E. de St Q. and Isaacson M. de St Q., Dimensional Methods in Engineering and Physics. New York: John Wiley and Sons, 1975, Chapter 2.

APPENDIX A

NOMENCLATURE

NOMENCLATURE

A_b = gross area of bolt

A_{gross} = gross area

A_{net} = net area

b_p = end-plate width

d = beam depth

d_b = nominal bolt diameter

d_e = edge distance

d_h = bolt head diameter

d_h' = equivalent bolt head diameter

E = modulus of elasticity

E_s = secant modulus

F = tee-hanger or beam flange applied force

F_{max} = maximum flange force

F_u = factored beam flange force

g = gage, distance between bolt centerlines in the same row

g_e = effective gage

h_t = bolt head thickness

I = moment of inertia

L = beam length

M_p = plastic moment capacity of beam

M_u = factored beam moment

p_b = distance between two rows of bolts

p_e = effective pitch

p_f = pitch, distance from the face of the stem (flange) to the centerline of the near bolt

P_t = bolt pretension force

s_b = length of the stiffener along the end-plate

s_s = length of the stiffener along the beam flange

s_h = length of the tee-stem

SF = scaling factor

t_{fb} = beam flange thickness

t_p = end-plate thickness

t_s = stiffener thickness

t_w = beam web thickness

T_a = near bolt force based on averaging the strains

T_c = near bolt force based on calculating the strain at centroid

T_n = measured near bolt force

T_{nm} = modified near bolt force

T_r = near bolt force from Von-Mises single layer analysis with strain calculated at centroid

T_u = factored bolt force

w_p = size of the fillet weld connecting the stiffener to the end-plate and to the beam flange

w_s = size of the fillet weld connecting the end-plate to the beam flange

w_u = uniform load

Z = plastic section modulus

δ = deflection

δ_a = displacement based on averaging the strains

δ_c = displacement based on calculating the strain at centroid

δ_r = displacement from Von-Mises single layer analysis with strain calculating at centroid

$(\delta_x)_{max}$ = maximum displacement in the end-plate

$\varepsilon_1, \varepsilon_2, \varepsilon_3$ = principal strains

ε_{eff} = effective strain

ε_y = yield strain

ε_u = ultimate strain

θ_c = connection rotation

θ_{max} = maximum beam end rotation

θ_s = equivalent simple beam end rotation

ν = Poisson's ratio

π_i = dependent or independent dimensionless parameter used for regression analysis

ψ_i = dependent or independent parameter used for regression analysis

$\sigma_1, \sigma_2, \sigma_3$ = principal stress

σ_a = maximum stress based on averaging the strains

σ_{by} = bolt yield stress

σ_{bu} = bolt ultimate stress

σ_c = maximum stress based on calculating the strain at centroid

σ_{eff} = effective stress

σ_r = maximum stress from Von-Mises single layer analysis with strain calculated at centroid

$(\sigma_x)_{max}$ = maximum bending stress (x-direction) in the end-plate

σ_y = yield stress

$(\sigma_y)_{max}$ = maximum bending stress (y-direction) in the end-plate

APPENDIX B

PARAMETRIC STUDY USING BUCKINGHAM'S PI-THEOREM

APPENDIX B

PARAMETRIC STUDY USING BUCKINGHAM'S PI-THEOREM

B.1 Independent and Dependent Variables

B.1.1 Independent Variables

The most significant geometry and force independent variables are: t_p = end-plate thickness, p_f = bolt pitch distance, d_d = bolt diameter, t_s = stiffener thickness, g = bolt gage distance, b_p = end-plate width, F = beam flange force and P_t = bolt pretension force. These eight independent variables were reduced to six dimensionless parameters or "Pi-terms" by applying the Buckingham's π Theorem[20]. The normalizing variable for the geometric related parameters was chosen as b_p, where as for the force related parameter, $8P_t$ was chosen as the normalizing variable. The force $8P_t$ corresponds to approximately $8(0.7A_b\ \sigma_{by})$, where A_b = gross area of the bolt and σ_{by} = yield stress of the bolt. Thus, the resulting dimensionless parameters associated with geometry and force are:

$\pi_1 = t_p/b_p$, the plate thickness parameter (B.1.1a)

$\pi_2 = p_f/b_p$, the bolt pitch parameter (B.1.1b)

$\pi_3 = d_b/b_p$, the bolt diameter parameter (B.1.1c)

$\pi_4 = t_s/b_p$, the stiffener thickness parameter (B.1.1d)

$\pi_5 = g/b_p$, the bolt gage parameter (B.1.1e)

$\pi_6 = F/8P_t$, the force parameter (B.1.1f)

B.1.2 Dependent Variables

The most significant dependent variables which are of primary concern in the solution are: $(\delta_x)_{max}$ = the maximum deflection of the end-plate, $(\sigma_y)_{max}$ = the maximum bending stress in the y-direction, $(\sigma_x)_{max}$ = the maximum bending stress in the x-direction, T_n = the near bolt force and T_{nm} = the modified near bolt force. For consistency, the dependent variables were also made dimensionless. The five dependent dimensionless parameters are:

1) The parameter for maximum deflection δ_x is defined as,

$$\pi_a = (\delta_x)_{max}/0.02 \tag{B.1.2a}$$

where the normalizing factor 0.02" is discussed in Reference 14 and Appendix F.

2) The parameter for maximum bending stress $(\sigma_y)_{max}$ in the y-direction is defined as,

$$\pi_{by} = (\sigma_y)_{max}/36.0 \tag{B.1.2b}$$

where the normalizing factor 36.0 is the yield stress of A36 steel.

3) The parameter for maximum bending stress $(\sigma_x)_{max}$ in the x-direction is defined as,

$$\pi_{bx} = (\sigma_x)_{max}/36.0 \tag{B.1.2c}$$

4) The parameter for near bolt force T_n is defined as,

$$\pi_{c1} = T_n/P_t \tag{B.1.2d}$$

where the normalizing factor P_t is the pretension force of the bolt.

5) The parameter for the modified near bolt force T_{nm} is defined as,

$$\pi_{c2} = T_{nm}/P_t \qquad \text{(B.1.2e)}$$

B.2 Predicting Equations and Conclusions

B.2.1 Equations

The cases considered for the analysis were discussed in Section 3.4. The computer package SPSS[19] was used to develop the equations. The predicting equations were sought in the following relationship

$$\pi_i = f_i\,(\pi_1, \pi_2, \pi_3, \pi_4, \pi_5, \pi_6) \qquad \text{(B.2.1)}$$

for i = a, by, bx, c1 and c2. The actual form of the equations was

$$\pi_i = c_{ni}\,\pi_1^{n_{1i}}\,\pi_2^{n_{2i}}\,\pi_3^{n_{3i}}\,\pi_4^{n_{4i}}\,\pi_5^{n_{5i}}\,\pi_6^{n_{6i}} \qquad \text{(B.2.2)}$$

where c_{nj}'s and n_{ij}'s are constants determined by the regression analyses. The technique used for regressing equation B.2.2 involved taking the logarithm of each of the quantities and then the general linear model with multipled regression was carried out and the constants were determined. The value of c_{nj}'s were obtained by simply exponentiating the value obtained from the regression analysis.

The best fit equations that were found are given in Figure B.1. The value of R^2 is indicated in the parentheses by the equations.

B.2.2 Results and Conclusions

The error (computed by comparing predicted and finite element analysis values) associated with the two stress parameter equations in most cases is greater than 25%. The error associated with the deflection parameter equation and the modified bolt force parameter equation is less than for the two stress equations. Figures B.2 and B.3 present the comparison of the values obtained from the prediction equations and those

$$\pi_a = ((\delta_x)_{max}/0.02) = (0.1147)\left(\frac{t_p}{b_p}\right)^{-.915}\left(\frac{p_f}{b_p}\right)^{.415}\left(\frac{d_b}{b_p}\right)^{.762}\left(\frac{t_s}{b_p}\right)^{-.319}\left(\frac{g}{b_p}\right)^{-2.152}\left(\frac{F}{8P_t}\right)^{1.361} \tag{B.2.3}$$

$(R^2 = 0.934)$

$$\pi_{by} = ((\sigma_y)_{max}/36.0) = (2.117)\left(\frac{t_p}{b_p}\right)^{-.959}\left(\frac{p_f}{b_p}\right)^{.472}\left(\frac{d_b}{b_p}\right)^{1.312}\left(\frac{t_s}{b_p}\right)^{-.169}\left(\frac{g}{b_p}\right)^{-.705}\left(\frac{F}{8P_t}\right)^{.792} \tag{B.2.4}$$

$(R^2 = 0.928)$

$$\pi_{bx} = ((\sigma_x)_{max}/36.0) = (7.667)\left(\frac{t_p}{b_p}\right)^{-1.022}\left(\frac{p_f}{b_p}\right)^{.489}\left(\frac{d_b}{b_p}\right)^{1.811}\left(\frac{t_s}{b_p}\right)^{-.123}\left(\frac{g}{b_p}\right)^{-1.383}\left(\frac{F}{8P_t}\right)^{1.261} \tag{B.2.5}$$

$(R^2 = 0.881)$

$$\pi_{c1} = (T_n/P_t) = (1.446)\left(\frac{t_p}{b_p}\right)^{-.511}\left(\frac{p_f}{b_p}\right)^{-.036}\left(\frac{d_b}{b_p}\right)^{.076}\left(\frac{t_s}{b_p}\right)^{-.036}\left(\frac{g}{b_p}\right)^{.080}\left(\frac{F}{8P_t}\right)^{.220} \tag{B.2.6}$$

$(R^2 = 0.773)$

$$\pi_{c2} = (T_{nm}/P_t) = (1.368)\left(\frac{t_p}{b_p}\right)^{-.050}\left(\frac{p_f}{b_p}\right)^{-.004}\left(\frac{d_b}{b_p}\right)^{.058}\left(\frac{t_s}{b_p}\right)^{-.032}\left(\frac{g}{b_p}\right)^{.043}\left(\frac{F}{8P_t}\right)^{.185} \tag{B.2.7}$$

$(R^2 = 0.805)$

Figure B.1 Best Fit Equation Using Buckingham's Pi-Theorem input from the finite element analysis for the deflection and the modified bolt force dependent parameters. Figures relating to the other three dependent parameters are not shown because of large error.

In Figure B.2, it can be seen that the low, intermediate, high and special series lie in distinct patterns. Thus, it was concluded that there should have been parameters reflecting the flexibility of the end-plate geometry or the level of the series (low, intermediate, high and special). A special technique was used to include the importance of the level of the series in the equations but the results were not significantly improved. A measure of end-plate flexibility is bending stiffness of the end-plate. Bending in one direction might be considered in terms of a span associated with the pitch and in the other direction with the gage. Possible flexibility or bending parameters then may be

$$\psi_7 = \frac{p_e^{\,3}}{b_p\, t_s^{\,3}} \tag{B.2.8}$$

with

$$p_e = p_f - d_b/4 - w_s \tag{B.2.9}$$

and

$$\psi_8 = \frac{g_e^{\,3}}{p_f\, t_s^{\,3}} \tag{B.2.10}$$

with

$$g_e = g/2 - d_b/4 - t_s/4. \tag{B.2.11}$$

These parameters significantly improved the accuracy of the resulting predicting equation as discussed in Chapter III.

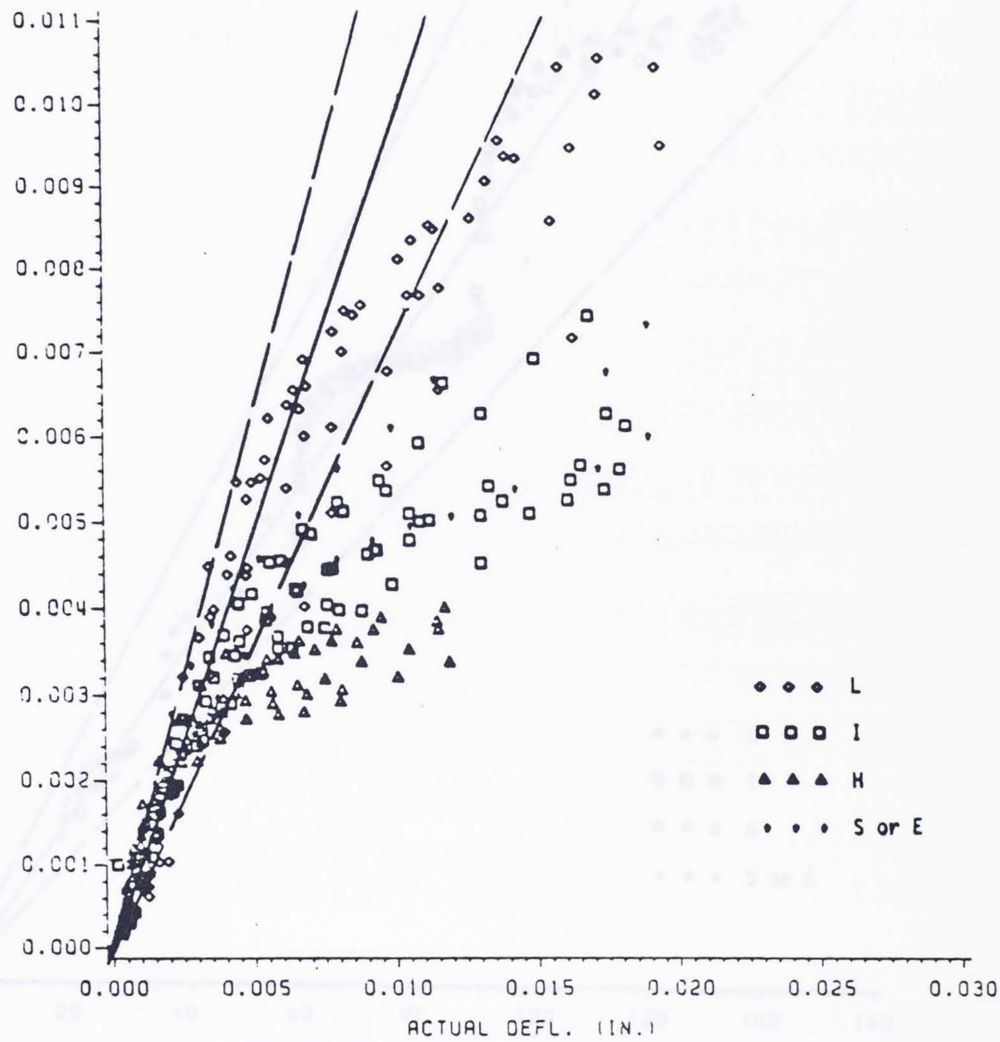

Figure B.2 Predicted Deflection vs. Actual Deflections using only Buckingham π - Terms

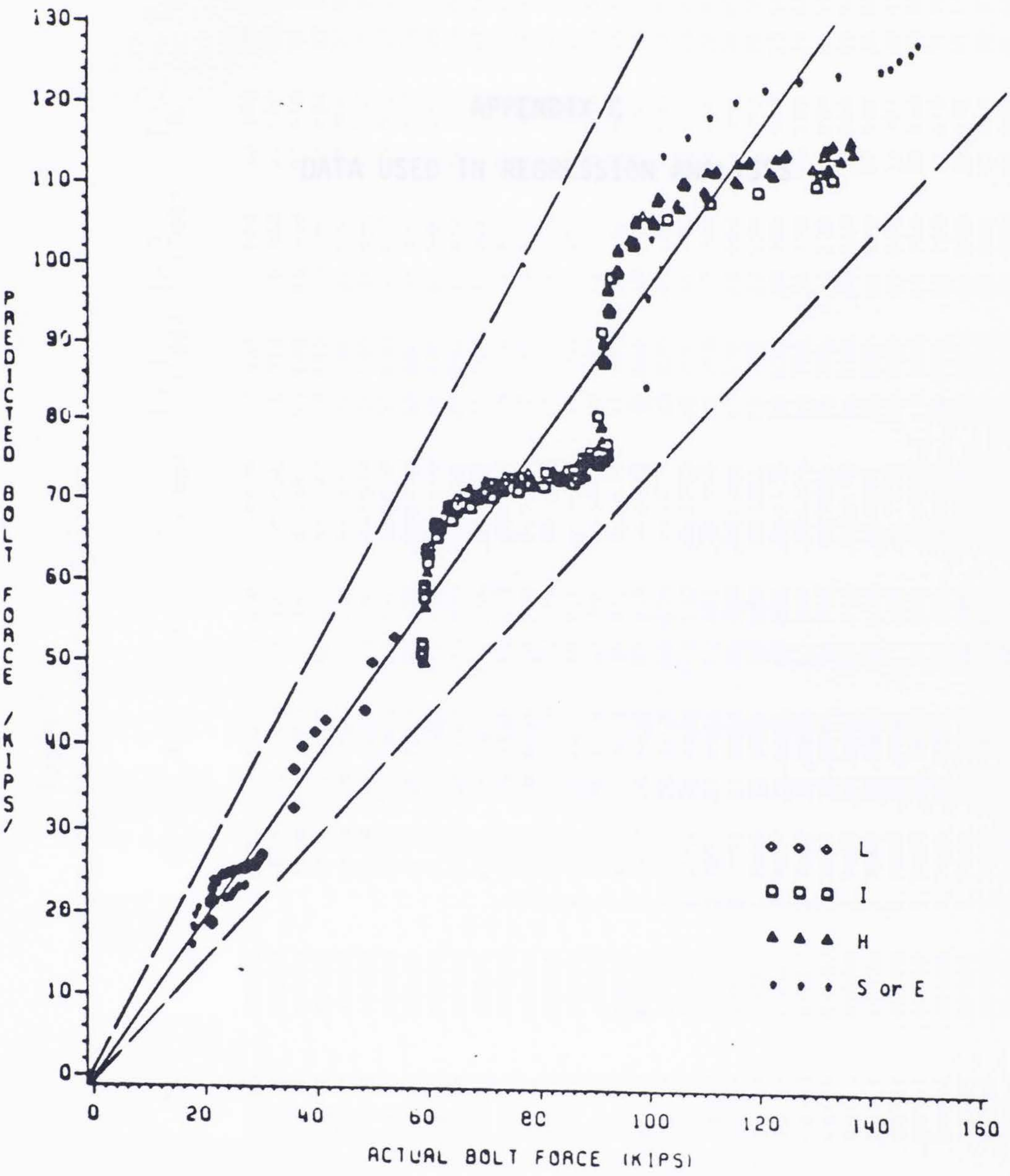

Figure B.3 Predicted Modified Bolt Force vs. Actual Modified Bolt Force using only Buckingham π - Terms

APPENDIX C

DATA USED IN REGRESSION ANALYSES

Table C.1
Data used in Regression Analyses

π_1	π_2	π_3	π_4	π_5	ψ_6	ψ_7	ψ_8	$(\delta_x)_{max}$	$(\sigma_y)_{max}$	$(\sigma_x)_{max}$	T_n	T_{nm}
.06220	.16111	.08951	.04111	.49500	.4128	34.1067	12.460	.000879	7.440	5.080	22.205	20.828
.06220	.16111	.08951	.04111	.49500	.4128	34.1067	24.920	.001626	9.710	9.060	22.180	20.894
.06220	.16111	.08951	.04111	.49500	.4128	34.1067	37.380	.002454	13.600	16.930	22.530	21.312
.06220	.16111	.08951	.04111	.49500	.4128	34.1067	49.830	.003392	18.890	19.340	23.490	22.280
.06220	.16111	.08951	.04111	.49500	.4128	34.1067	62.290	.004427	24.040	24.090	25.390	23.991
.06220	.16111	.08951	.04111	.49500	.4128	34.1067	74.750	.005544	29.140	31.890	27.700	25.998
.06220	.16111	.08951	.04111	.49500	.4128	34.1067	87.210	.006810	32.020	32.600	29.910	27.929
.06220	.16111	.08951	.04111	.49500	.4128	34.1067	99.670	.008850	35.690	35.990	31.970	28.776
.06220	.16111	.08951	.04111	.49500	.4128	34.1067	112.130	.011418	35.020	41.540	33.040	29.190
.06220	.16111	.08951	.04111	.49500	.4128	34.1067	124.580	.014355	37.850	42.950	34.150	29.660
.06220	.16111	.08951	.04111	.49500	.4128	34.1067	137.040	.015906	38.580	43.500	34.590	29.940
.06220	.20780	.08951	.04111	.49500	1.4357	26.4428	12.460	.001080	8.210	6.810	22.133	20.812
.06220	.20780	.08951	.04111	.49500	1.4357	26.4428	24.920	.002015	12.550	12.670	22.028	20.850
.06220	.20780	.08951	.04111	.49500	1.4357	26.4428	37.880	.003052	17.950	19.510	22.399	21.323
.06220	.20780	.08951	.04111	.49500	1.4357	26.4428	49.830	.004190	24.260	25.980	24.901	21.384
.06220	.20780	.08951	.04111	.49500	1.4357	26.4428	62.290	.005413	30.580	31.640	26.504	22.907
.06220	.20780	.08951	.04111	.49500	1.4357	26.4428	74.750	.006897	33.400	37.600	28.659	24.849
.06220	.20780	.08951	.04111	.49500	1.4357	26.4428	87.210	.008579	36.060	38.690	30.582	26.796
.06220	.20780	.08951	.04111	.49500	1.4357	26.4428	99.670	.011271	35.400	41.140	31.605	28.888
.06220	.20780	.08951	.04111	.49500	1.4357	26.4428	112.130	.013759	35.200	41.790	32.660	29.294
.06220	.24000	.08951	.04111	.49500	2.7007	22.8951	12.460	.001215	8.390	7.700	22.100	20.812
.06220	.24000	.08951	.04111	.49500	2.7007	22.8951	24.920	.002280	13.570	14.440	21.952	20.828
.06220	.24000	.08951	.04111	.49500	2.7007	22.8951	37.880	.003461	19.360	22.050	22.352	21.345
.06220	.24000	.08951	.04111	.49500	2.7007	22.8951	49.830	.004779	24.810	28.780	23.570	22.594
.06220	.24000	.08951	.04111	.49500	2.7007	22.8951	62.290	.006223	32.750	35.770	25.599	24.480
.06220	.24000	.08951	.04111	.49500	2.7007	22.8951	74.750	.007851	36.350	38.230	27.924	26.580
.06220	.24000	.08951	.04111	.49500	2.7007	22.8951	87.210	.010178	36.230	40.460	29.986	28.506
.06220	.24000	.08951	.04111	.49500	2.7007	22.8951	99.670	.013291	35.500	42.610	31.549	28.957
.06220	.24000	.08951	.04111	.49500	2.7007	22.8951	112.130	.017235	34.700	43.800	32.701	29.410
.06220	.24000	.11680	.04111	.49500	1.7426	20.7822	21.210	.001586	12.330	17.760	38.630	35.600
.06220	.24000	.11680	.04111	.49500	1.7426	20.7822	42.430	.003010	19.690	32.220	38.610	35.760
.06220	.24000	.11680	.04111	.49500	1.7426	20.7822	63.640	.004730	30.620	41.540	39.970	37.190
.06220	.24000	.11680	.04111	.49500	1.7426	20.7822	84.860	.006814	32.050	42.960	42.260	39.470
.06220	.24000	.11680	.04111	.49500	1.7426	20.7822	106.070	.010915	33.410	44.600	44.050	41.410
.06220	.24000	.14400	.04111	.49500	.9404	18.8101	26.400	.001903	13.900	13.900	53.800	48.500
.06220	.24000	.14400	.04111	.49500	.9404	18.8101	52.800	.003923	25.120	21.420	55.230	49.909
.06220	.24000	.14400	.04111	.49500	.9404	18.8101	79.200	.006772	33.220	20.230	59.530	53.924
.06220	.24000	.08951	.03579	.49500	2.7007	23.3229	12.460	.001250	8.550	7.190	22.092	20.812
.06220	.24000	.08951	.03579	.49500	2.7007	23.3229	24.920	.002347	13.910	13.550	21.944	20.828
.06220	.24000	.08951	.03579	.49500	2.7007	23.3229	37.380	.003582	20.070	20.820	22.433	21.433

π_1	π_2	π_3	π_4	π_5	ψ_6	ψ_7	ψ_8	$(\delta_x)_{max}$	$(\sigma_y)_{max}$	$(\sigma_x)_{max}$	T_n	T_{nm}
.06220	.24000	.08951	.03579	.49500	2.7007	23.3229	49.830	.004948	26.820	27.330	23.692	22.726
.06220	.24000	.08951	.03579	.49500	2.7007	23.3229	62.290	.006452	33.840	34.110	25.923	24.772
.06220	.24000	.08951	.03579	.49500	2.7007	23.3229	74.750	.008282	35.970	37.980	28.149	26.807
.06220	.24000	.08951	.03579	.49500	2.7007	23.3229	87.210	.010651	35.850	39.680	30.345	28.680
.06220	.24000	.08951	.03579	.49500	2.7007	23.3229	99.670	.013966	34.990	41.910	31.800	29.038
.06220	.24000	.08951	.03579	.49500	2.7007	23.3229	112.130	.017316	34.600	42.620	32.766	29.448
.06220	.24000	.08951	.08011	.49500	2.7007	19.9174	12.460	.001069	7.630	7.280	22.129	20.823
.06220	.24000	.08951	.08011	.49500	2.7007	19.9174	24.920	.002004	12.120	14.320	22.024	20.861
.06220	.24000	.08951	.08011	.49500	2.7007	19.9174	37.380	.002992	16.920	25.080	22.200	21.147
.06220	.24000	.08951	.08011	.49500	2.7007	19.9174	49.830	.004086	22.280	32.490	23.036	22.049
.06220	.24000	.08951	.08011	.49500	2.7007	19.9174	62.290	.005273	27.910	38.660	24.360	23.353
.06220	.24000	.08951	.08011	.49500	2.7007	19.9174	74.750	.006660	34.320	40.270	26.418	25.261
.06220	.24000	.08951	.08011	.49500	2.7007	19.9174	87.210	.008167	37.470	41.850	28.558	27.203
.06220	.24000	.08951	.08011	.49500	2.7007	19.9174	99.670	.010494	37.400	42.890	30.491	28.700
.06220	.24000	.08951	.08011	.49500	2.7007	19.9174	112.130	.012737	37.380	43.530	31.531	29.000
.06220	.24000	.08951	.08011	.49500	2.7007	19.9174	124.580	.016293	36.500	44.860	32.648	29.440
.06220	.24000	.08951	.08011	.49500	2.7007	19.9174	137.040	.019316	36.200	45.440	33.393	29.808
.06220	.24000	.08951	.04111	.53420	2.7007	29.7501	12.460	.001208	8.310	5.330	22.100	20.828
.06220	.24000	.08951	.04111	.53420	2.7007	29.7501	24.920	.002267	13.460	10.790	21.954	20.850
.06220	.24000	.08951	.04111	.53420	2.7007	29.7501	37.380	.003448	19.370	16.860	22.381	21.400
.06220	.24000	.08951	.04111	.53420	2.7007	29.7501	49.830	.004763	25.850	22.350	23.594	22.660
.06220	.24000	.08951	.04111	.53420	2.7007	29.7501	62.290	.006184	32.460	28.920	25.649	24.568
.06220	.24000	.08951	.04111	.53420	2.7007	29.7501	74.750	.007792	35.130	32.160	28.064	26.752
.06220	.24000	.08951	.04111	.53420	2.7007	29.7501	87.210	.009777	35.800	33.600	30.354	28.684
.06220	.24000	.08951	.04111	.53420	2.7007	29.7501	99.670	.011629	36.930	35.100	31.332	28.917
.06220	.24000	.08951	.04111	.53420	2.7007	29.7501	112.130	.015587	36.390	36.740	32.748	29.443
.06220	.24000	.08951	.04111	.53420	2.7007	29.7501	124.580	.019500	36.000	37.000	33.750	29.900
.06220	.24000	.08951	.04111	.57891	2.7007	39.0968	12.460	.001202	8.240	3.630	22.100	20.828
.06220	.24000	.08951	.04111	.57891	2.7007	39.0968	24.920	.002257	13.380	7.940	21.951	20.861
.06220	.24000	.08951	.04111	.57891	2.7007	39.0968	37.380	.003441	19.310	12.630	22.409	21.450
.06220	.24000	.08951	.04111	.57891	2.7007	39.0968	49.830	.004756	25.790	17.760	23.625	22.726
.06220	.24000	.08951	.04111	.57891	2.7007	39.0968	62.290	.006168	32.320	23.100	25.703	24.662
.06220	.24000	.08951	.04111	.57891	2.7007	39.0968	74.750	.007773	34.980	26.320	28.199	26.917
.06220	.24000	.08951	.04111	.57891	2.7007	39.0968	87.210	.009735	37.250	27.724	30.542	28.705
.06220	.24000	.08951	.04111	.57891	2.7007	39.0968	99.670	.011569	37.680	28.220	31.284	28.944
.06220	.24000	.08951	.04111	.57891	2.7007	39.0968	112.130	.016314	37.170	31.860	32.910	29.549
.17473	.16110	.11680	.04110	.53420	.0076	1.3723	37.720	.000513	5.160	2.020	61.325	58.823
.17473	.16110	.11680	.04110	.53420	.0076	1.3723	75.430	.000893	5.510	5.490	61.546	59.108
.17473	.16110	.11680	.04110	.53420	.0076	1.3723	113.150	.001342	6.190	9.690	62.068	59.650
.17473	.16110	.11680	.04110	.53420	.0076	1.3723	150.860	.001947	8.110	13.955	63.629	61.073
.17473	.16110	.11680	.04110	.53420	.0076	1.3723	188.580	.002699	10.790	16.772	66.445	63.540
.17473	.16110	.11680	.04110	.53420	.0076	1.3723	226.290	.003553	13.730	19.395	70.208	66.789
.17473	.16110	.11680	.04110	.53420	.0076	1.3723	264.000	.004477	16.910	22.843	74.887	70.772
.17473	.16110	.11680	.04110	.53420	.0076	1.3723	301.720	.005444	20.340	26.176	80.197	75.266
.17473	.16110	.11680	.04110	.53420	.0076	1.3723	339.440	.006456	24.130	29.390	85.928	88.107

π_1	π_2	π_3	π_4	π_5	ψ_6	ψ_7	ψ_8	$(\delta_x)_{max}$	$(\sigma_y)_{max}$	$(\sigma_x)_{max}$	T_n	T_{nm}
.17473	.16110	.11680	.04110	.53420	.0076	1.3723	377.150	.007609	24.620	34.640	91.831	85.148
.17473	.16110	.11680	.04110	.53420	.0076	1.3723	414.870	.009025	25.840	42.370	98.142	87.161
.17473	.16110	.11680	.04110	.53420	.0076	1.3723	452.580	.010882	27.530	47.310	101.027	89.007
.17473	.16110	.11680	.04110	.53420	.0076	1.3723	490.300	.013798	28.190	50.410	105.688	89.738
.17473	.16110	.11680	.04110	.53420	.0076	1.3723	528.000	.017388	28.470	51.590	111.629	92.190
.17473	.20780	.11680	.04110	.53420	.0329	1.0639	37.720	.000545	4.550	2.270	61.214	58.779
.17473	.20780	.11680	.04110	.53420	.0329	1.0639	75.430	.001023	6.000	5.440	61.550	59.210
.17473	.20780	.11680	.04110	.53420	.0329	1.0639	113.150	.001589	8.160	8.620	62.204	59.952
.17473	.20780	.11680	.04110	.53420	.0329	1.0639	150.860	.002365	11.190	11.390	64.265	61.873
.17473	.20780	.11680	.04110	.53420	.0329	1.0639	188.580	.003282	14.680	14.100	67.552	64.802
.17473	.20780	.11680	.04110	.53420	.0329	1.0639	226.290	.004298	18.510	18.220	71.824	68.550
.17473	.20780	.11680	.04110	.53420	.0329	1.0639	264.000	.005401	22.500	24.030	77.224	73.208
.17473	.20780	.11680	.04110	.53420	.0329	1.0639	301.720	.006530	26.540	28.010	82.989	78.164
.17473	.20780	.11680	.04110	.53420	.0329	1.0639	339.440	.007772	28.650	32.930	89.128	83.454
.17473	.20780	.11680	.04110	.53420	.0329	1.0639	377.150	.009265	29.330	39.840	95.591	87.009
.17473	.20780	.11680	.04110	.53420	.0329	1.0639	414.870	.010497	30.120	43.140	98.742	87.578
.17473	.20780	.11680	.04110	.53420	.0329	1.0639	452.580	.013332	29.900	46.860	102.947	89.093
.17473	.20780	.11680	.04110	.53420	.0329	1.0639	490.300	.016576	30.200	49.040	107.899	91.445
.17473	.20780	.11680	.04110	.53420	.0329	1.0639	528.000	.018167	30.280	49.200	109.485	91.890
.17473	.20780	.14400	.04110	.53420	.0152	.9714	57.330	.000709	6.560	3.900	94.517	90.512
.17473	.20780	.14400	.04110	.53420	.0152	.9714	114.650	.001313	8.520	8.070	95.191	91.309
.17473	.20780	.14400	.04110	.53420	.0152	.9714	171.980	.002054	11.510	12.710	96.696	92.843
.17473	.20780	.14400	.04110	.53420	.0152	.9714	229.300	.003136	15.900	16.861	101.446	97.100
.17473	.20780	.14400	.04110	.53420	.0152	.9714	286.630	.004401	20.960	21.510	108.423	103.215
.17473	.20780	.14400	.04110	.53420	.0152	.9714	343.960	.005825	26.500	30.730	117.407	110.978
.17473	.20780	.14400	.04110	.53420	.0152	.9714	401.280	.007571	28.710	38.790	127.482	119.741
.17473	.20780	.14400	.04110	.53420	.0152	.9714	458.610	.009864	29.670	41.660	139.641	130.369
.17473	.20780	.14400	.04110	.53420	.0152	.9714	515.930	.013032	30.050	43.240	150.684	133.340
.17473	.20780	.11680	.03579	.53420	.0329	1.0826	37.720	.000518	4.480	1.840	61.236	58.792
.17473	.20780	.11680	.03579	.53420	.0329	1.0826	75.430	.001210	5.720	4.680	61.550	59.192
.17473	.20780	.11680	.03579	.53420	.0329	1.0826	113.150	.001481	7.720	7.530	62.138	59.857
.17473	.20780	.11680	.03579	.53420	.0329	1.0826	150.860	.002170	10.320	10.500	63.867	61.482
.17473	.20780	.11680	.03579	.53420	.0329	1.0826	188.580	.003001	13.380	14.800	66.777	64.091
.17473	.20780	.11680	.03579	.53420	.0329	1.0826	226.290	.003927	16.840	20.880	70.641	69.888
.17473	.20780	.11680	.03579	.53420	.0329	1.0826	264.000	.004921	20.430	27.430	75.363	71.572
.17473	.20780	.11680	.03579	.53420	.0329	1.0826	301.720	.005961	24.100	31.660	80.754	76.200
.17473	.20780	.11680	.03579	.53420	.0329	1.0826	339.440	.007023	27.820	36.040	86.393	81.036
.17473	.20780	.11680	.03579	.53420	.0329	1.0826	377.150	.008178	29.610	41.340	92.375	86.170
.17473	.20780	.11680	.03579	.53420	.0329	1.0826	414.870	.009692	29.890	46.570	98.250	87.316
.17473	.20780	.11680	.03579	.53420	.0329	1.0826	452.580	.010848	30.150	46.210	99.603	88.295
.17473	.20780	.11680	.03579	.53420	.0329	1.0826	490.300	.013080	30.400	48.260	103.377	89.209
.17473	.20780	.11680	.03579	.53420	.0329	1.0826	528.000	.017506	30.200	49.710	111.273	92.306
.17473	.20780	.11680	.08010	.53420	.0329	.9330	37.720	.000503	4.560	1.720	61.258	58.801
.17473	.20780	.11680	.08010	.53420	.0329	.9330	75.430	.000932	5.680	4.530	61.583	59.206
.17473	.20780	.11680	.08010	.53420	.0329	.9330	113.150	.001437	7.660	7.360	62.189	59.877

π_1	π_2	π_3	π_4	π_5	ψ_6	ψ_7	ψ_8	$(\delta_x)_{max}$	$(\sigma_y)_{max}$	$(\sigma_x)_{max}$	T_n	T_{nm}
.17473	.20780	.11680	.08010	.53420	.0329	.9330	150.860	.002107	10.240	9.880	63.913	61.499
.17473	.20780	.11680	.08010	.53420	.0329	.9330	188.580	.002919	13.300	12.130	66.787	64.078
.17473	.20780	.11680	.08010	.53420	.0329	.9330	226.290	.003830	16.690	20.340	70.655	67.469
.17473	.20780	.11680	.08010	.53420	.0329	.9330	264.000	.004794	20.230	29.930	75.139	71.363
.17473	.20780	.11680	.08010	.53420	.0329	.9330	301.720	.005815	23.870	34.560	80.500	75.969
.17473	.20780	.11680	.08010	.53420	.0329	.9330	339.440	.006867	27.620	39.610	86.136	80.800
.17473	.20780	.11680	.08010	.53420	.0329	.9330	377.150	.008006	29.690	44.460	92.159	85.970
.17473	.20780	.11680	.08010	.53420	.0329	.9330	452.580	.009352	29.800	46.700	98.164	87.260
.17473	.20780	.11680	.08010	.53420	.0329	.9330	490.300	.011194	29.940	47.710	100.826	88.225
.17473	.20780	.11680	.08010	.53420	.0329	.9330	528.000	.014758	29.960	48.300	107.343	90.614
.17473	.20780	.11680	.08010	.53420	.0329	.9330	565.730	.016220	30.000	48.690	108.961	91.427
.17473	.20780	.11680	.04110	.49500	.0329	.8121	37.720	.000570	4.740	2.220	61.231	58.788
.17473	.20780	.11680	.04110	.49500	.0329	.8121	75.430	.001068	6.100	5.429	61.559	59.215
.17473	.20780	.11680	.04110	.49500	.0329	.8121	113.150	.001654	8.210	8.660	62.248	59.984
.17473	.20780	.11680	.04110	.49500	.0329	.8121	150.860	.002458	11.290	11.530	64.393	61.975
.17473	.20780	.11680	.04110	.49500	.0329	.8121	188.580	.003397	14.880	15.030	67.717	64.949
.17473	.20780	.11680	.04110	.49500	.0329	.8121	226.290	.004438	18.750	20.720	72.024	68.723
.17473	.20780	.11680	.04110	.49500	.0329	.8121	264.000	.005560	22.790	26.800	77.372	73.355
.17473	.20780	.11680	.04110	.49500	.0329	.8121	301.720	.006723	26.940	31.630	83.236	78.396
.17473	.20780	.11680	.04110	.49500	.0329	.8121	339.440	.007981	29.120	37.360	89.453	83.748
.17473	.20780	.11680	.04110	.49500	.0329	.8121	377.150	.009452	29.300	44.380	96.044	87.046
.17473	.20780	.11680	.04110	.49500	.0329	.8121	452.580	.011728	29.200	46.550	100.065	88.060
.17473	.20780	.11680	.04110	.49500	.0329	.8121	490.300	.014940	29.820	47.530	105.001	89.881
.17473	.20780	.11680	.04110	.49500	.0329	.8121	528.000	.016887	30.030	48.600	107.211	90.909
.17473	.20780	.11680	.04110	.57890	.0329	1.4091	37.720	.000517	4.370	2.290	61.192	58.775
.17473	.20780	.11680	.04110	.57890	.0329	1.4091	75.430	.000974	5.960	5.420	61.523	59.201
.17473	.20780	.11680	.04110	.57890	.0329	1.4091	113.150	.001513	8.120	8.510	62.156	59.912
.17473	.20780	.11680	.04110	.57890	.0329	1.4091	150.860	.002257	10.970	11.180	64.138	61.753
.17473	.20780	.11680	.04110	.57890	.0329	1.4091	188.580	.003150	14.480	13.300	67.398	64.664
.17473	.20780	.11680	.04110	.57890	.0329	1.4091	226.290	.004148	18.260	17.750	71.778	68.492
.17473	.20780	.11680	.04110	.57890	.0329	1.4091	264.000	.005220	22.230	20.980	77.074	73.057
.17473	.20780	.11680	.04110	.57890	.0329	1.4091	301.720	.006321	26.230	24.310	82.765	77.947
.17473	.20780	.11680	.04110	.57890	.0329	1.4091	339.440	.007477	29.200	27.930	88.743	83.081
.17473	.20780	.11680	.04110	.57890	.0329	1.4091	377.150	.008805	29.430	32.700	94.968	86.947
.17473	.20780	.11680	.04110	.57890	.0329	1.4091	452.580	.010500	29.500	39.310	99.208	87.691
.17473	.20780	.11680	.04110	.57890	.0329	1.4091	490.300	.013019	29.560	44.050	103.008	89.083
.17473	.20780	.11680	.04110	.57890	.0329	1.4091	528.000	.016103	30.170	47.140	108.014	91.084
.17473	.20780	.11680	.04110	.57890	.0329	1.4091	565.730	.017954	30.180	47.700	110.162	92.153
.28805	.16110	.14400	.08010	.57890	.0004	.3303	57.330	.000266	4.450	.100	95.067	91.287
.28805	.16110	.14400	.08010	.57890	.0004	.3303	114.650	.000325	5.020	2.190	95.863	92.004
.28805	.16110	.14400	.08010	.57890	.0004	.3303	171.980	.000435	5.640	5.440	96.801	92.865
.28805	.16110	.14400	.08010	.57890	.0004	.3303	229.310	.000660	6.120	9.730	98.612	94.398
.28805	.16110	.14400	.08010	.57890	.0004	.3303	286.630	.000953	6.390	15.030	101.003	96.394
.28805	.16110	.14400	.08010	.57890	.0004	.3303	343.960	.001314	6.810	20.770	103.776	98.705
.28805	.16110	.14400	.08010	.57890	.0004	.3303	401.290	.001805	8.910	27.740	107.620	101.915

π_1	π_2	π_3	π_4	π_5	ψ_6	ψ_7	ψ_8	$(\delta_x)_{max}$	$(\sigma_y)_{max}$	$(\sigma_x)_{max}$	T_n	T_{nm}
.28805	.16110	.14400	.08010	.57890	.0004	.3303	458.610	.002399	11.260	30.650	112.531	106.026
.28805	.16110	.14400	.08010	.57890	.0004	.3303	515.940	.003050	13.720	29.710	118.088	110.665
.28805	.16110	.14400	.08010	.57890	.0004	.3303	573.270	.003779	16.340	29.600	124.667	116.128
.28805	.16110	.14400	.08010	.57890	.0004	.3303	630.590	.004707	19.220	36.870	132.853	122.981
.28805	.16110	.14400	.08010	.57890	.0004	.3303	687.920	.005824	20.990	42.560	142.980	131.592
.28805	.16110	.14400	.08010	.57890	.0004	.3303	745.250	.006718	20.800	48.770	153.490	133.064
.28805	.16110	.14400	.08010	.57890	.0004	.3303	802.580	.008036	20.920	49.560	160.058	132.284
.28805	.24000	.14400	.08010	.57890	.0083	.2217	57.330	.000291	4.400	.780	94.747	91.144
.28805	.24000	.14400	.08010	.57890	.0083	.2217	114.650	.000392	5.030	3.870	95.196	91.607
.28805	.24000	.14400	.08010	.57890	.0083	.2217	171.980	.000582	5.610	7.680	96.050	92.418
.28805	.24000	.14400	.08010	.57890	.0083	.2217	229.310	.000922	6.240	13.090	97.798	93.980
.28805	.24000	.14400	.08010	.57890	.0083	.2217	286.630	.001514	8.420	16.580	101.259	97.017
.28805	.24000	.14400	.08010	.57890	.0083	.2217	343.960	.002180	10.770	20.140	105.356	100.570
.28805	.24000	.14400	.08010	.57890	.0083	.2217	401.290	.002957	13.450	23.340	110.606	105.083
.28805	.24000	.14400	.08010	.57890	.0083	.2217	458.610	.003779	16.440	24.070	116.355	110.005
.28805	.24000	.14400	.08010	.57890	.0083	.2217	515.940	.004680	19.110	28.440	123.033	115.686
.28805	.24000	.14400	.08010	.57890	.0083	.2217	573.270	.005636	22.540	33.730	130.406	121.928
.28805	.24000	.14400	.08010	.57890	.0083	.2217	630.590	.006820	26.110	39.460	139.652	129.797
.28805	.24000	.14400	.08010	.57890	.0083	.2217	687.920	.008073	26.660	45.330	150.164	132.585
.28805	.24000	.14400	.08010	.57890	.0083	.2217	745.250	.010050	26.230	49.590	156.995	134.885
.28805	.24000	.14400	.08010	.57890	.0083	.2217	802.580	.011880	26.080	53.430	162.738	137.070
.28805	.24000	.11680	.08010	.57890	.0149	.2417	37.720	.000228	3.130	.460	61.334	59.106
.28805	.24000	.11680	.08010	.57890	.0149	.2417	75.430	.000295	3.570	2.420	61.545	59.338
.28805	.24000	.11680	.08010	.57890	.0149	.2417	113.150	.000413	3.860	4.900	61.943	59.724
.28805	.24000	.11680	.08010	.57890	.0149	.2417	150.860	.000606	3.910	8.250	62.644	60.360
.28805	.24000	.11680	.08010	.57890	.0149	.2417	188.580	.000966	4.870	11.440	64.062	61.616
.28805	.24000	.11680	.08010	.57890	.0149	.2417	226.290	.001398	6.310	13.800	65.854	63.186
.28805	.24000	.11680	.08010	.57890	.0149	.2417	264.000	.001904	7.810	15.970	68.110	65.143
.28805	.24000	.11680	.08010	.57890	.0149	.2417	301.720	.002452	9.770	17.970	70.665	67.354
.28805	.24000	.11680	.08010	.57890	.0149	.2417	339.440	.003076	11.730	19.790	73.862	70.081
.28805	.24000	.11680	.08010	.57890	.0149	.2417	377.160	.003842	13.870	21.650	78.183	73.748
.28805	.24000	.11680	.08010	.57890	.0149	.2417	414.870	.004680	16.100	25.030	83.111	77.908
.28805	.24000	.11680	.08010	.57890	.0149	.2417	452.590	.005566	18.380	29.450	88.394	82.374
.28805	.24000	.11680	.08010	.57890	.0149	.2417	490.300	.006497	20.720	35.300	94.082	86.816
.28805	.24000	.11680	.08010	.57890	.0149	.2417	528.020	.007474	23.170	39.650	99.619	87.329
.28805	.24000	.11680	.08010	.57890	.0149	.2417	565.730	.008787	25.610	44.610	102.041	88.113
.28805	.24000	.11680	.08010	.57890	.0149	.2417	603.450	.010460	25.890	53.320	105.684	89.325
.28805	.24000	.11680	.08010	.57890	.0149	.2417	641.170	.011506	26.200	55.130	107.055	89.911
.28805	.24000	.14400	.03579	.57890	.0083	.2548	57.330	.000318	4.480	1.620	94.650	91.078
.28805	.24000	.14400	.03579	.57890	.0083	.2548	114.650	.000456	5.190	4.920	95.050	91.517
.28805	.24000	.14400	.03579	.57890	.0083	.2548	171.980	.000681	5.830	9.190	95.893	92.328
.28805	.24000	.14400	.03579	.57890	.0083	.2548	229.310	.001147	6.960	15.080	98.050	94.271
.28805	.24000	.14400	.03579	.57890	.0083	.2548	286.630	.001820	9.400	18.896	101.764	97.533
.28805	.24000	.14400	.03579	.57890	.0083	.2548	343.960	.002594	12.120	22.450	106.383	101.542
.28805	.24000	.14400	.03579	.57890	.0083	.2548	401.290	.003481	15.120	25.690	112.319	106.620

π_1	π_2	π_3	π_4	π_5	ψ_6	ψ_7	ψ_8	$(\delta_x)_{max}$	$(\sigma_y)_{max}$	$(\sigma_x)_{max}$	T_n	T_{nm}
.28805	.24000	.14400	.03579	.57890	.0083	.2548	458.610	.004432	18.260	25.190	118.874	112.214
.28805	.24000	.14400	.03579	.57890	.0083	.2548	515.940	.005436	21.430	25.200	125.965	118.251
.28805	.24000	.14400	.03579	.57890	.0083	.2548	573.270	.006570	25.080	30.910	133.812	124.961
.28805	.24000	.14400	.03579	.57890	.0083	.2548	630.590	.007905	26.770	40.420	143.152	132.014
.28805	.24000	.14400	.03579	.57890	.0083	.2548	687.920	.009486	26.310	51.110	152.132	133.474
.28805	.24000	.14400	.03579	.57890	.0083	.2548	745.250	.011719	25.320	57.250	161.325	136.752
.28805	.24000	.14400	.04110	.57890	.0083	.2507	57.330	.000314	4.460	1.510	94.664	91.086
.28805	.24000	.14400	.04110	.57890	.0083	.2507	114.650	.000446	5.160	4.760	95.069	91.529
.28805	.24000	.14400	.04110	.57890	.0083	.2507	171.980	.000666	5.790	8.950	95.914	92.336
.28805	.24000	.14400	.04110	.57890	.0083	.2507	229.310	.001111	6.840	14.750	98.006	94.218
.28805	.24000	.14400	.04110	.57890	.0083	.2507	286.630	.001772	9.240	18.500	101.682	97.447
.28805	.24000	.14400	.04110	.57890	.0083	.2507	343.960	.002529	11.900	22.050	106.219	101.386
.28805	.24000	.14400	.04110	.57890	.0083	.2507	401.290	.003393	14.670	25.290	111.984	106.329
.28805	.24000	.14400	.04110	.57890	.0083	.2507	458.610	.004325	17.860	24.700	118.448	111.841
.28805	.24000	.14400	.04110	.57890	.0083	.2507	515.940	.005310	21.090	25.580	125.470	117.817
.28805	.24000	.14400	.04110	.57890	.0083	.2507	573.270	.006405	24.600	29.110	133.243	124.449
.28805	.24000	.14400	.04110	.57890	.0083	.2507	630.590	.007722	26.740	40.500	142.470	131.951
.28805	.24000	.14400	.04110	.57890	.0083	.2507	687.920	.009192	26.600	49.090	151.349	133.154
.28805	.24000	.14400	.04110	.57890	.0083	.2507	745.250	.011457	26.000	57.845	160.845	136.500
.28805	.24000	.14400	.08010	.49500	.0083	.1224	57.330	.000337	4.940	.130	94.828	91.253
.28805	.24000	.14400	.08010	.49500	.0083	.1224	114.650	.000468	5.520	3.280	95.375	91.799
.28805	.24000	.14400	.08010	.49500	.0083	.1224	171.980	.000673	6.070	6.960	96.240	92.614
.28805	.24000	.14400	.08010	.49500	.0083	.1224	229.310	.001003	6.430	12.170	97.840	94.065
.28805	.24000	.14400	.08010	.49500	.0083	.1224	286.630	.001598	8.380	16.710	101.308	97.099
.28805	.24000	.14400	.08010	.49500	.0083	.1224	343.960	.002298	10.670	13.200	105.576	100.800
.28805	.24000	.14400	.08010	.49500	.0083	.1224	401.290	.003115	13.300	18.840	111.019	105.477
.28805	.24000	.14400	.08010	.49500	.0083	.1224	458.610	.003997	16.090	23.980	117.034	110.638
.28805	.24000	.14400	.08010	.53420	.0083	.1639	57.330	.000316	4.670	.400	94.789	91.208
.28805	.24000	.14400	.08010	.53420	.0083	.1639	114.650	.000433	5.270	3.521	95.288	91.708
.28805	.24000	.14400	.08010	.53420	.0083	.1639	171.980	.000631	5.840	7.370	96.148	92.520
.28805	.24000	.14400	.08010	.53420	.0083	.1639	229.310	.000974	6.340	12.740	97.875	94.074
.28805	.24000	.14400	.08010	.53420	.0083	.1639	286.630	.001580	8.460	16.690	101.449	97.201
.28805	.24000	.14400	.08010	.53420	.0083	.1639	343.960	.002257	10.750	20.520	105.575	100.788
.28805	.24000	.14400	.08010	.53420	.0083	.1639	401.290	.003049	13.420	19.890	110.887	105.354
.28805	.24000	.14400	.08010	.53420	.0083	.1639	458.610	.003893	16.200	26.460	116.627	110.294
.28805	.24000	.14400	.08010	.53420	.0083	.1639	515.940	.004819	19.220	30.920	123.455	116.102
.28805	.24000	.14400	.08010	.53420	.0083	.1639	573.270	.005824	22.340	36.810	131.136	122.611
.28805	.24000	.14400	.08010	.53420	.0083	.1639	630.590	.007121	26.050	38.780	141.182	131.162
.28805	.24000	.14400	.08010	.53420	.0083	.1639	687.920	.008618	26.380	42.430	151.238	132.989
.08610	.19360	.10760	.04303	.60240	.2786	25.7578	10.580	.000526	6.660	3.610	18.563	17.561
.08610	.19360	.10760	.04303	.60240	.2786	25.7578	21.170	.000963	7.060	7.610	18.577	17.645
.08610	.19360	.10760	.04303	.60240	.2786	25.7578	31.750	.001468	9.870	11.420	18.859	17.971
.08610	.19360	.10760	.04303	.60240	.2786	25.7578	42.330	.002044	13.050	15.840	19.470	18.600
.08610	.19360	.10760	.04303	.60240	.2786	25.7578	52.910	.002774	18.330	19.920	21.227	20.140
.08610	.19360	.10760	.04303	.60240	.2786	25.7578	63.500	.003516	23.350	25.440	23.084	21.766

π_1	π_2	π_3	π_4	π_5	ψ_6	ψ_7	ψ_8	$(\delta_x)_{max}$	$(\sigma_y)_{max}$	$(\sigma_x)_{max}$	T_n	T_{nm}
.08610	.19360	.10760	.04303	.60240	.2786	25.7578	74.080	.004268	28.280	29.400	24.974	23.399
.08610	.19360	.10760	.04303	.60240	.2786	25.7578	84.660	.005198	31.330	35.800	26.926	24.428
.08610	.19360	.10760	.04303	.60240	.2786	25.7578	95.250	.006613	34.950	37.790	28.029	24.735
.08610	.19360	.10760	.04303	.60240	.2786	25.7578	105.830	.008003	36.530	38.780	28.875	25.075
.08610	.19360	.10760	.04303	.60240	.2786	25.7578	116.410	.009893	35.900	40.340	29.906	25.515
.08610	.19360	.10760	.04303	.60240	.2786	25.7578	126.990	.011421	35.130	41.050	30.532	25.847
.08610	.19360	.10760	.04303	.60240	.2786	25.7578	137.580	.017526	35.090	44.940	32.706	26.872
.08610	.19360	.10760	.04303	.60240	.2786	25.7578	148.160	.018964	35.000	45.000	33.173	27.192
.19048	.15880	.09530	.06350	.47630	.0066	.4522	62.290	.000568	4.030	.690	103.236	99.283
.19048	.15880	.09530	.06350	.47630	.0066	.4522	124.570	.000982	4.500	2.970	103.561	99.706
.19048	.15880	.09530	.06350	.47630	.0066	.4522	186.860	.001468	4.910	5.790	104.160	100.382
.19048	.15880	.09530	.06350	.47630	.0066	.4522	249.140	.002074	5.130	9.750	105.483	101.640
.19048	.15880	.09530	.06350	.47630	.0066	.4522	311.430	.002837	6.240	13.520	104.008	102.698
.19048	.15880	.09530	.06350	.47630	.0066	.4522	373.720	.003697	8.050	16.210	111.602	107.117
.19048	.15880	.09530	.06350	.47630	.0066	.4522	436.000	.004658	10.040	18.580	116.247	111.154
.19048	.15880	.09530	.06350	.47630	.0066	.4522	498.290	.005682	12.180	20.830	121.727	115.883
.19048	.15880	.09530	.06350	.47630	.0066	.4522	560.570	.006766	14.410	22.950	127.990	121.237
.19048	.15880	.09530	.06350	.47630	.0066	.4522	622.860	.007941	16.670	25.140	135.323	127.485
.19048	.15880	.09530	.06350	.47630	.0066	.4522	685.150	.009201	18.940	27.390	143.655	134.558
.19048	.15880	.09530	.06350	.47630	.0066	.4522	747.430	.010536	21.220	29.420	152.770	142.294
.19048	.15880	.09530	.06350	.47630	.0066	.4522	809.720	.012001	22.970	36.340	162.722	144.075
.19048	.15880	.09530	.06350	.47630	.0066	.4522	872.000	.014263	24.420	43.660	167.462	145.638
.19048	.15880	.09530	.06350	.47630	.0066	.4522	934.290	.017207	24.670	45.720	173.631	147.808
.19048	.15880	.09530	.06350	.47630	.0066	.4522	996.580	.018987	24.930	54.280	176.419	149.012
.06220	.24000	.08951	.04111	.49500	2.7007	22.8951	12.460	.001215	8.390	7.700	22.100	20.812
.06220	.24000	.08951	.04111	.49500	2.7007	22.8951	24.920	.002280	13.570	14.440	21.952	20.828
.06220	.24000	.08951	.04111	.49500	2.7007	22.8951	37.880	.003461	19.360	22.050	22.352	21.345
.06220	.24000	.08951	.04111	.49500	2.7007	22.8951	49.830	.004779	24.810	28.780	23.570	22.594
.06220	.24000	.08951	.04111	.49500	2.7007	22.8951	62.290	.006223	32.750	35.770	25.599	24.480
.06220	.24000	.08951	.04111	.49500	2.7007	22.8951	74.750	.007851	36.350	38.230	27.924	26.580
.06220	.24000	.08951	.04111	.49500	2.7007	22.8951	87.210	.010178	36.230	40.460	29.986	28.506
.06220	.24000	.08951	.04111	.49500	2.7007	22.8951	99.670	.013291	35.500	42.610	31.549	28.957
.06220	.24000	.08951	.04111	.49500	2.7007	22.8951	112.130	.017235	34.700	43.800	32.701	29.410
.06220	.20780	.08951	.04111	.49500	1.4357	26.4428	12.460	.001080	8.210	6.810	22.133	20.812
.06220	.20780	.08951	.04111	.49500	1.4357	26.4428	24.920	.002015	12.550	12.670	22.028	20.850
.06220	.20780	.08951	.04111	.49500	1.4357	26.4428	37.880	.003052	17.950	19.510	22.399	21.323
.06220	.20780	.08951	.04111	.49500	1.4357	26.4428	49.830	.004190	24.260	25.980	24.901	21.384
.06220	.20780	.08951	.04111	.49500	1.4357	26.4428	62.290	.005413	30.580	31.640	26.504	22.907
.06220	.20780	.08951	.04111	.49500	1.4357	26.4428	74.750	.006897	33.400	37.600	28.659	24.849
.06220	.20780	.08951	.04111	.49500	1.4357	26.4428	87.210	.008579	36.060	38.690	30.582	26.796
.06220	.20780	.08951	.04111	.49500	1.4357	26.4428	99.670	.011271	35.400	41.140	31.605	28.888
.06220	.20780	.08951	.04111	.49500	1.4357	26.4428	112.130	.013759	35.200	41.790	32.660	29.294
.06220	.20780	.08951	.04111	.49500	1.4357	26.4428	12.460	.001080	8.210	6.810	22.133	20.812
.06220	.20780	.08951	.04111	.49500	1.4357	26.4428	24.920	.002015	12.550	12.670	22.028	20.850
.06220	.20780	.08951	.04111	.49500	1.4357	26.4428	37.880	.003052	17.950	19.510	22.399	21.323

π_1	π_2	π_3	π_4	π_5	ψ_6	ψ_7	ψ_8	$(\delta_x)_{max}$	$(\sigma_y)_{max}$	$(\sigma_x)_{max}$	T_n	T_{nm}
.06220	.20780	.08951	.04111	.49500	1.4357	26.4428	49.830	.004190	24.260	25.980	24.901	21.384
.06220	.20780	.08951	.04111	.49500	1.4357	26.4428	62.290	.005413	30.580	31.640	26.504	22.907
.06220	.20780	.08951	.04111	.49500	1.4357	26.4428	74.750	.006897	33.400	37.600	28.659	24.849
.06220	.20780	.08951	.04111	.49500	1.4357	26.4428	87.210	.008579	36.060	38.690	30.582	26.796
.06220	.20780	.08951	.04111	.49500	1.4357	26.4428	99.670	.011271	35.400	41.140	31.605	28.888
.06220	.20780	.08951	.04111	.49500	1.4357	26.4428	112.130	.013759	35.200	41.790	32.660	29.294
.17473	.20780	.11680	.04110	.53420	.0329	1.0639	37.720	.000545	4.550	2.270	61.214	58.779
.17473	.20780	.11680	.04110	.53420	.0329	1.0639	75.430	.001023	6.000	5.440	61.550	59.210
.17473	.20780	.11680	.04110	.53420	.0329	1.0639	113.150	.001589	8.160	8.620	62.204	59.952
.17473	.20780	.11680	.04110	.53420	.0329	1.0639	150.860	.002365	11.190	11.390	64.265	61.873
.17473	.20780	.11680	.04110	.53420	.0329	1.0639	188.580	.003282	14.680	14.100	67.552	64.802
.17473	.20780	.11680	.04110	.53420	.0329	1.0639	226.290	.004298	18.510	18.220	71.824	68.550
.17473	.20780	.11680	.04110	.53420	.0329	1.0639	264.000	.005401	22.500	24.030	77.224	73.208
.17473	.20780	.11680	.04110	.53420	.0329	1.0639	301.720	.006530	26.540	28.010	82.989	78.164
.17473	.20780	.11680	.04110	.53420	.0329	1.0639	339.440	.007772	28.650	32.930	89.128	83.454
.17473	.20780	.11680	.04110	.53420	.0329	1.0639	377.150	.009265	29.330	39.840	95.591	87.009
.17473	.20780	.11680	.04110	.53420	.0329	1.0639	414.870	.010497	30.120	43.140	98.742	87.578
.17473	.20780	.11680	.04110	.53420	.0329	1.0639	452.580	.013332	29.900	46.860	102.947	89.093
.17473	.20780	.11680	.04110	.53420	.0329	1.0639	490.300	.016576	30.200	49.040	107.899	91.445
.17473	.20780	.11680	.04110	.53420	.0329	1.0639	528.000	.018167	30.280	49.200	109.485	91.890
.17473	.20780	.11680	.04110	.53420	.0329	1.0639	37.720	.000545	4.550	2.270	61.214	58.779
.17473	.20780	.11680	.04110	.53420	.0329	1.0639	75.430	.001023	6.000	5.440	61.550	59.210
.17473	.20780	.11680	.04110	.53420	.0329	1.0639	113.150	.001589	8.160	8.620	62.204	59.952
.17473	.20780	.11680	.04110	.53420	.0329	1.0639	150.860	.002365	11.190	11.390	64.265	61.873
.17473	.20780	.11680	.04110	.53420	.0329	1.0639	188.580	.003282	14.680	14.100	67.552	64.802
.17473	.20780	.11680	.04110	.53420	.0329	1.0639	226.290	.004298	18.510	18.220	71.824	68.550
.17473	.20780	.11680	.04110	.53420	.0329	1.0639	264.000	.005401	22.500	24.030	77.224	73.208
.17473	.20780	.11680	.04110	.53420	.0329	1.0639	301.720	.006530	26.540	28.010	82.989	78.164
.17473	.20780	.11680	.04110	.53420	.0329	1.0639	339.440	.007772	28.650	32.930	89.128	83.454
.17473	.20780	.11680	.04110	.53420	.0329	1.0639	377.150	.009265	29.330	39.840	95.591	87.009
.17473	.20780	.11680	.04110	.53420	.0329	1.0639	414.870	.010497	30.120	43.140	98.742	87.578
.17473	.20780	.11680	.04110	.53420	.0329	1.0639	452.580	.013332	29.900	46.860	102.947	89.093
.17473	.20780	.11680	.04110	.53420	.0329	1.0639	490.300	.016576	30.200	49.040	107.899	91.445
.17473	.20780	.11680	.04110	.53420	.0329	1.0639	528.000	.018167	30.280	49.200	109.485	91.890
.17473	.20780	.11680	.04110	.53420	.0329	1.0639	37.720	.000545	4.550	2.270	61.214	58.779
.17473	.20780	.11680	.04110	.53420	.0329	1.0639	75.430	.001023	6.000	5.440	61.550	59.210
.17473	.20780	.11680	.04110	.53420	.0329	1.0639	113.150	.001589	8.160	8.620	62.204	59.952
.17473	.20780	.11680	.04110	.53420	.0329	1.0639	150.860	.002365	11.190	11.390	64.265	61.873
.17473	.20780	.11680	.04110	.53420	.0329	1.0639	188.580	.003282	14.680	14.100	67.552	64.802
.17473	.20780	.11680	.04110	.53420	.0329	1.0639	226.290	.004298	18.510	18.220	71.824	68.550
.17473	.20780	.11680	.04110	.53420	.0329	1.0639	264.000	.005401	22.500	24.030	77.224	73.208
.17473	.20780	.11680	.04110	.53420	.0329	1.0639	301.720	.006530	26.540	28.010	82.989	78.164
.17473	.20780	.11680	.04110	.53420	.0329	1.0639	339.440	.007772	28.650	32.930	89.128	83.454
.17473	.20780	.11680	.04110	.53420	.0329	1.0639	377.150	.009265	29.330	39.840	95.591	87.009
.17473	.20780	.11680	.04110	.53420	.0329	1.0639	414.870	.010497	30.120	43.140	98.742	87.578

π_1	π_2	π_3	π_4	π_5	ψ_6	ψ_7	ψ_8	$(\delta_x)_{max}$	$(\sigma_y)_{max}$	$(\sigma_x)_{max}$	T_n	T_{nm}
.17473	.20780	.11680	.04110	.53420	.0329	1.0639	452.580	.013332	29.900	46.860	102.947	89.093
.17473	.20780	.11680	.04110	.53420	.0329	1.0639	490.300	.016576	30.200	49.040	107.899	91.445
.17473	.20780	.11680	.04110	.53420	.0329	1.0639	528.000	.018167	30.280	49.200	109.485	91.890
.28805	.24000	.14400	.08010	.57890	.0083	.2217	57.330	.000291	4.400	.780	94.747	91.144
.28805	.24000	.14400	.08010	.57890	.0083	.2217	114.650	.000392	5.030	3.870	95.196	91.607
.28805	.24000	.14400	.08010	.57890	.0083	.2217	171.980	.000582	5.610	7.680	96.050	92.418
.28805	.24000	.14400	.08010	.57890	.0083	.2217	229.310	.000922	6.240	13.090	97.798	93.980
.28805	.24000	.14400	.08010	.57890	.0083	.2217	286.630	.001514	8.420	16.580	101.259	97.017
.28805	.24000	.14400	.08010	.57890	.0083	.2217	343.960	.002180	10.770	20.140	105.356	100.570
.28805	.24000	.14400	.08010	.57890	.0083	.2217	401.290	.002957	13.450	23.340	110.606	105.083
.28805	.24000	.14400	.08010	.57890	.0083	.2217	458.610	.003779	16.440	24.070	116.355	110.005
.28805	.24000	.14400	.08010	.57890	.0083	.2217	515.940	.004680	19.110	28.440	123.033	115.686
.28805	.24000	.14400	.08010	.57890	.0083	.2217	573.270	.005636	22.540	33.730	130.406	121.928
.28805	.24000	.14400	.08010	.57890	.0083	.2217	630.590	.006820	26.110	39.460	139.652	129.797
.28805	.24000	.14400	.08010	.57890	.0083	.2217	687.920	.008073	26.660	45.330	150.164	132.585
.28805	.24000	.14400	.08010	.57890	.0083	.2217	745.250	.010050	26.230	49.590	156.995	134.885
.28805	.24000	.14400	.08010	.57890	.0083	.2217	802.580	.011880	26.080	53.430	162.738	137.070
.28805	.24000	.14400	.08010	.57890	.0083	.2217	57.330	.000291	4.400	.780	94.747	91.144
.28805	.24000	.14400	.08010	.57890	.0083	.2217	114.650	.000392	5.030	3.870	95.196	91.607
.28805	.24000	.14400	.08010	.57890	.0083	.2217	171.980	.000582	5.610	7.680	96.050	92.418
.28805	.24000	.14400	.08010	.57890	.0083	.2217	229.310	.000922	6.240	13.090	97.798	93.980
.28805	.24000	.14400	.08010	.57890	.0083	.2217	286.630	.001514	8.420	16.580	101.259	97.017
.28805	.24000	.14400	.08010	.57890	.0083	.2217	343.960	.002180	10.770	20.140	105.356	100.570
.28805	.24000	.14400	.08010	.57890	.0083	.2217	401.290	.002957	13.450	23.340	110.606	105.083
.28805	.24000	.14400	.08010	.57890	.0083	.2217	458.610	.003779	16.440	24.070	116.355	110.005
.28805	.24000	.14400	.08010	.57890	.0083	.2217	515.940	.004680	19.110	28.440	123.033	115.686
.28805	.24000	.14400	.08010	.57890	.0083	.2217	573.270	.005636	22.540	33.730	130.406	121.928
.28805	.24000	.14400	.08010	.57890	.0083	.2217	630.590	.006820	26.110	39.460	139.652	129.797
.28805	.24000	.14400	.08010	.57890	.0083	.2217	687.920	.008073	26.660	45.330	150.164	132.585
.28805	.24000	.14400	.08010	.57890	.0083	.2217	745.250	.010050	26.230	49.590	156.995	134.885
.28805	.24000	.14400	.08010	.57890	.0083	.2217	802.580	.011880	26.080	53.430	162.738	137.070
.28805	.24000	.14400	.08010	.57890	.0083	.2217	57.330	.000291	4.400	.780	94.747	91.144
.28805	.24000	.14400	.08010	.57890	.0083	.2217	114.650	.000392	5.030	3.870	95.196	91.607
.28805	.24000	.14400	.08010	.57890	.0083	.2217	171.980	.000582	5.610	7.680	96.050	92.418
.28805	.24000	.14400	.08010	.57890	.0083	.2217	229.310	.000922	6.240	13.090	97.798	93.980
.28805	.24000	.14400	.08010	.57890	.0083	.2217	286.630	.001514	8.420	16.580	101.259	97.017
.28805	.24000	.14400	.08010	.57890	.0083	.2217	343.960	.002180	10.770	20.140	105.356	100.570
.28805	.24000	.14400	.08010	.57890	.0083	.2217	401.290	.002957	13.450	23.340	110.606	105.083
.28805	.24000	.14400	.08010	.57890	.0083	.2217	458.610	.003779	16.440	24.070	116.355	110.005
.28805	.24000	.14400	.08010	.57890	.0083	.2217	515.940	.004680	19.110	28.440	123.033	115.686
.28805	.24000	.14400	.08010	.57890	.0083	.2217	573.270	.005636	22.540	33.730	130.406	121.928
.28805	.24000	.14400	.08010	.57890	.0083	.2217	630.590	.006820	26.110	39.460	139.652	129.797
.28805	.24000	.14400	.08010	.57890	.0083	.2217	687.920	.008073	26.660	45.330	150.164	132.585
.28805	.24000	.14400	.08010	.57890	.0083	.2217	745.250	.010050	26.230	49.590	156.995	134.885
.28805	.24000	.14400	.08010	.57890	.0083	.2217	802.580	.011880	26.080	53.430	162.738	137.070

APPENDIX D

TEE-HANGER TEST RESULTS

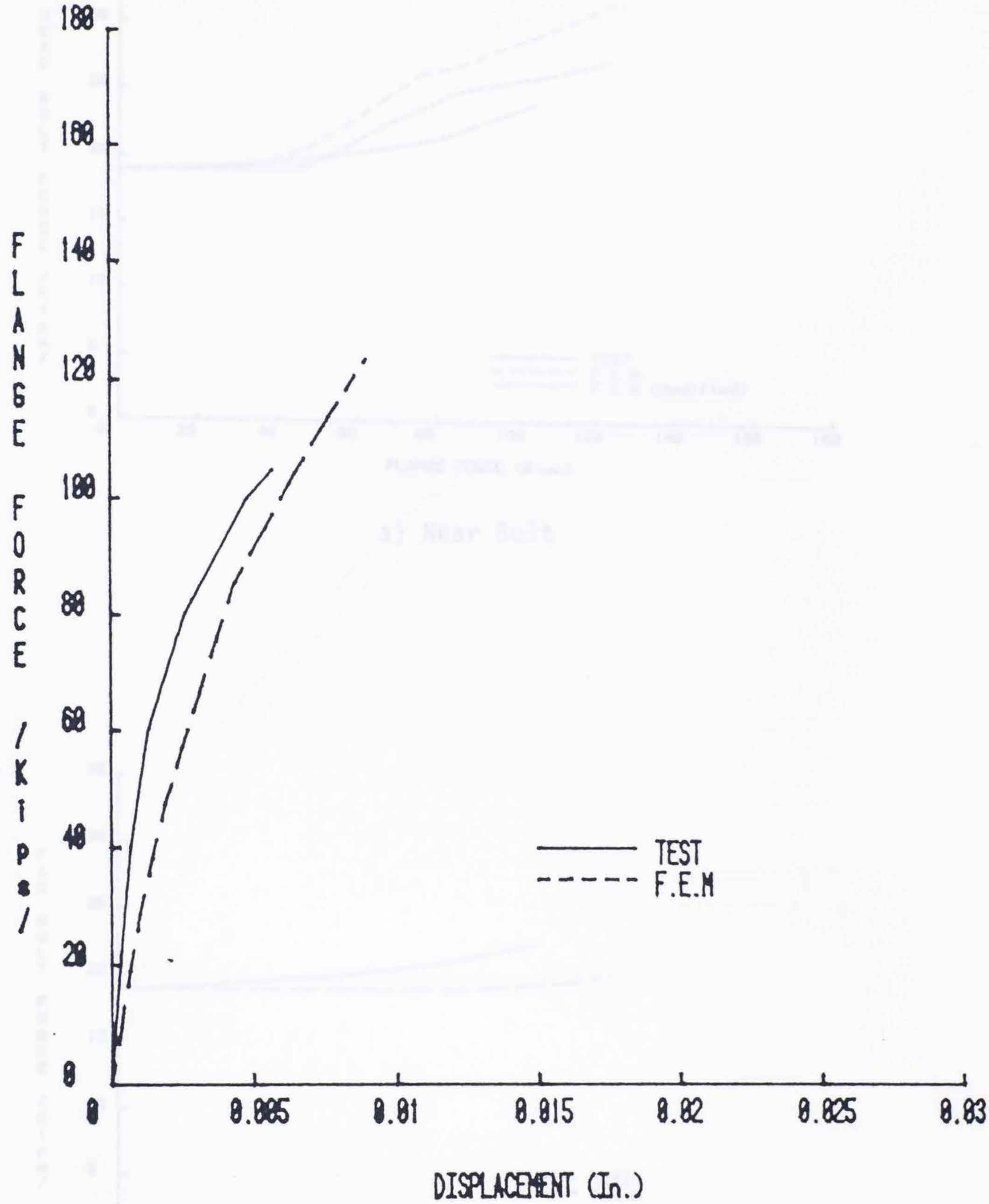

Figure D.1 Flange Force vs. Plate Separation, Test TH-1

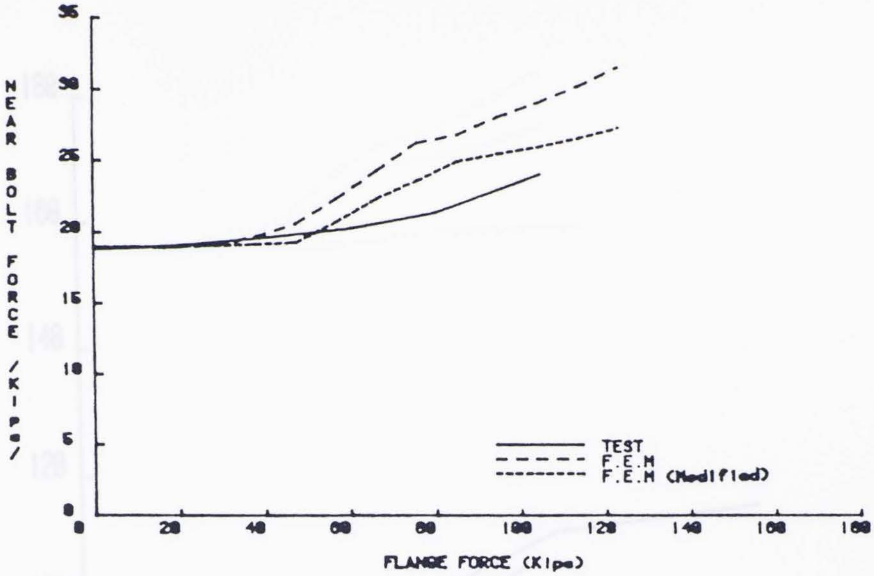

a) Near Bolt

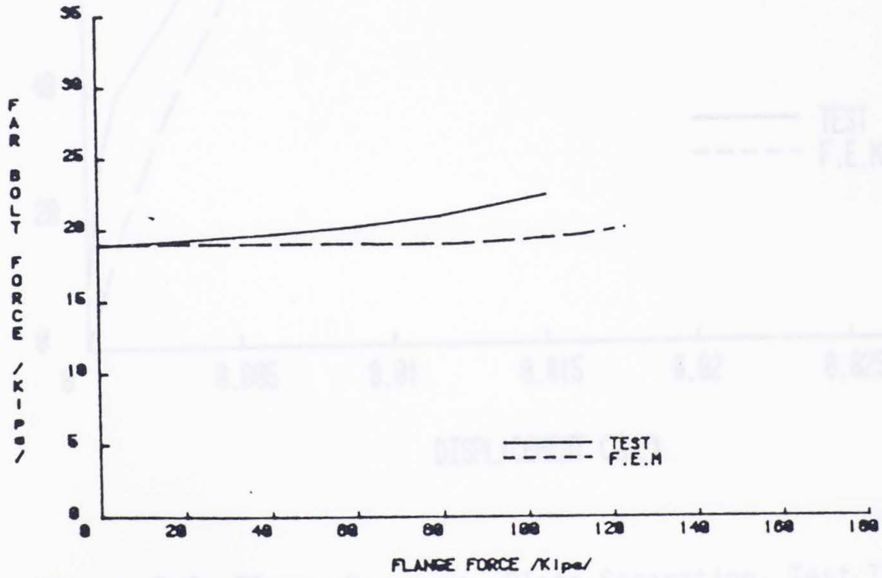

b) Far Bolt

Figure D.2 Bolt Force vs. Flange Force, Test TH-1

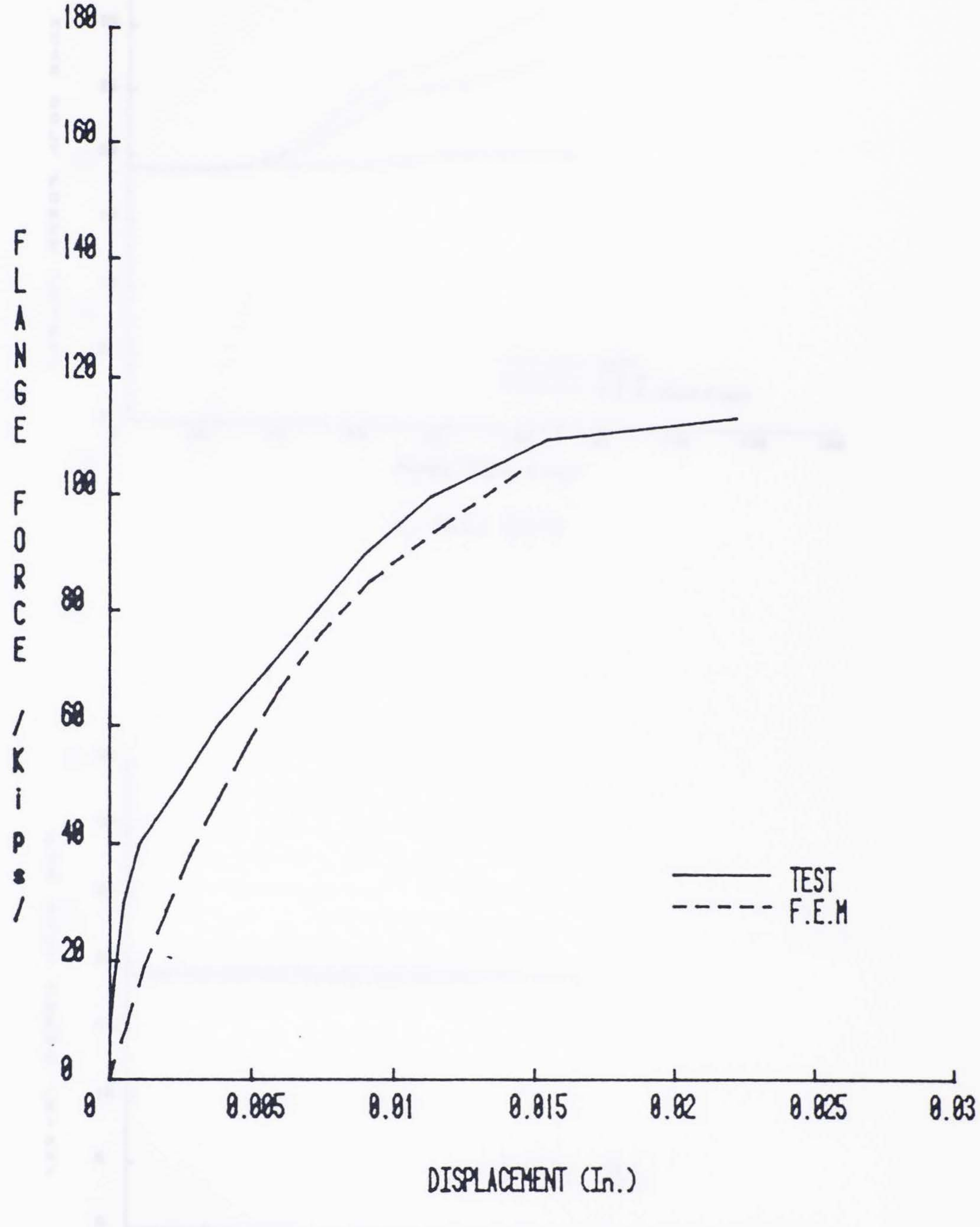

Figure D.3 Flange Force vs. Plate Separation, Test TH-2

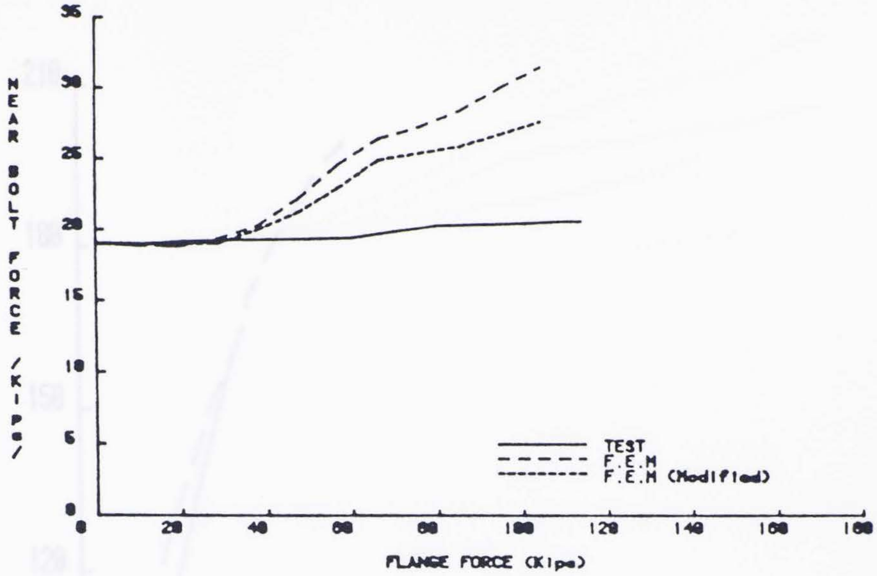

a) Near Bolt

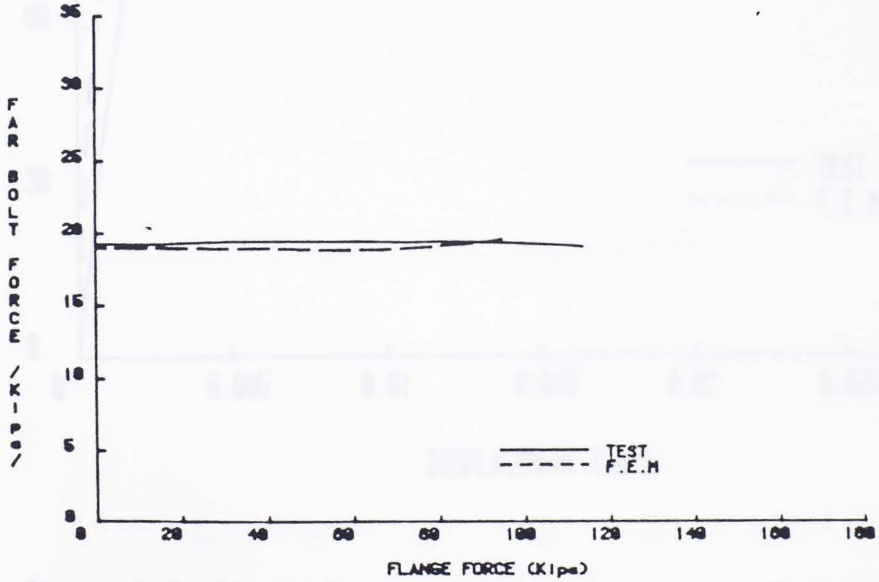

b) Far Bolt

Figure D.4 Bolt Force vs. Flange Force, Test TH-2

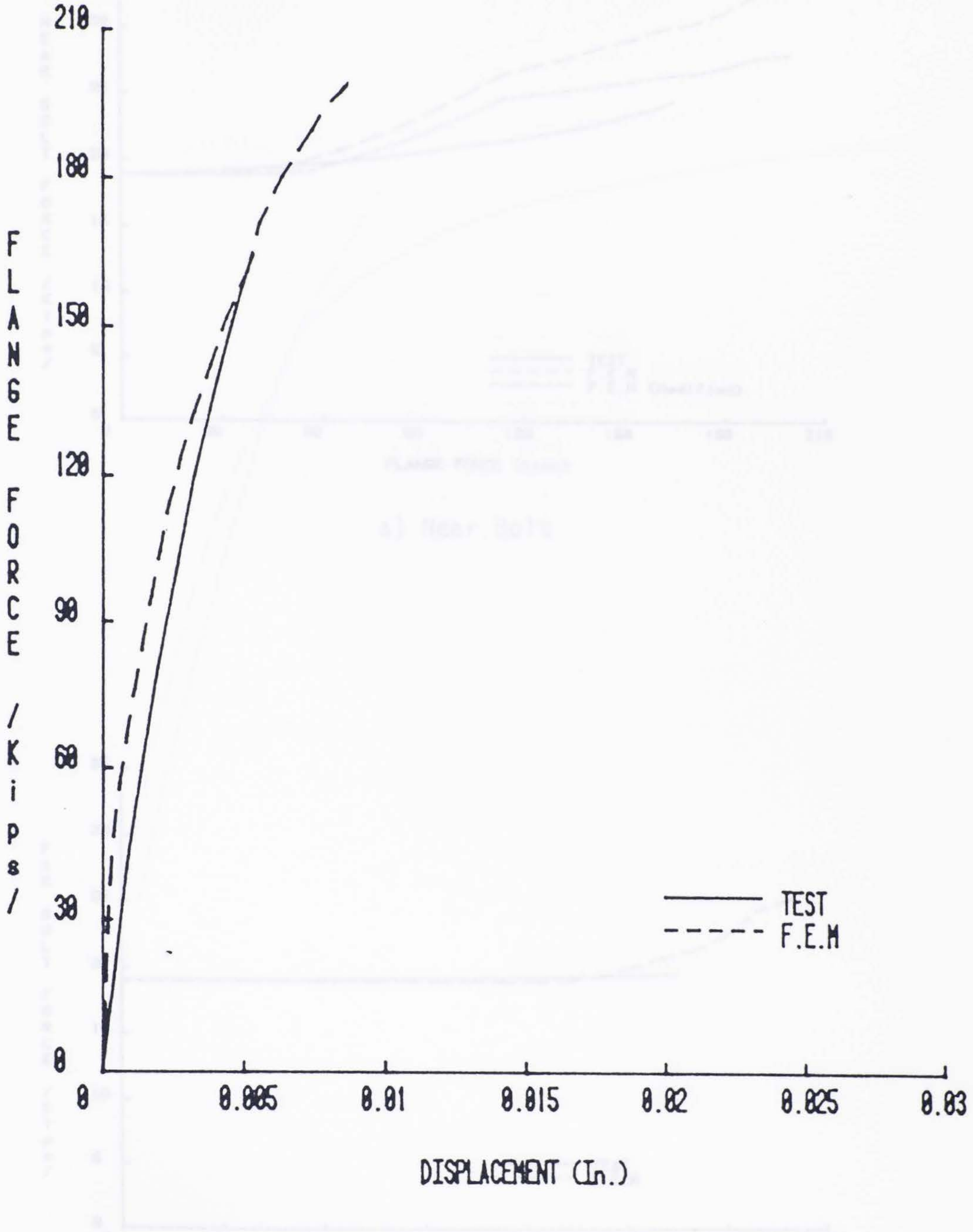

Figure D.5 Flange Force vs. Plate Separation, Test TH-3

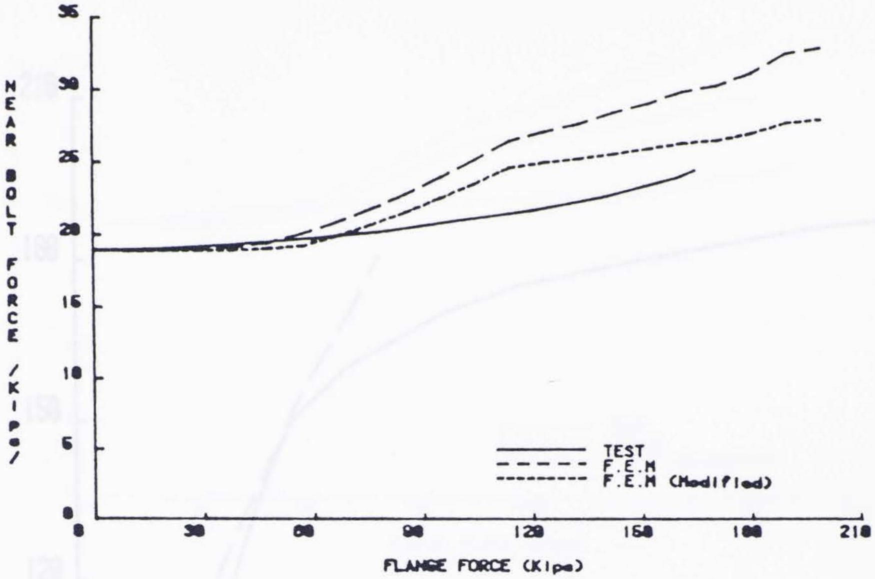

a) Near Bolt

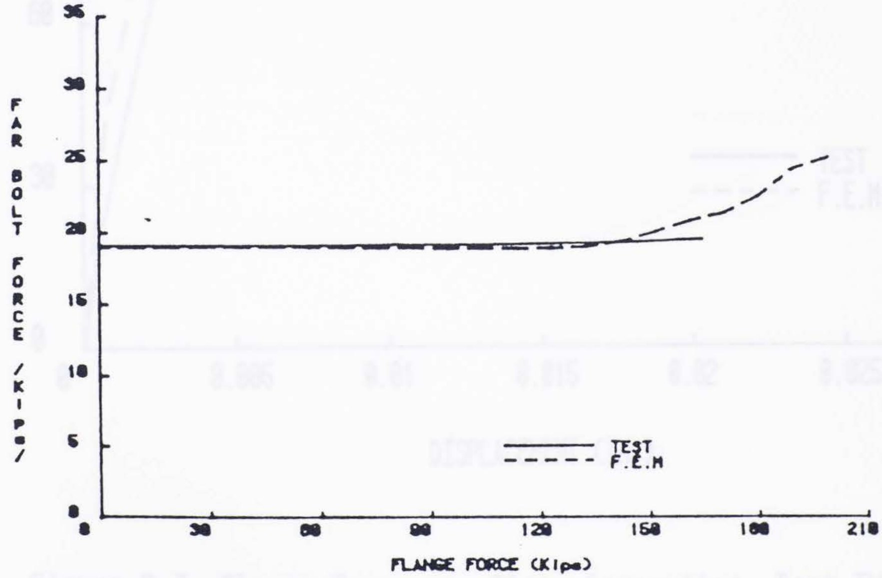

b) Far Bolt

Figure D.6 Bolt Force vs. Flange Force, Test TH-3

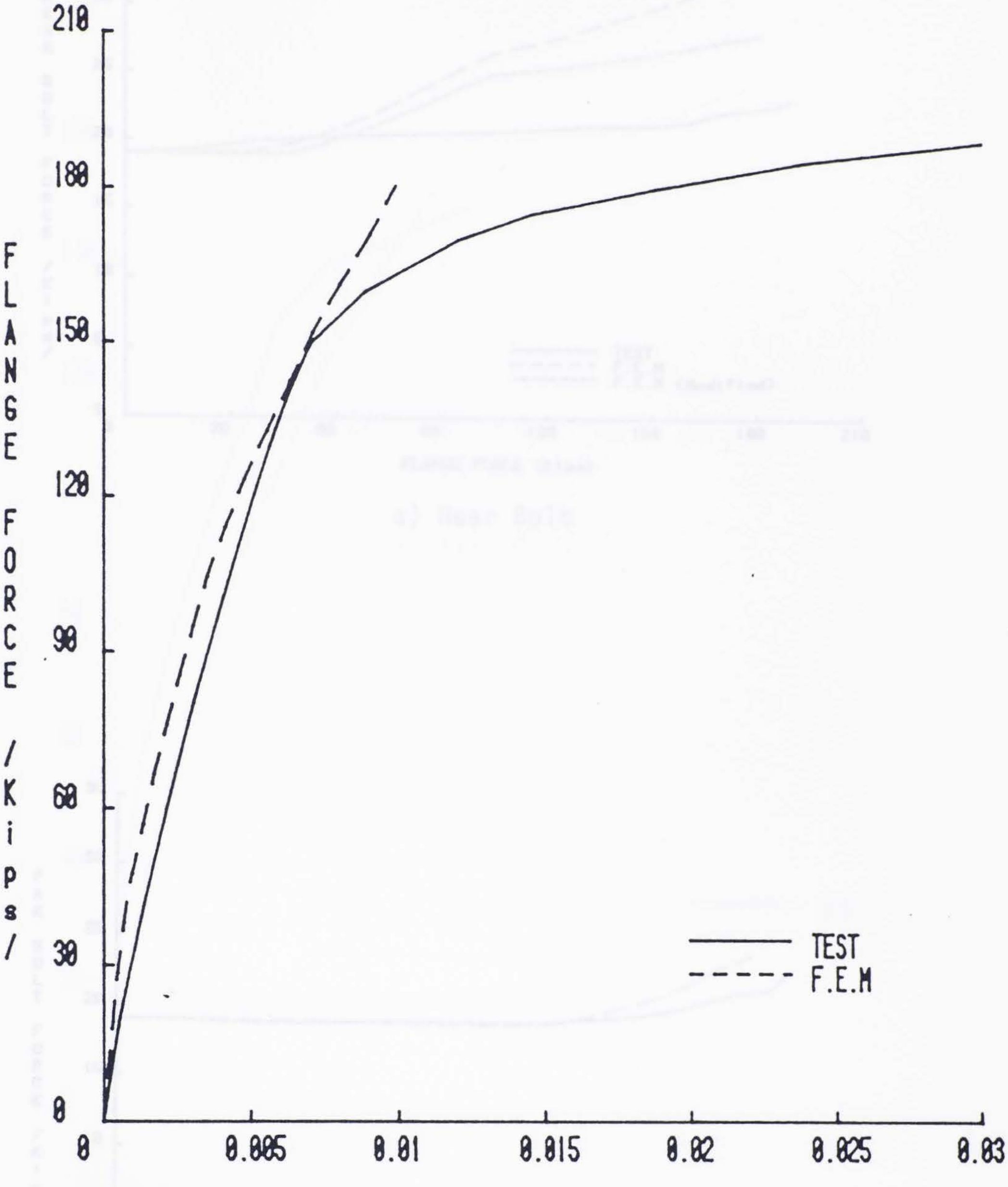

Figure D.7 Flange Force vs. Plate Separation, Test TH-4

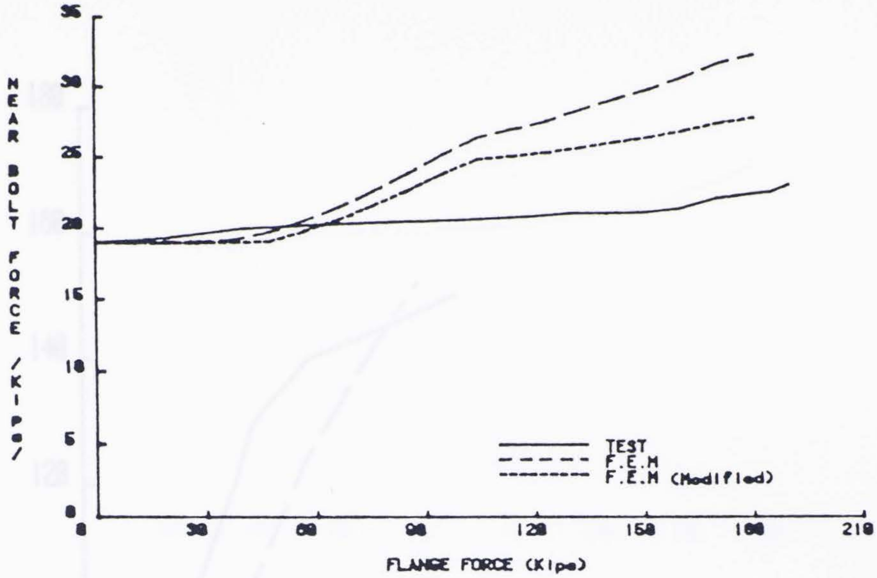

a) Near Bolt

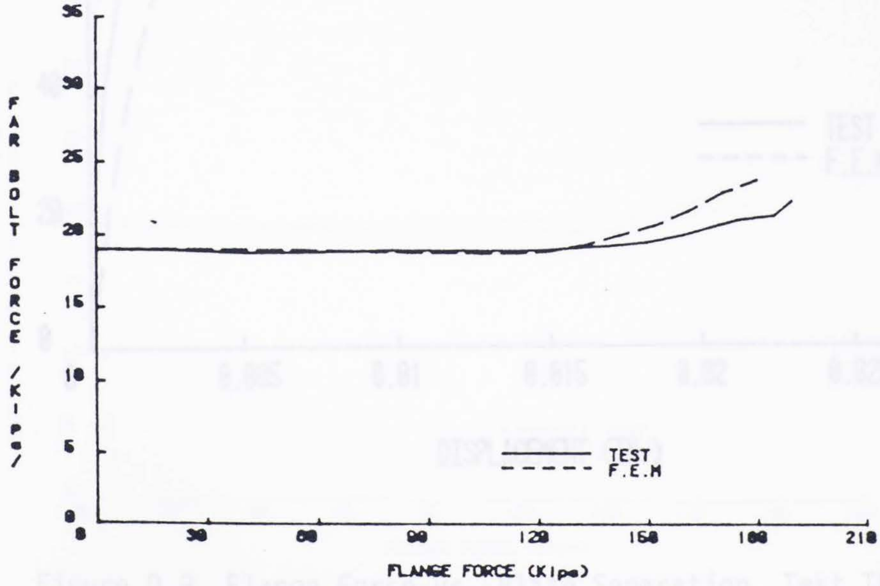

b) Far Bolt

Figure D.8 Bolt Force vs. Flange Force, Test TH-4

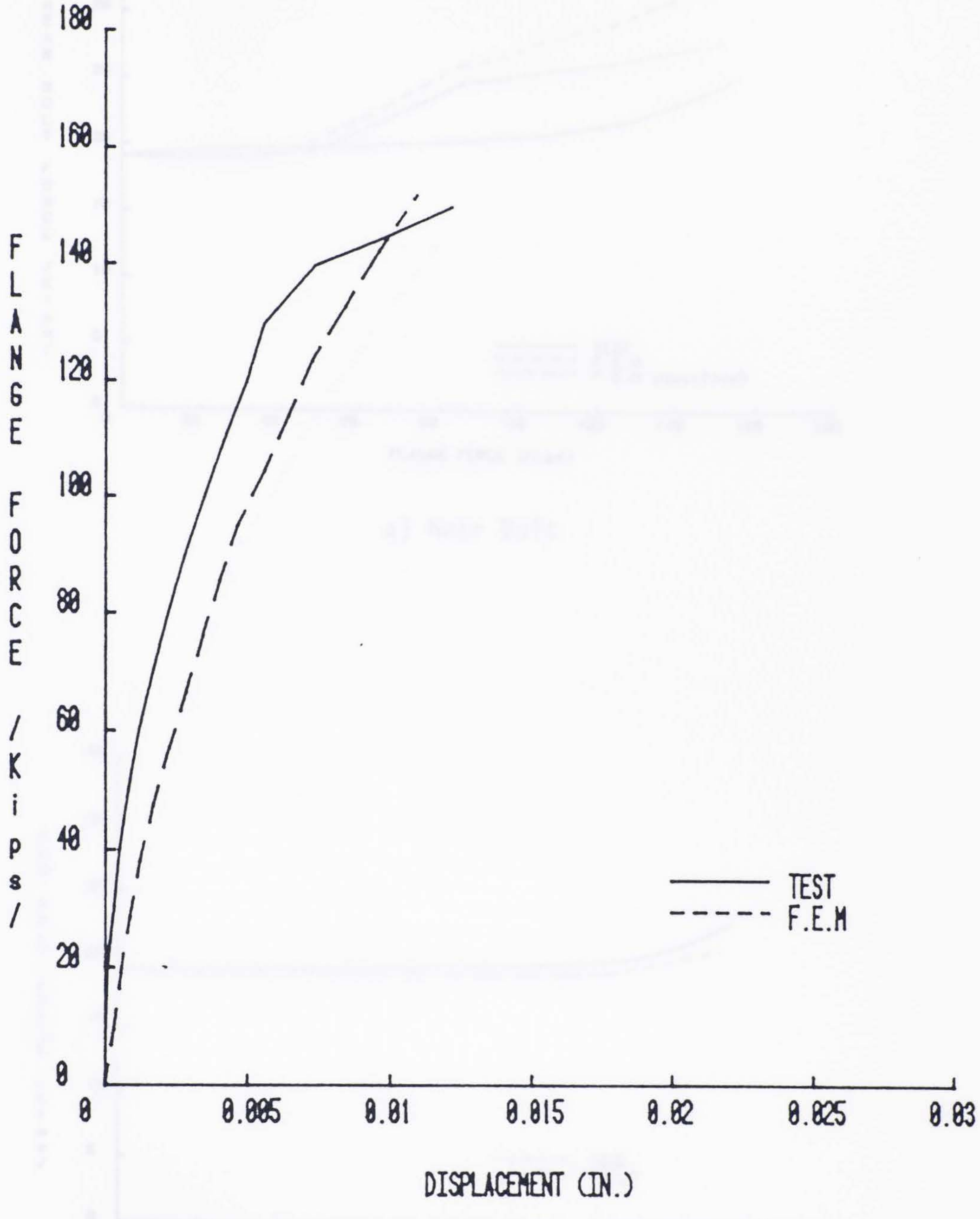

Figure D.9 Flange Force vs. Plate Separation, Test TH-5

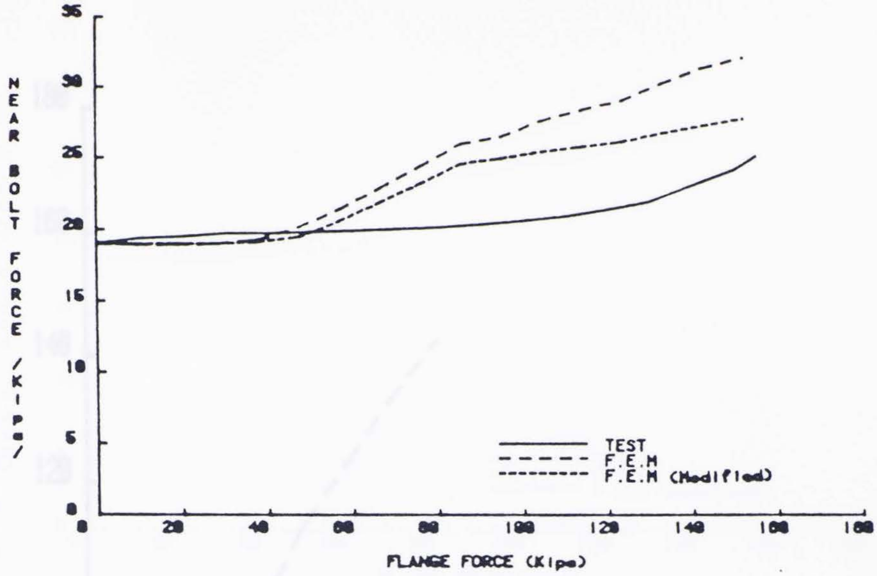

a) Near Bolt

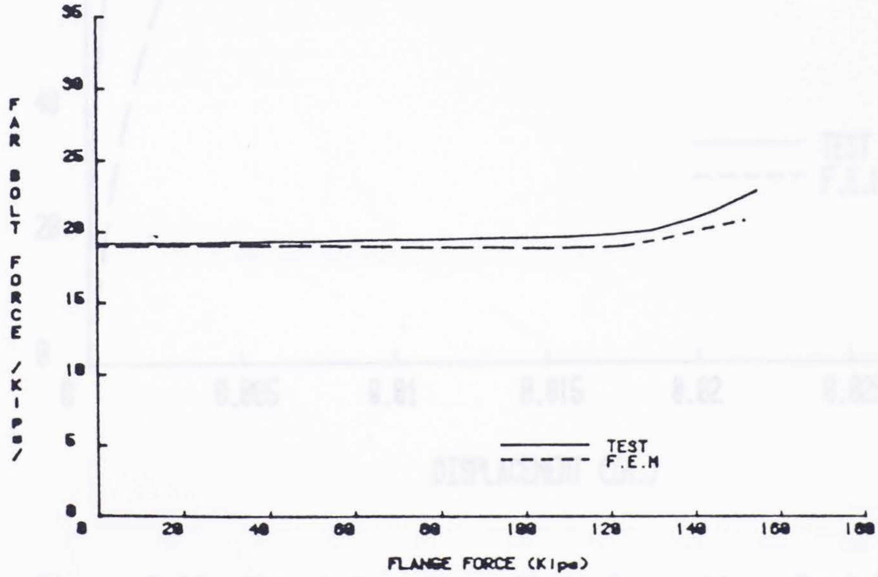

b) Far Bolt

Figure D.10 Bolt Force vs. Flange Force, Test TH-5

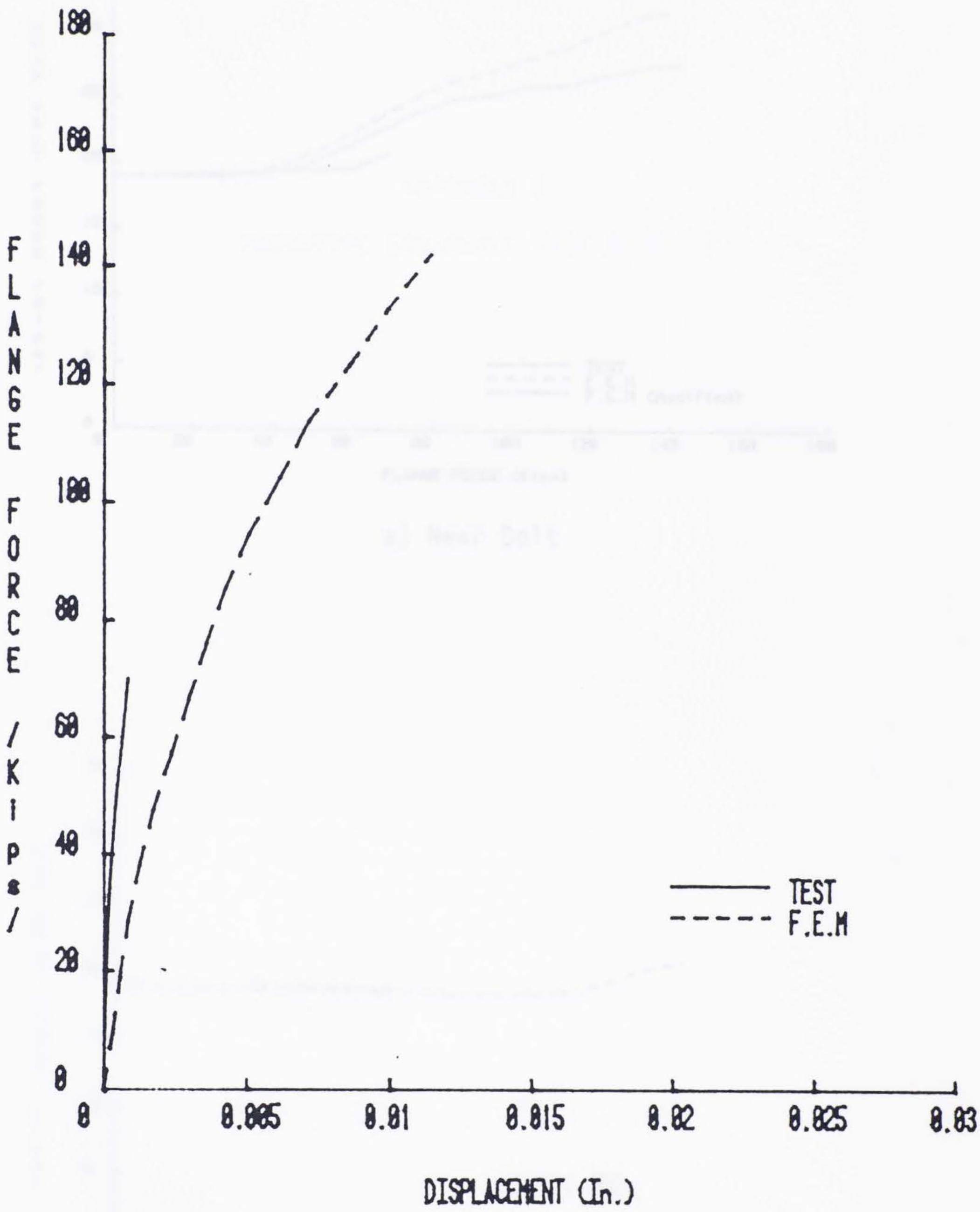

Figure D.11 Flange Force vs. Plate Separation, Test TH-6

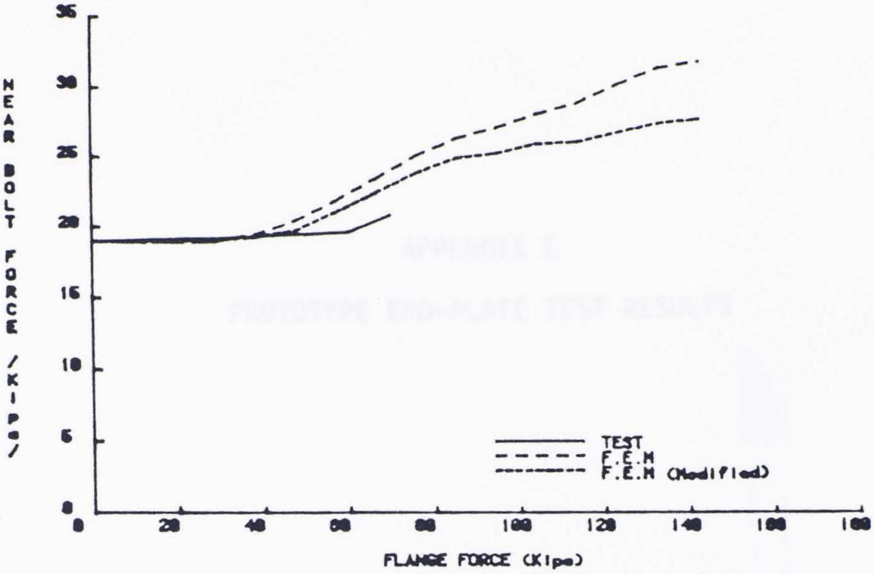

a) Near Bolt

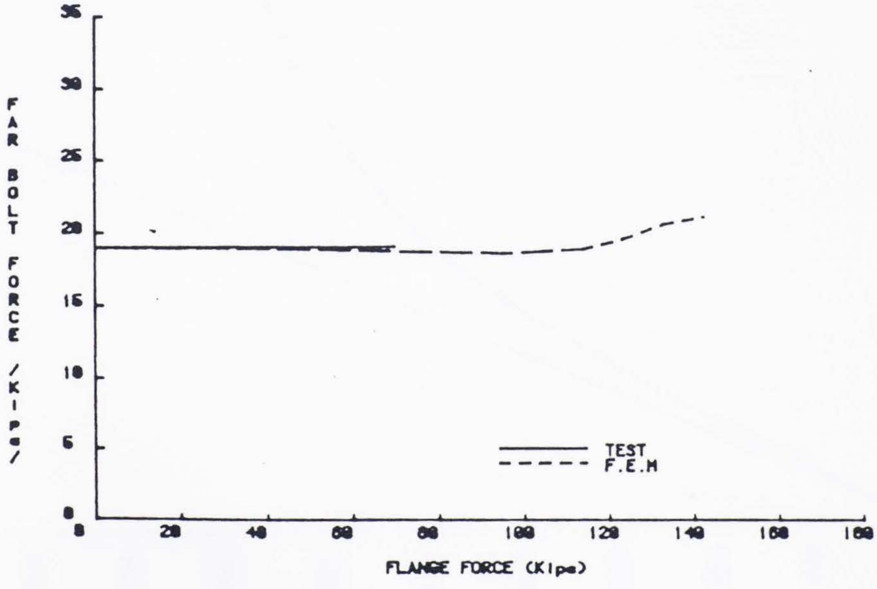

b) Far Bolt

Figure D.12 Bolt Force vs. Flange Force, Test TH-6

APPENDIX E

PROTOTYPE END-PLATE TEST RESULTS

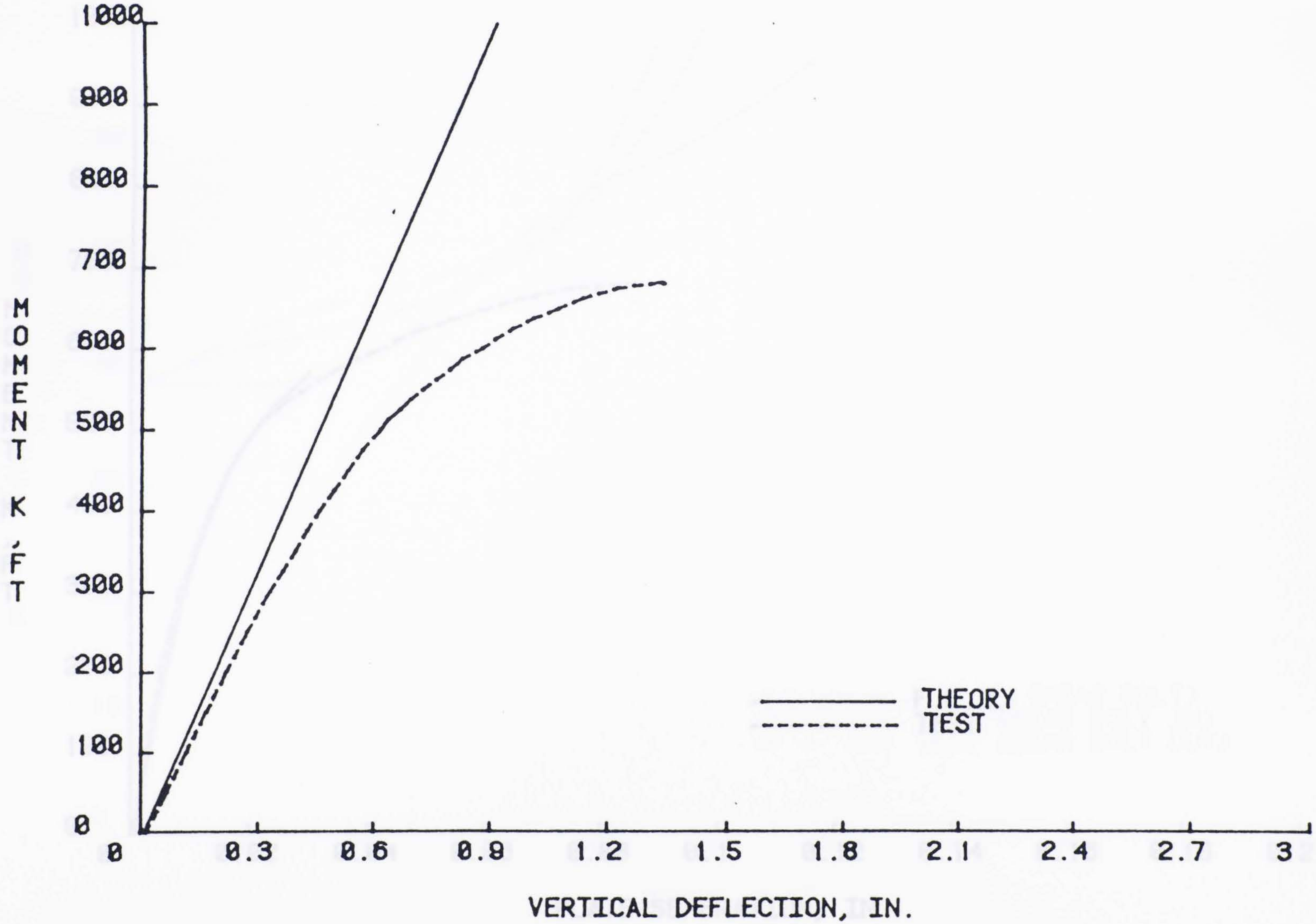

Figure E.1 Midspan Moment vs. Vertical Deflection, Test EP-1

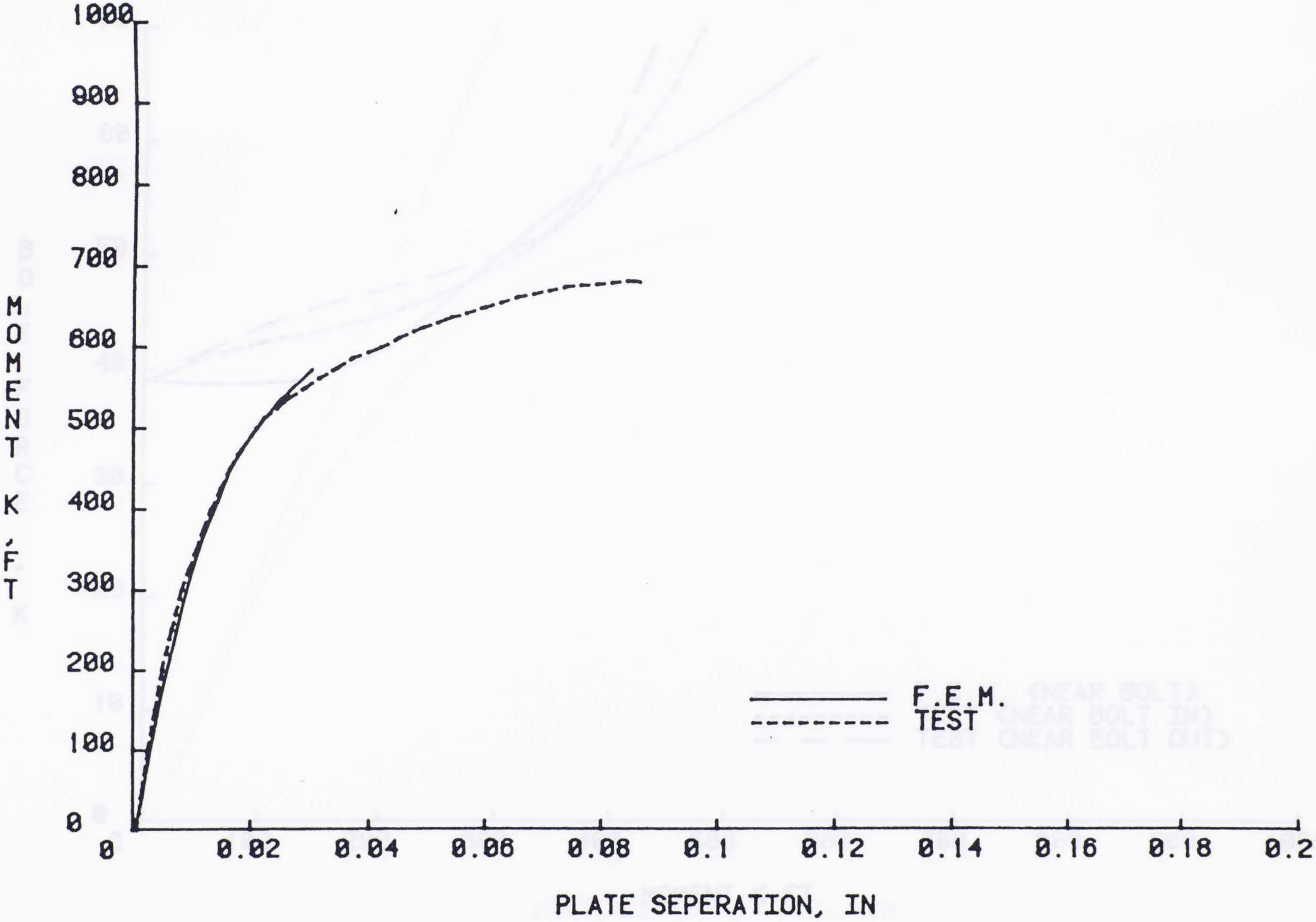

Figure E.2 Midspan Moment versus Plate Separation, Test EP-1

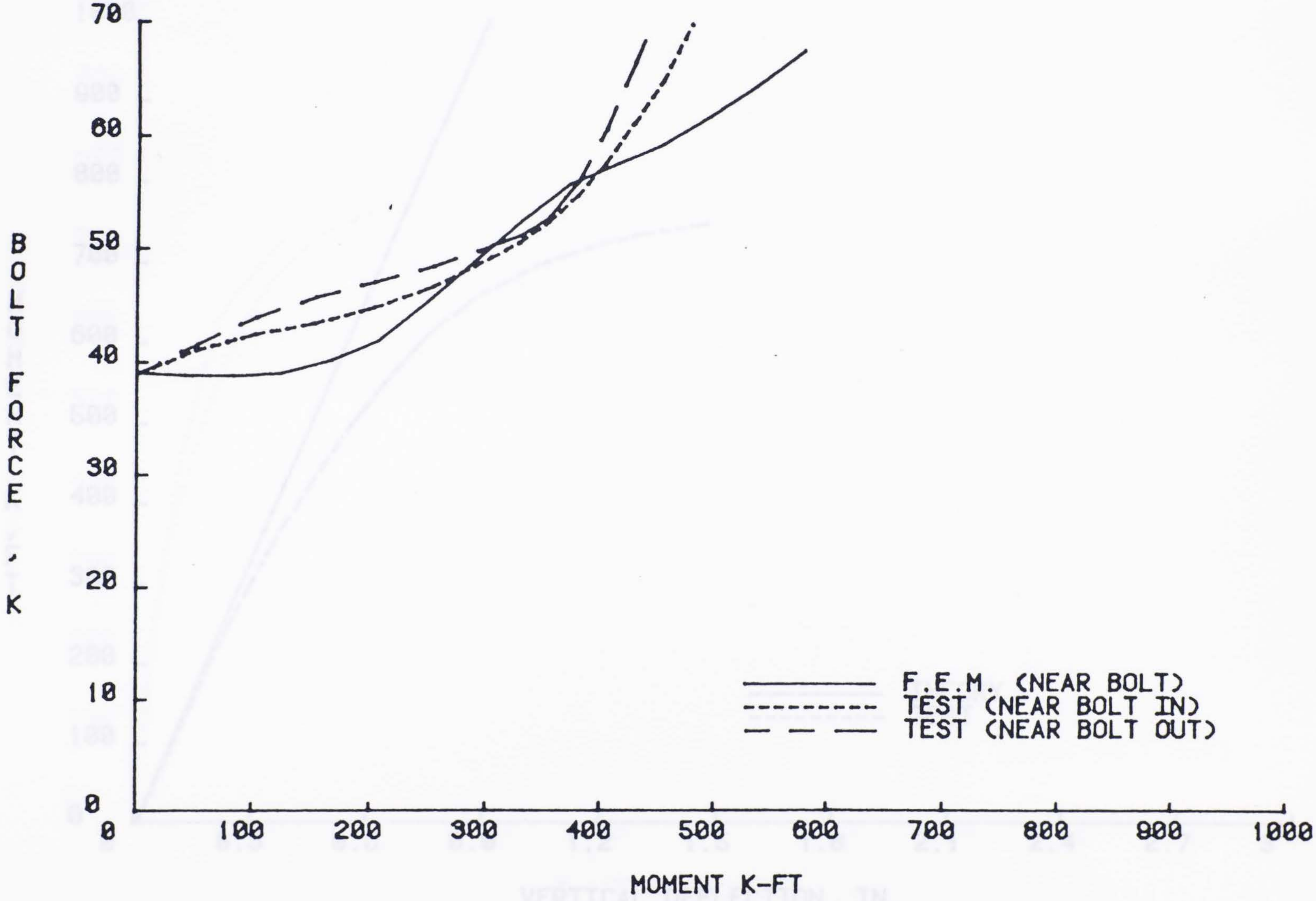

Figure E.3 Near Bolt Forces vs. Midspan Moment, Test EP-1

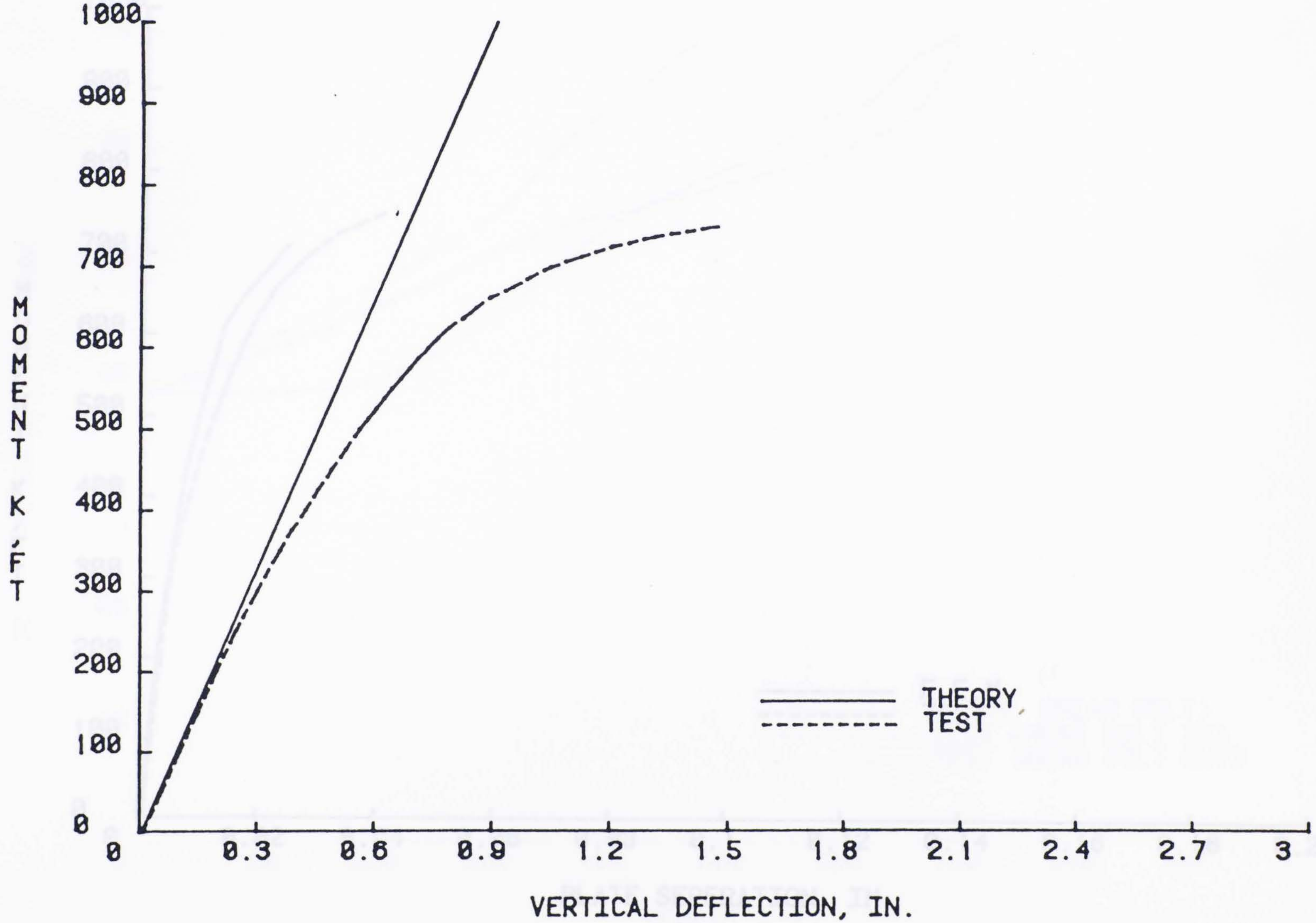

Figure E.4 Midspan Moment vs. Vertical Deflection, Test EP-2

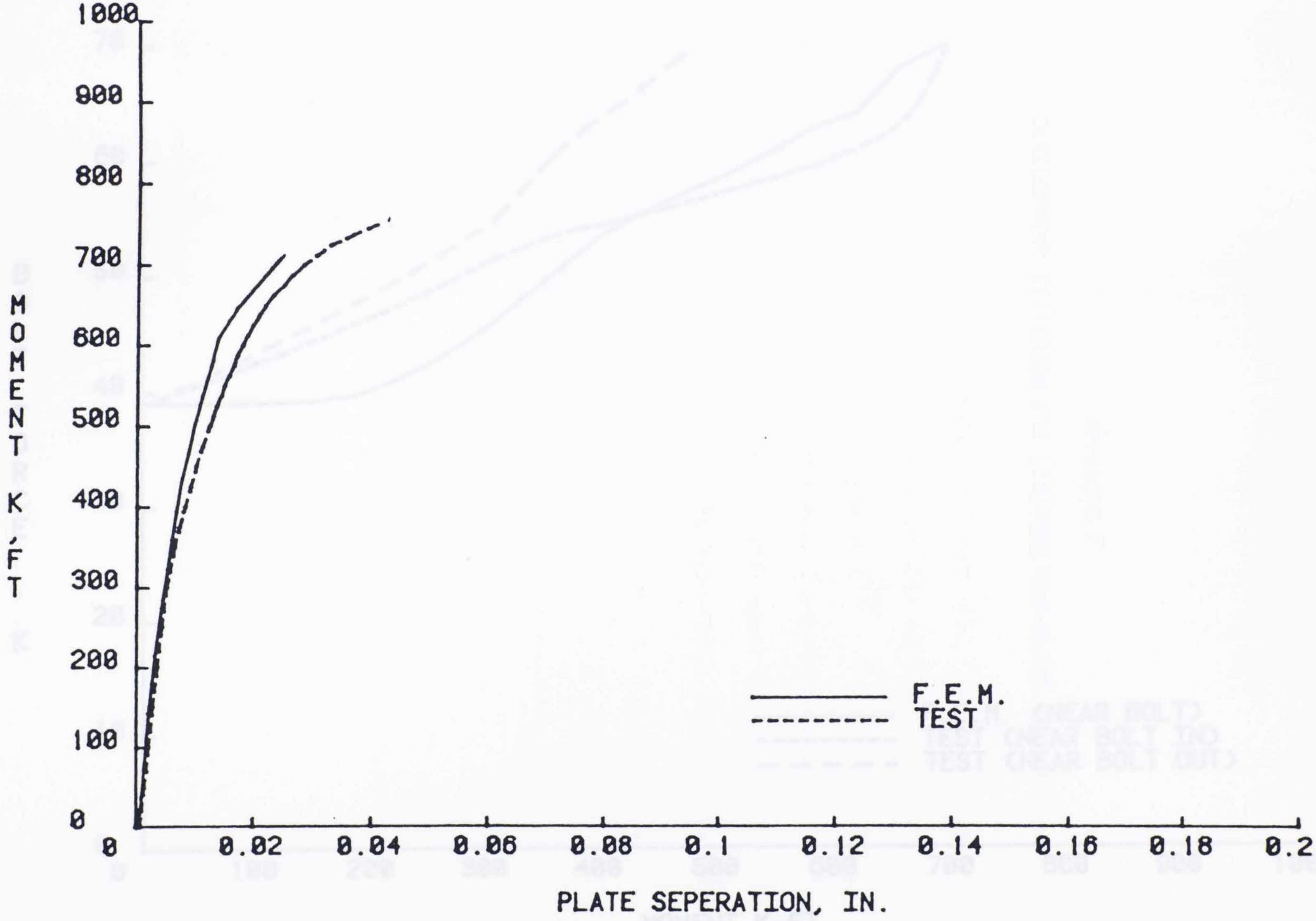

Figure E.5 Midspan Moment vs. Plate Separation, Test EP-2

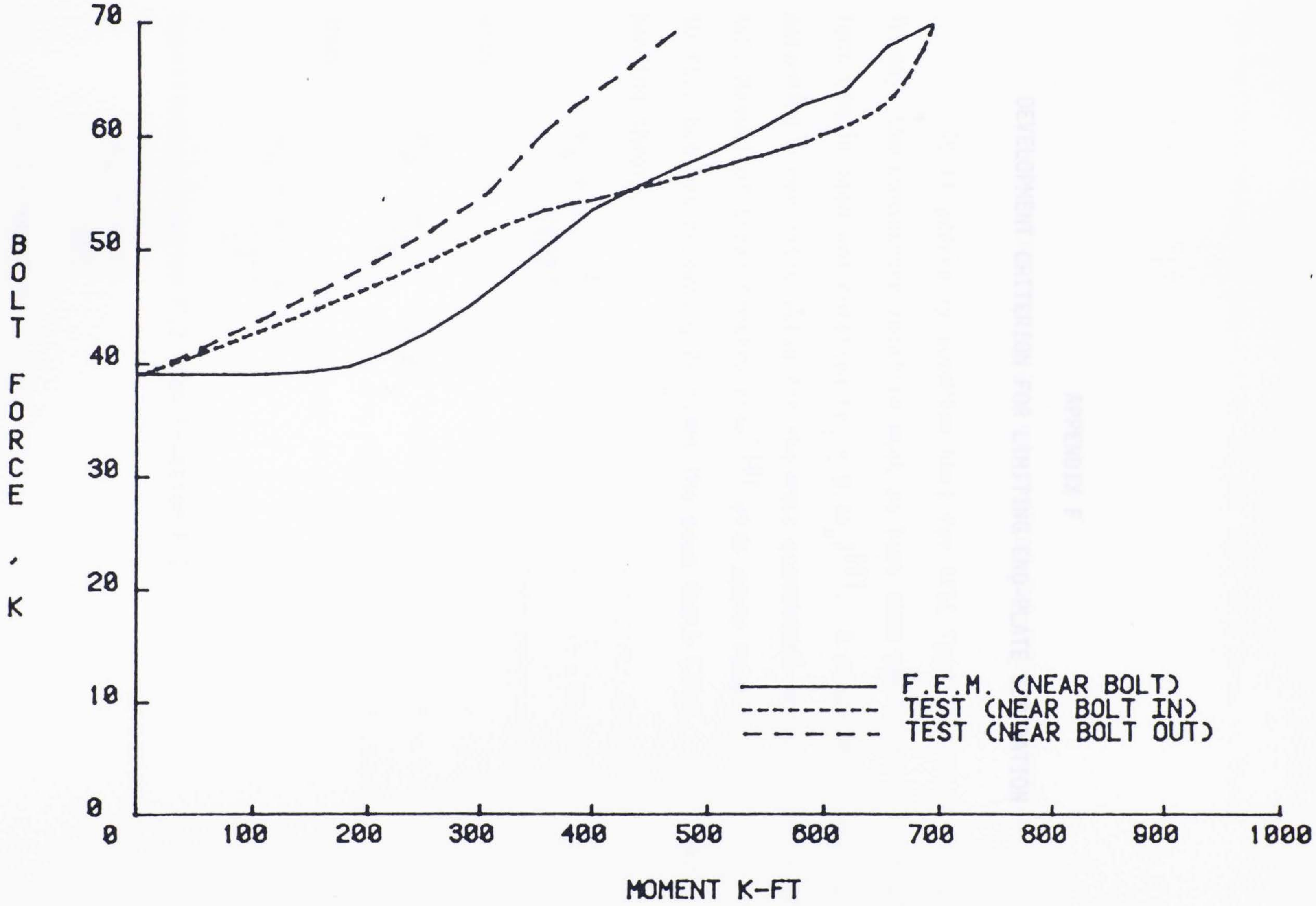

Figure E.6 Near Bolt Forces vs. Midspan Moment, Test EP-2

APPENDIX F

DEVELOPMENT CRITERION FOR LIMITING END-PLATE SEPARATION

It is generally accepted that for AISC Type 1 construction (rigid-frame), the connection rotation must be less than one-tenth of an equivalent simple beam end rotation ($\phi_c \leq 0.1\phi_s$)(5). A study was conducted to determine a realistic value for the most economical beams listed in the AISC Manual of Steel Construction(10) with spans ranging from 15 ft. to 50 ft., but not exceeding 24 times the beam depth (24d). From simple bending theory

$$\theta_s = \frac{w_u L^3}{24EI} \tag{F.1}$$

with

$$M_p = \frac{w_u L^2}{8} = Z\sigma_y \tag{F.2}$$

then

$$w_u = \frac{8\sigma_y Z}{L^2} \tag{F.3}$$

Substituting Equation F.3 into Equation F.1

$$\theta_s = \frac{\sigma_y ZL}{3EI} \tag{F.4}$$

For a Type 1 connection

$$\theta_{max} = 0.1\ \theta_s \tag{F.5}$$

APPENDIX F

DEVELOPMENT CRITERION FOR LIMITING END-PLATE SEPARATION

It is generally accepted that for AISC Type I construction (rigid-frame), the connection rotation must be less than one-tenth of an equivalent simple beam end rotation ($\theta_c \leq 0.1\theta_s$)[5]. A study was conducted to determine a realistic value for the most economical beams listed in the AISC Manual of Steel Construction[10] with spans ranging from 15 ft. to 50 ft., but not exceeding 24 times the beam depth (24d). From simple bending theory

$$\theta_s = \frac{w_u L^3}{24EI} \tag{F.1}$$

with

$$M_p = \frac{w_u L^2}{8} = Z\sigma_y \tag{F.2}$$

then

$$w_u = \frac{8\sigma_y Z}{L^2} \tag{F.3}$$

Substituting Equation F.3 into Equation F.1

$$\theta_s = \frac{\sigma_y ZL}{3EI} \tag{F.4}$$

For a Type I connection

$$\theta_{max} = 0.1\ \theta_s \tag{F.5}$$

The maximum end-plate separation at the tension flange is then

$$\delta = 0.1\ \theta_s d \qquad \text{(F.6)}$$

Substituting Equation F.4 into Equation F.6

$$\delta = 0.1\frac{(\sigma_Y ZL)}{3EI} \qquad \text{(F.7)}$$

which may be rewritten as

$$\delta = \lambda L \qquad \text{(F.8)}$$

where

$$\lambda = \frac{0.1\sigma_Y Z}{3EI} \qquad \text{(F.9)}$$

Values of λ are listed in the Table F.1 for several representative beam sections at a span of 24d. The value is almost constant and a typical value of 9.5×10^{-5} is used for further calculations. With this value of λ and a typical span of 35 ft., the value of δ is 0.04 in. For rigid frame construction, the limitation on rotation on one side of the connection is $0.05\theta_s$. Thus, the value of the maximum allowable plate separation has been adopted as 0.02 in.